Introduction to RADAR systems

Third Edition

Merrill I. Skolnik

McGRAW-HILL INTERNATIONAL EDITIONS
Electrical Engineering Series

chapter

7

Radar Clutter

7.1 INTRODUCTION TO RADAR CLUTTER

Clutter is the term used by radar engineers to denote *unwanted* echoes from the natural environment. It implies that these unwanted echoes "clutter" the radar and make difficult the detection of wanted targets. Clutter includes echoes from land, sea, weather (particularly rain), birds, and insects. At the lower radar frequencies, echoes from ionized meteor trails and aurora also can produce clutter. The electronic warfare technique known as *chaff,** although not an example of the natural environment, is usually considered as clutter since it is unwanted and resembles clutter from rain. Clutter is generally distributed in spatial extent in that it is much larger in physical size than the radar resolution cell. There are also "point," or discrete, clutter echoes, such as TV and water towers, buildings, and other similar structures that produce large backscatter. Large clutter echoes can mask echoes from desired targets and limit radar capability. When clutter is much larger than receiver noise, the optimum radar waveform and signal processing can be quite different from that employed when only receiver noise is the dominant limitation on sensitivity.

Radar echoes from the environment are not always undesired. Reflections from storm clouds, for example, can be a nuisance to a radar that must detect aircraft; but storm clouds

*Chaff is an electronic countermeasure that consists of a large number of thin passive reflectors, often metallic foil strips. When released from an aircraft they are quickly dispersed by the wind to form a highly reflecting cloud. A relatively small bundle of chaff can form a cloud with a radar cross section comparable to that of a large aircraft.

containing rain are what the radar meteorologist wants to detect in order to measure rainfall rate over a large area. The backscatter echoes from land can interfere with many applications of radar, but they are the target of interest for ground-mapping radar, synthetic aperture radars, and radars that observe earth resources. Thus the same environmental echo might be the desired signal in one application and the undesired clutter echo in another. The observation of land, sea, weather and other natural phenomena by radar and other sensors for the purpose of determining something about the environment is known as *remote sensing of the environment,* or simply *remote sensing.* All radars, strictly speaking, are remote sensors; but the term is usually applied only to those radars whose major function is to observe the natural environment for the purpose of extracting information about the environment. A prime example of a radar used for remote sensing is the doppler weather radar.

Echoes from land or sea are examples of *surface clutter.* Echoes from rain and chaff are examples of *volume clutter.* The magnitude of the echo from distributed surface clutter is proportional to the area illuminated. In order to have a measure of the clutter echo that is independent of the illuminated area, the *clutter cross section per unit area,* denoted by the symbol σ^0, is commonly used to describe surface clutter. It is given as

$$\sigma^0 = \frac{\sigma_c}{A_c} \qquad [7.1]$$

where σ_c is the radar cross section of the clutter occupying an area A_c. The symbol σ^0 is spoken, and sometimes written, as *sigma zero.* It has also been called the *scattering coefficient, differential scattering cross section, normalized radar reflectivity, backscattering coefficient,* and *normalized radar cross section* (*NRCS*). The zero is a superscript since the subscript is reserved for the polarization employed. Sigma zero is a dimensionless quantity, and is often expressed in decibels with a reference value of one m^2/m^2.

Similarly, a cross section per unit volume is used to characterize volume clutter. It is defined as

$$\eta = \frac{\sigma_c}{V_c} \qquad [7.2]$$

where σ_c in this case is the radar cross section of the clutter that occupies a volume V_c. Clutter cross section per unit volume, η, is sometimes called the *reflectivity.*

In the next section, the radar range equation for targets in surface clutter is derived along with a brief review of the general character of scattering from surface clutter. This is followed by descriptions of radar echoes from land, sea, weather, and the atmosphere. The chapter concludes by describing methods that might be used to enhance the detection of targets in clutter.

7.2 SURFACE-CLUTTER RADAR EQUATION

The radar equation describing the detection of a target in surface clutter is different from the radar equation discussed in Chap. 2, where it was assumed that detection sensitivity

was limited by receiver noise. The radar equation for detection of a target in clutter leads to different design guidelines than the radar equation for detection of a target when limited by receiver noise.

Low Grazing Angle Consider the geometry of Fig. 7.1 which depicts a radar illuminating the surface at a grazing angle ψ. Assume the grazing angle is small. A small grazing angle usually implies that the extent of the resolution cell in the range dimension is determined by the radar pulse width τ rather than the elevation beamwidth. The width of the cell in the cross-range dimension is determined by the azimuth beamwidth θ_B and the range R. From the simple radar equation [such as Eq. (1.7) of Sec. 1.2] the received echo power P_r is

$$P_r = \frac{P_t G A_e \sigma}{(4\pi)^2 R^4} \qquad [7.3]$$

where

P_t = transmitter power, W
G = antenna gain
A_e = antenna effective aperture, m^2
R = range, m
σ = radar cross section of the scatterer, m^2

When the echo is from a target (rather than from clutter), we let $P_r = S$ (received target signal power) and $\sigma = \sigma_t$ (target cross section). The signal power returned from a target is then

$$S = \frac{P_t G A_e \sigma_t}{(4\pi)^2 R^4} \qquad [7.4]$$

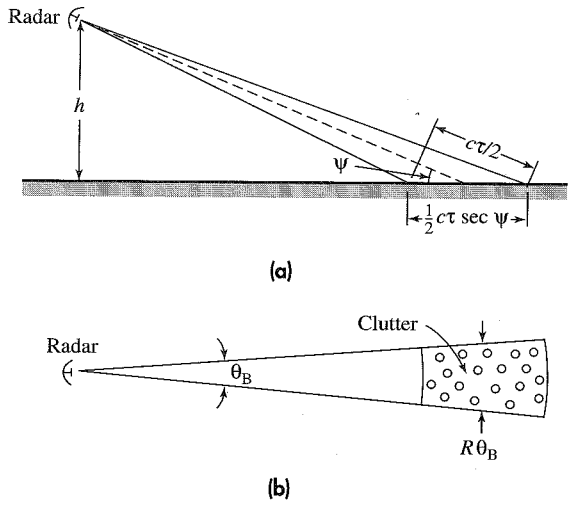

Figure 7.1 Geometry of radar surface clutter. (a) Elevation view showing the extent of the surface illuminated by the radar pulse, (b) plan view showing the illuminated clutter patch (or resolution cell) consisting of individual, independent scatterers.

When the echo is from clutter, the cross section σ becomes $\sigma_c = \sigma^0 A_c$, where the area A_c of the radar resolution cell is given from Fig. 7.1 as

$$A_c = R\theta_B (c\tau/2) \sec \psi \qquad [7.5]$$

θ_B = two-way azimuth beamwidth, c = velocity of propagation, τ = pulsewidth, and ψ = grazing angle (defined with respect to the tangent to the surface). The extent of the area A_c in the range coordinate (the range resolution) is $c\tau/2$, where the factor of 2 in the denominator accounts for the two-way propagation of radar. With these definitions, the radar equation for the surface-clutter echo-signal power C is

$$C = \frac{P_t G A_e \sigma^0 \theta_B (c\tau/2) \sec \psi}{(4\pi)^2 R^3} \qquad [7.6]$$

The received echo power C from surface clutter is seen to vary inversely as the cube of the range rather than the fourth power, as was the case for point targets in free space.

When the echo from surface clutter is large compared to receiver noise, the signal-to-clutter ratio is Eq. (7.4) divided by Eq. (7.6), or

$$\frac{S}{C} = \frac{\sigma_t}{\sigma^0 R \theta_B (c\tau/2) \sec \psi} \qquad [7.7]$$

If the maximum range $R_{\max}$ corresponds to the minimum discernible signal-to-clutter ratio $(S/C)_{\min}$, then the radar equation for the detection of a target in surface clutter at low grazing angle is

$$R_{\max} = \frac{\sigma_t}{(S/C)_{\min} \sigma^0 \theta_B (c\tau/2) \sec \psi} \qquad [7.8]$$

If pulse compression is used, the pulse width τ is that of the compressed pulse.

The azimuth beamwidth θ_B in the above equations is the two-way beamwidth. When the gaussian function can be used to approximate the beam shape (which is usually a good assumption), the two-way beamwidth is smaller than the one-way beamwidth by $\sqrt{2}$. (If the one-way beamwidth is used to calculate σ^0, the value of σ^0 will be lower by 1.5 dB than if the two-way beamwidth were used.)

The radar equation for surface clutter, Eq. (7.8), is quite different from the noise-dominated radar equation derived in Sec 1.2. The range appears as the first power rather than the fourth power as in the usual radar equation [Eq. (7.3)]. This results in greater variation of the maximum range of a clutter-dominated radar than a noise-dominated one when there is uncertainty or variability in the parameters of the radar equation. For example, if the target cross section in Eq. (7.8) were to change by a factor of two, the maximum range would also change by a factor of two. However, the same change of a factor of two in target cross section would only cause a variation in range of 1.2 (the fourth root of 2) when radar performance is determined by receiver noise alone.

There are other significant differences that affect radar design when clutter is the dominant limitation. The transmitter power does not appear explicitly in the surface-clutter radar equation. Increasing the transmitter power will increase the target signal, but the clutter echo will also increase by the same amount. Thus there is no net gain in the

detectability of desired targets. The only requirement on the transmitter power when Eq. (7.8) is used is that it be great enough to cause the clutter power at the radar receiver to be large compared to receiver noise.

Neither the antenna gain nor effective aperture enters explicitly, except as affected by the azimuth beamwidth θ_B. Equation (7.8) indicates that the narrower the azimuth beamwidth, the greater the range. Also, the narrower the pulse width, the greater the range, which is just the opposite of conventional radar detection of target echo signals in noise. A long pulse is desired when the radar is dominated by noise so as to increase the signal-to-noise energy ratio. A long pulse, on the other hand, decreases the signal-to-clutter ratio.

If the statistics of the clutter echoes are similar to the statistics of receiver noise (gaussian probability density function), the minimum signal-to-clutter ratio in Eq. (7.8) can be selected similarly to that for the signal-to-noise ratio as described in Chap. 2. Gaussian statistics, however, are rarely applicable to sea clutter and seldom for land clutter, unless the resolution cell is large. Therefore, the selection of the minimum signal-to-clutter ratio required for detection of a target in sea clutter can be difficult. When no other information is available concerning the statistics of clutter, many engineers will cautiously use the gaussian model that is used for receiver noise—and hope for the best. Even if the clutter can be described by gaussian statistics, clutter echoes do not vary with time in the same manner as receiver noise. The temporal correlation of successive clutter echoes has to be taken into account.

Radars integrate (add together) a number of echoes from a target to enhance detection, as was discussed in Sec. 2.6. Integration of pulses is generally much less effective when detection is limited by clutter than when limited by receiver noise. The statistics of receiver noise are independent (uncorrelated) in a time equal to $1/B$, where B = receiver bandwidth (usually measured in the IF portion of the radar receiver). When pulses are integrated, the sum of the noise-power fluctuations do not increase as rapidly as does the sum of the target echoes so that increased signal-to-noise ratio is obtained as the number of pulses integrated is increased. On the other hand, with perfectly stationary clutter (rocks or fence posts, for example), the clutter echo does not fluctuate from pulse to pulse. It builds up at the same rate as the target signal. There is no increase in signal-to-clutter ratio, so that integrating pulses provides no benefit. Sea clutter, however, changes with time, but slowly. At X band, for example, the decorrelation time of sea clutter is about several milliseconds. One might talk about an effective number, n_{eff}, of pulses integrated for incorporating in the numerator of Eq. (7.8), but it is likely to be much smaller than the n_{eff} for a noise-limited radar with the same number of received pulses. It is much more difficult to determine n_{eff} for clutter than for noise. Because of the uncertainties in determining n_{eff} for clutter, the conservative engineer might omit any gain due to pulse integration when detection is dominated by stationary or slowly changing clutter rather than receiver noise.

System losses also are not included explicitly in the radar equation of Eq. (7.8). Many of the system losses mentioned in Sec. 2.12 affect the target and clutter echo signals the same. Losses, therefore, have less effect on detection when signals are limited by clutter than when signals are limited by receiver noise. As long as losses do not make invalid the assumption that the clutter echo is large compared to receiver noise, losses have a lesser effect than in a noise-dominated radar.

High Grazing Angle Next consider the case where the radar observes surface clutter near perpendicular incidence. The clutter area viewed by the radar is determined by the antenna beamwidths θ_B and ϕ_B in the two principal planes. The clutter illuminated area A_c in Eq. (7.1) is $(\pi/4)R\theta_B R\phi_B/2 \sin \psi$, where ψ = grazing angle and R = range. The factor $\pi/4$ accounts for the elliptical shape of the illuminated area, and the factor of 2 in the denominator is necessary since in this case θ_B and ϕ_B are the one-way beamwidths. Substituting $\sigma = \sigma^0 A_c$ in Eq. (7.3), letting $P_r = C$ (the clutter echo power), and taking $G = \pi^2/\theta_B\phi_B$,[1] the clutter radar equation in this case is

$$C = \frac{\pi P_t A_e \sigma^0}{128 R^2 \sin \psi} \qquad [7.9]$$

The clutter power is seen to vary inversely as the square of the range. This equation applies to the echo power received from the ground by a radar altimeter or the remote sensing radar known as a scatterometer. An equation for detecting a target at high grazing angles could be derived, but this represents a situation not often found in practice.

Grazing, Incidence, and Depression Angles In most of this chapter, the grazing angle is used to describe the aspect at which clutter is viewed. There are two other angles that are sometimes used instead of the grazing angle (Fig. 7.2). The *incidence angle* is defined with respect to the normal to the surface; the *grazing angle* is defined with respect to the tangent to the surface; and the *depression angle* is defined with respect to the local horizontal at the radar. The incidence angle is the complement of the grazing angle. When the earth's surface can be considered smooth and flat, the depression angle and the grazing angle are the same. When the earth's curvature must be taken into account, as in spaceborne radars, the depression angle can be quite different from the grazing angle. The incidence angle is usually used when considering earth backscatter at near perpendicular incidence, as in the altimeter and the scatterometer. The grazing angle is preferred in most other applications. Some engineers (as in references 3 and 4) prefer to use the depression angle when a rough or varying earth's surface is viewed at low grazing angles since it might be easier to determine than the grazing angle when the earth is not a flat surface.

Variation of Surface Clutter with Grazing Angle The general form of surface clutter as a function of grazing angle is shown in Fig. 7.3. There are three different scattering regions. At high grazing angles, the radar echo is due mainly to reflections from clutter that can be represented as a number of individual *planar facets* oriented so that the incident

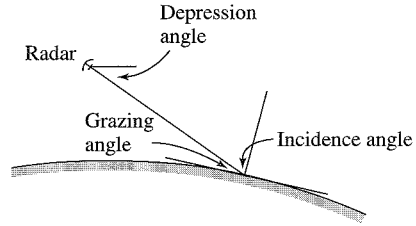

Figure 7.2 Angles used in describing geometry of the radar and surface clutter.

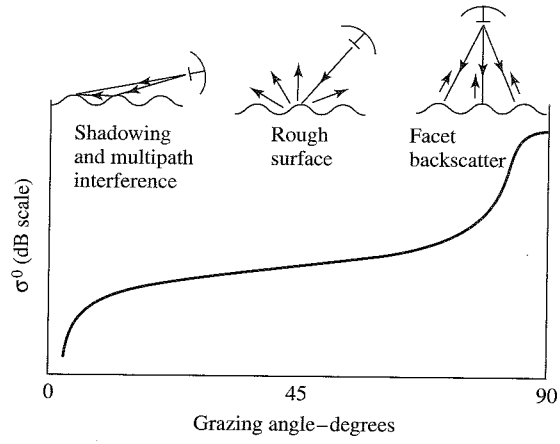

Figure 7.3 General nature of the variation of surface clutter as a function of grazing angle, showing the three major scattering regions.

energy is directed back to the radar. The backscatter can be quite large at high grazing angles. At the intermediate grazing angles, scattering is somewhat similar to that from a *rough surface.* At low grazing angles, back scattering is influenced by *shadowing* (masking) and by *multipath propagation.* Shadowing of the trough regions by the crests of waves prevents low-lying scatterers from being illuminated. Multipath reduces the energy propagating at low angles because of cancellation of the direct energy by the out-of-phase surface-reflected energy (similar to the multipath phenomenon described in Sec. 8.2). The curve drawn in Fig. 7.3 is descriptive of the general character of both land and sea scattering; but there are significant differences in the details depending on the particular type of clutter. The difference between the maximum clutter at perpendicular incidence and the minimum clutter at grazing incidence can be many tens of dB.

Mean and Median Values The characteristics of clutter echoes are usually given in statistical terms. It is often described either by the mean (average) value of σ^0 or the median (the value exceeded 50 percent of the time). For a Rayleigh probability density function, the difference between the mean and the median is small (a few percent); but for non-Rayleigh distributions, the mean and the median can be quite different. In some cases, the accuracy of clutter measurements might not be sufficient to make a distinction between the mean and the median. Nevertheless, when using clutter data, it is best to know whether it is the mean or the median that is being used. According to Nathanson,[2] the mean value is much better behaved than the median. The median can vary depending on the siting, pulse duration, masking, and other factors.

For proper radar design, the probability density function of the clutter echoes should be known so that the receiver detector can be designed appropriately. Unfortunately, when the statistics of the clutter cannot be described by the classical Rayleigh probability density function, it is often difficult to define a specific quantitative statistical description. For this reason, many radar designs have been based on the mean value of the clutter σ^0 rather than some statistical model. Further discussion of surface-clutter probability density functions is given later in Sec. 7.5.

7.3 LAND CLUTTER

The general nature of land clutter at low, medium, and high grazing angles is described in this section.

Land Clutter at Low Grazing Angles An extensive multiple-frequency database of land clutter at low angles was acquired by the MIT Lincoln Laboratory and reported by J. B. Billingsley and J. F. Larrabee.[3] This is one of the few collections of land clutter data that have been obtained over a wide variety of terrain, with good "ground truth," good calibration, and observations over a long period of time. The Lincoln Laboratory data provides much better understanding than previously, and it has caused some earlier notions about the nature of land clutter to be modified.

Forty-two different sites widely dispersed geographically across North America were measured, with most of the sites in western Canada. Measurements were made over a period of almost 3 years with an average time of 17 days at a site. Some sites were visited more than once to determine seasonal variations. Measurements were made at five frequencies: VHF (167 MHz), UHF (435 MHz), *L* (1.23 GHz), *S* (3.24 GHz), and *X* (9.2 GHz) bands. The radars were mobile with antennas mounted on a tower that could be extended to heights of 30, 60, or 100 ft. Range resolution was either 150 m or 36 m at VHF and UHF. At the other three frequencies, the resolution was either 150 m or 15 m. Both vertical and horizontal polarizations were employed. The rms accuracy of the clutter echo measurements over all sites was said to be 2 dB, a very good value for field operations.

The radar measured $\sigma^0 F^4$ (called *clutter strength* in the Lincoln Laboratory Report), where σ^0 is the clutter cross-section per unit area and F is the *propagation factor* that sometimes appears in the radar equation to account for propagation effects such as multipath reflections, diffraction, and attenuation. The authors define the propagation factor F as the "ratio of the incident field that actually exists at the clutter cell being measured to the incident field that would exist there if the clutter cell existed by itself in free space." Even though one might wish to separate clutter backscatter (σ^0) from propagation effects (F), it is difficult to do so and it is not generally done. (Many of the measurements of σ^0 reported in the literature are measurements of $\sigma^0 F^4$ even though they might be said to be of σ^0.)

Clutter observations were made at low depression angles, at ranges from 1 to 25 or 50 km or more. The depression angle was used rather than the grazing angle since it was difficult to define the grazing angle over a non-flat surface such as natural terrain. The depression angle in the Lincoln Laboratory report is "the complement of the incidence angle at the backscattering terrain point under consideration." This definition of depression angle includes the effect of earth curvature on the angle of illumination but not the effect of the local terrain slope.

The results of the Lincoln Laboratory measurements are summarized in Fig. 7.4 and Table 7.1. Clutter strength is given as the median value of the measured means by terrain type and frequency. The values in the figure and table were averaged over both vertical and horizontal polarizations, and with both 150 m and 15 or 36 m range resolution. This

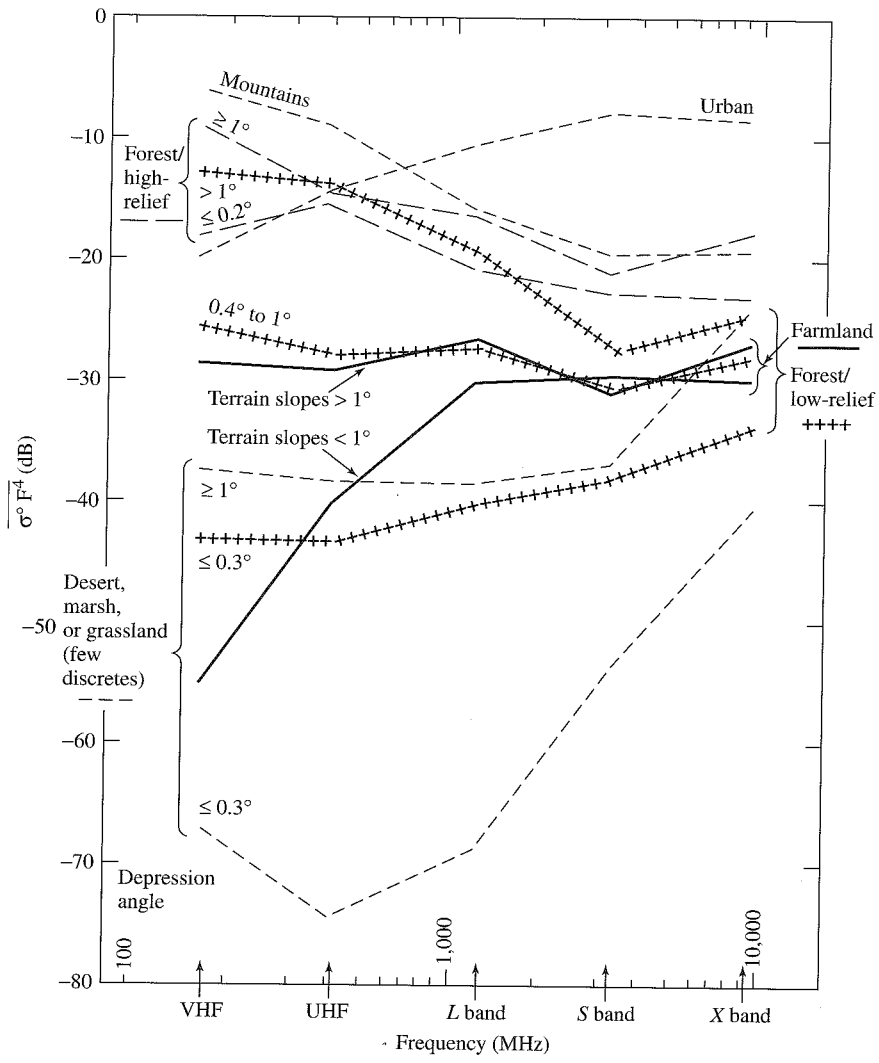

Figure 7.4 Mean clutter strength as a function of frequency for various terrain types.
(From J. B. Billingsley and J. F. Larrabee.[3] Reprinted with permission of MIT Lincoln Laboratory, Lexington, Massachusetts.)

averaging was done since the variations of the mean clutter echo with both polarization and resolution were small, generally about 1 or 2 dB.

Figure 7.5 shows the mean value of rural clutter strength (no urban areas are included) as a function of frequency, measured over 36 sites. The mean values are almost independent of frequency. The average of the means is 29.2 dB, and all five values lie within 1.7 dB of this value. The standard deviation is indicated by the vertical bars, and the extreme horizontal bars in the figure represent the extremes of the measurements at each frequency. The values in Fig. 7.5 are *before* terrain classification. The corresponding one-sigma patch-to-patch variation in mean clutter strength by frequency band *after* terrain classification is 3.9, 3.8, 2.9, 2.7, and 2.3 dB at VHF, UHF, *L*, *S*, and *X* bands,

Table 7.1 Median value of mean land clutter strength over many measurements* by terrain type and frequency

Terrain Type	Median Value of $\sigma^0 F^4$ (dB)				
	Frequency Band				
	VHF	UHF	*L* Band	*S* Band	*X* Band
URBAN	−20.9	−16.0	−12.6	−10.1	−10.8
MOUNTAINS	−7.6	−10.6	−17.5	−21.4	−21.6
FOREST/HIGH-RELIEF (Terrain Slopes > 2°)					
High depression angle (>1°)	−10.5	−16.1	−18.2	−23.6	−19.9
Low depression angle (≤0.2°)	−19.5	−16.8	−22.6	−24.6	−25.0
FOREST/LOW-RELIEF (Terrain slopes < 2°)					
High depression angle (>1°)	−14.2	−15.7	−20.8	−29.3	−26.5
Intermediate depression angle (0.4° to 1°)	−26.2	−29.2	−28.6	−32.1	−29.7
Low depression angle (≤0.3°)	−43.6	−44.1	−41.4	−38.9	−35.4
AGRICULTURAL/HIGH-RELIEF (Terrain Slopes > 2°)	−32.4	−27.3	−26.9	−34.8	−28.8
AGRICULTURAL/LOW-RELIEF					
Moderately low-relief (1° < terrain slopes < 2°)	−27.5	−30.9	−28.1	−32.5	−28.4
Very low-relief (terrain slopes < 1°)	−56.0	−41.1	−31.6	−30.9	−31.5
DESERT, MARSH, OR GRASSLAND (Few discretes)					
High depression angle (≥1°)	−38.2	−39.4	−39.6	−37.9	−25.6
Low depression angle (≤0.3°)	−66.8	−74.0	−68.6	−54.4	−42.0

*Medianized (central) values within groups of like-classified measurements in a given frequency band, including both *V*- and *H*-polarizations and high (15 or 36 m) and low (150 m) range resolution.

respectively. If the terrain can be separated by class (as it is in Fig. 7.4 and Table 7.1), the variability in all bands is substantially reduced.

Some of the other findings of this comprehensive measurement program were:

- Most of the significant land clutter echoes at low angles come from spatially localized or discrete vertical features associated with the high regions of the visible landscape (such as trees, tree lines, buildings, fences, or high points of the terrain). Low regions of terrain are shadowed at low grazing angles so that the clutter is spatially patchy. Clutter occurs "within kilometer-sized macroregions of general geometric visibility, each containing hundreds or thousands of spatial resolution cells." Groups of cells that produce a strong return are often separated by cells with weak echoes or just receiver noise. (The patchiness of the clutter is what gives rise at low grazing angles to interclutter visibility, Sec. 7.8).

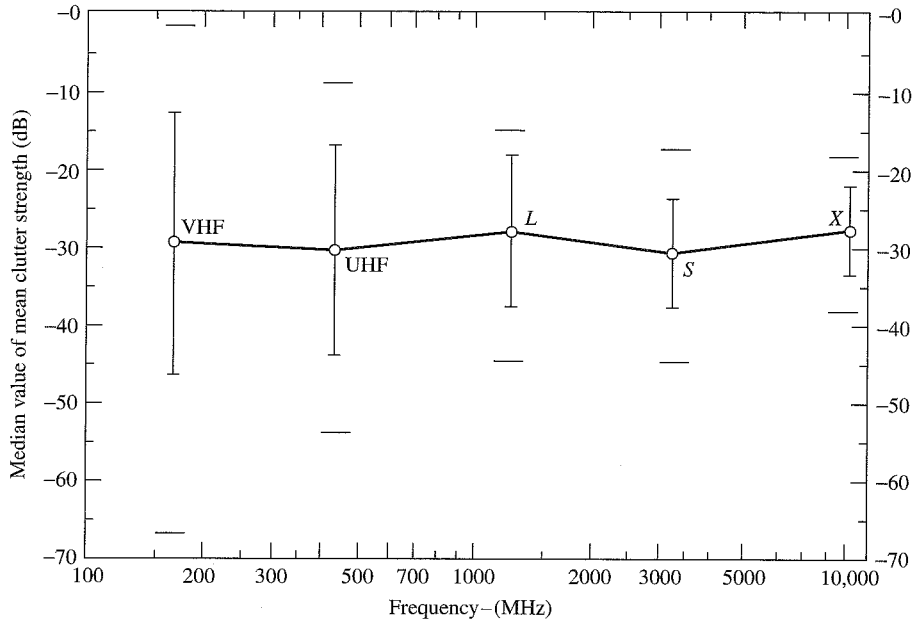

Figure 7.5 General dependence at low depression angles of the mean value of land clutter (circles), standard deviation (vertical lines), and the extreme measured values (horizontal bars) as a function of frequency at 36 rural sites.
(After J. B. Billingsley and J. F. Larrabee.[3])

- Over the range of depression angles employed in these measurements, the mean clutter strengths increase and the cell-to-cell fluctuations decrease with increasing angle. This is attributed to the reduction in masking with increasing angle. At the lower angles where masking occurs, the statistics can be represented by the Weibull probability density function. At depression angles of 6 to 8°, clutter is no longer spiky and is represented by the Rayleigh probability density.
- The difference between vertical and horizontal polarization is small, typically about 1 or 2 dB. The median difference between polarizations over all frequencies is 1.5 dB and the standard deviation is 2.8 dB, with little apparent dependence on frequency. (An exception is at VHF in steep mountainous terrain where the measurements show that the mean clutter strength is 7 to 8 dB greater with vertical polarization than with horizontal.) There was also little apparent dependence of the polarization on the range resolutions that were used. Even though the nominal calibration accuracy is 2 dB over all sites, the authors of reference 3 "accept the conclusion that, on average, the mean ground clutter strength is often 2 dB or so stronger at vertical polarization than at horizontal." They suggest that this may be due to the vertical orientation of many discrete clutter scatterers.
- The variation of clutter echo due to weather or season was found to be small, usually less than 1.5 dB for weather and 3 dB for changes in season. This was believed to be related to low-angle clutter being dominated by discrete scatterers.

- The effect of vertical discrete objects on the overall clutter strength is large even when they are relatively sparse. They contribute to clutter in a major way and are relatively unchanged with season. For example, the telephone lines, trees, and the fence around a wheat field are much more significant scatterers than the wheat itself. Even though the wheat field changes appearance with the seasons, it has little effect on the overall clutter strength. The echo from a tree line contributes strong clutter echoes no matter whether the trees are in leaf or bare, wet or dry.
- When a ground-based radar experiences strong clutter from visible terrain at ranges of 100 km or more, it is generally due to echoes from mountains that rise high enough to be within the line-of-sight of the radar. The echoes from mountains at long range are significantly greater when viewed with VHF than with microwave frequencies.
- Forests provide mean clutter echoes at VHF that are 10 to 15 dB stronger than at microwaves. This is attributed to the decreased loss at the lower frequencies when propagating radar energy through forests. Clutter from farmland, however, is 20 or 30 dB less at VHF than at microwaves since multipath (Sec. 8.2) is more of a factor with relatively flat, smooth surfaces. (Multipath, when it is present, reduces the energy at low angles.)
- Since forests tend to destroy the multipath, forest clutter echoes at high illumination angles are more likely to be the intrinsic value of σ^0 rather than $\sigma^0 F^4$.
- The median difference of the mean ground clutter strength between the low (150 m) and high resolutions (15 or 36 m) used in these measurements is less than 2 dB. Thus, on average, over many measurements, there is no significant difference expected between low and high range-resolution.
- Although the mean value of the clutter echo signal does not depend on resolution, the *variation* of the clutter echo amplitudes is a function of resolution. The smaller the resolution cell, the less the averaging within the cell and the greater is the variability from cell to cell. Reference 3 provides measurements of the ratio of the standard deviation to the mean, the skewness (third central moment), and kurtosis (fourth central moment) for the seven major terrain types at the five frequencies. Tables of the 50-, 70-, and 90-percentile levels are also given.
- Many past radar designs were based on only the mean value of the expected clutter. Different types of clutter, however, might have the same mean value, but quite different statistical variations. Figure. 7.6a is a histogram of the clutter for a particular region of forest at *X* band. Its mean is about the same as the histogram from farmlands shown in Fig. 7.6b. The distributions, however, are seen to be quite different. It should not be expected that the performance of a radar design based only on the mean value of clutter will be the same in these two regions. The mean-to-median ratio for forest in this case was 8 dB and for level farmland it was a very large value of 33 dB. The histograms for VHF over these same two sites are shown in Figs. 7.6c and d. The means are quite different in these two cases. The mean-to-median ratio was 4 dB for forest and 15 dB for farmland.
- The most likely day-to-day difference in the mean clutter strength was 0.2 dB, the average difference was about 1 dB, and the one-sigma range of variability beyond

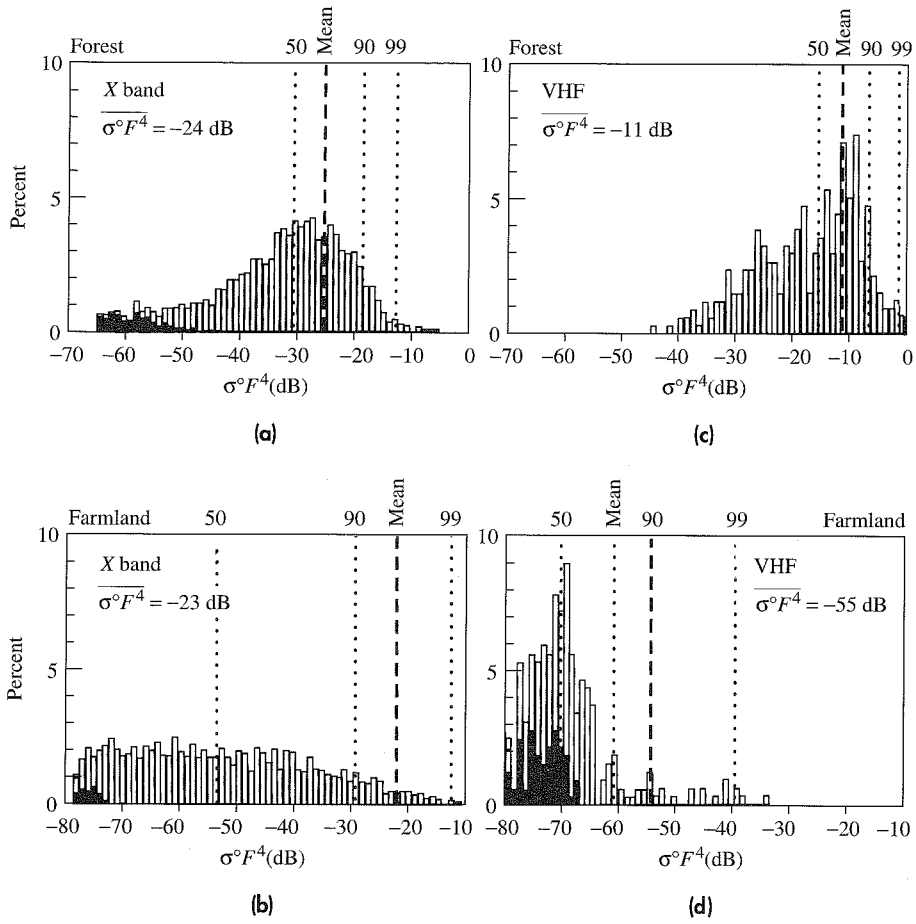

Figure 7.6 Examples of histograms of *X*-band land clutter at low depression angles in (a) a particular region of forest and (b) a particular level-farmland; both with the same approximate mean value of clutter strength, but with different statistical distributions. Histograms for the same terrain, but at VHF, are shown in (c) and (d). Black values are receiver noise.

(From J. B. Billingsley and J. F. Larrabee.[3] Reprinted with permission of MIT Lincoln Laboratory, Lexington, Massachusetts.)

the mean was 2.5 dB. Occasionally when the day-to-day difference was large (near 10 dB), it was attributed to measurement equipment malfunctions or singular events such as a train passing through the scene.

- It is said that land clutter's most salient attribute is its variability. This needs to be kept in mind when designing a radar to detect targets in clutter. The design should be conservative in order to provide reliable detection over a wide range of possible clutter values.

Figure 7.7 is an X-band PPI display of the clutter seen at Gull Lake West, in Manitoba, Canada, one of the sites measured by Lincoln Laboratory. The maximum range is 7 km, range resolution is 15 m, and the polarization is horizontal. Cells with $\sigma^0 F^4 \geq -40$ dB are shown in white. The area outlined in black lines in the northwest is a sector in which much of the data was recorded. This particular area is a forested wetland out to 3.5 km range, followed by a swampy open pond from 3.5 to 5 km, then to a higher sand dune along the shore of Lake Winnipeg between 5 and 6 km. Beyond that is the water of Lake Winnipeg. This PPI display illustrates that land clutter consists of many different kinds of textures and degrees of spatial correlation. It shows that clutter does not occur as "random salt and pepper."

The cumulative amplitude distributions of the X-band echo from rural low-relief and rural high-relief terrain are shown in Fig. 7.8 as a function of depression angle.[4] By low relief is meant slopes $<2°$ and variations in height <100 ft; and by high relief, slopes $>2°$ and variations in height >100 ft. At the higher depression angles, the slope of the distribution approaches that of the Rayleigh, which indicates that microshadowing of the clutter is small at higher angles.

Figure 7.9, derived from Billingsley,[4] shows the variation of the mean and median values for low- and high-relief rural land clutter. At the top of this figure are values of the Weibull skewness parameter, which is mentioned later in Sec. 7.5 and Eq. (7.18).

Further information about the Lincoln Laboratory ground-clutter measurements can be found in the detailed reports by Billingsley.[3–5]

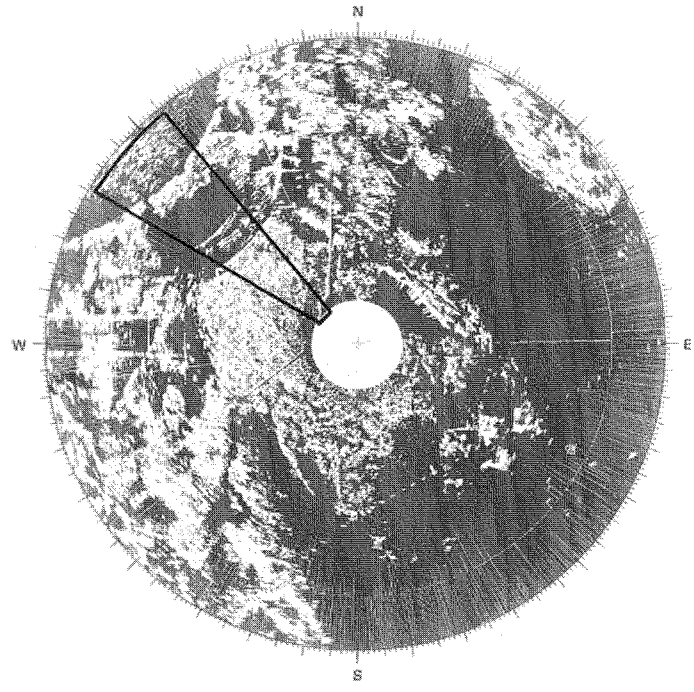

Figure 7.7 PPI clutter map at Gull Lake West, Manitoba, Canada. Cells with $\sigma^0 F^4 \geq -40$ dB are shown in white. (From J. B. Billingsley and J. F. Larrabee.[3] Reprinted with permission of MIT Lincoln Laboratory, Lexington, Massachusetts.)

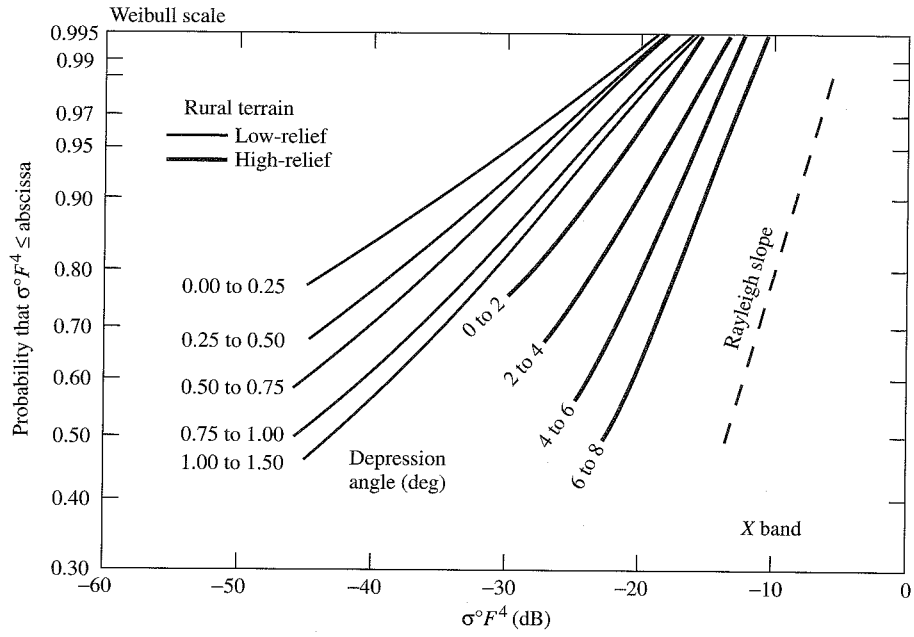

Figure 7.8 Cumulative amplitude probability distributions as a function of depression angle for X-band clutter from rural terrain of low and high relief. A straight line on this graph indicates Weibull clutter. The slope for a Rayleigh distribution (Weibull with $\alpha = 2$) is shown for comparison. (From J. B. Billingsley.[4] Reprinted with permission of MIT Lincoln Laboratory, Lexington, Massachusetts.)

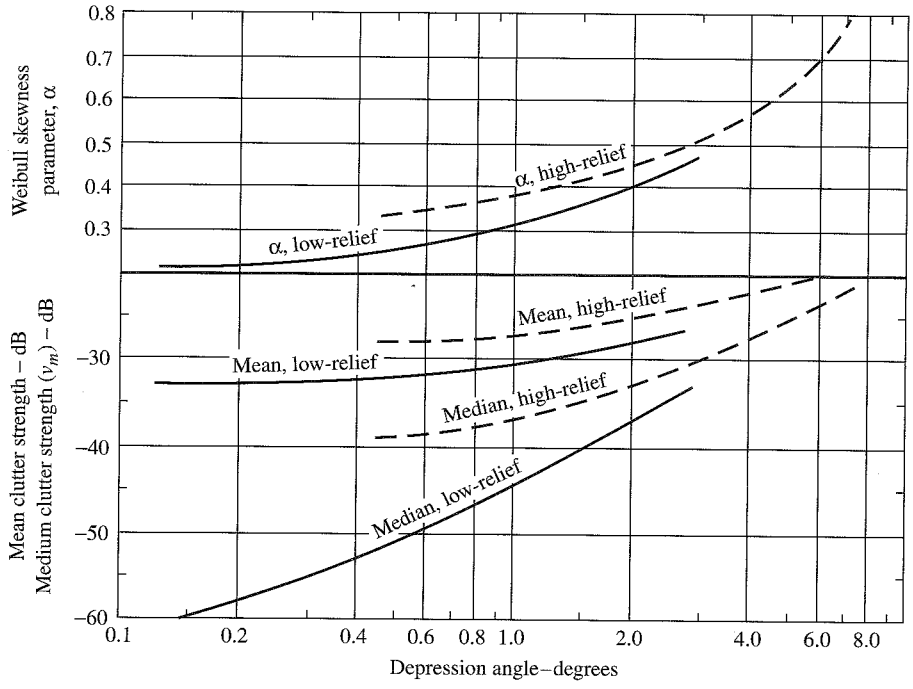

Figure 7.9 Mean and median values of low- and high-relief rural terrain as a function of depression angle. The upper curves give the Weibull skewness parameter. (After J. Billingsley.[4])

Land Clutter at Medium Grazing Angles There exist many measurements of land clutter at medium grazing angles, from a few degrees to about 70° (see, for example, references 2,6,9,10,12,15,17–19). Much of the information in this angle regime has been obtained from aircraft or spacecraft, where there is poor ground truth about the nature of the clutter being viewed by the radar. Radars mounted on portable "cherry pickers" also have been used to acquire data at medium grazing angles, especially by those interested in remote sensing. Ground truth is easier to obtain with this type of instrumentation since the radar is a short distance from the clutter and one can readily discern its nature. Radars mounted on cherry pickers, however, do not obtain the highly averaged values possible with airborne or spaceborne sensors.

An example of the average value of clutter that might be typical of North America in the summer is shown in Fig. 7.10. This figure was derived from data presented by Moore et al.[6] It represents a combination of measurements made by the Skylab S-193 scatterometer (at 13.9 GHz) and the University of Kansas "microwave-active-spectrometer system"* mounted on a cherry picker. The ground-based cherry-picker radars could operate from 1 to 18 GHz. The data from the cherry-picker radars were combined by Moore et al. by comparing the 13.8-GHz ground-based data with the 13.9-GHz Skylab measurements. The absolute level of the model was determined by the Skylab measurements, but the relationships among the other frequencies were set by the ground-based measurements. The curve in Fig. 7.10 for L band combines the horizontal and vertical polarizations, and represents an average over the two years for which measurements were reported. The X-band values at low grazing angles were taken from the means averaged over all terrain types, as presented by Billingsley.[4] The dashed portion of the curve is a bold interpolation.

Many experimental measurements of land clutter seem to indicate that the value of sigma zero at grazing angles from a few degrees to perhaps 70° is approximately

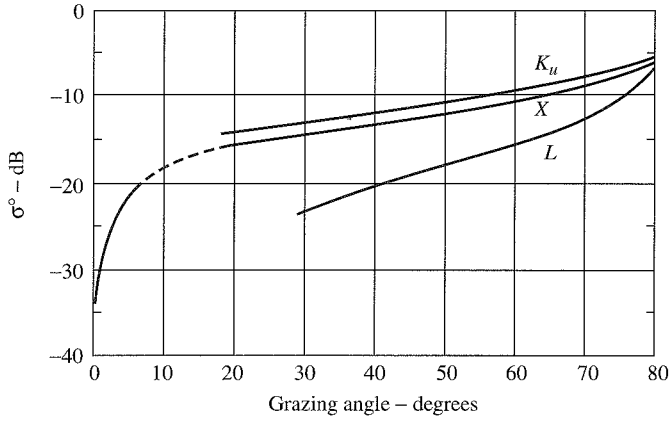

Figure 7.10 Clutter sigma zero that might be typical of North America in the summer.
(After Moore et al.[6] Courtesy of the IEEE. The X-band values at low angles are taken from Billingsley.[4])

*A radar by any other name is still a radar.

proportional to the sine of the grazing angle ψ. For this reason, land clutter is sometimes described by the parameter γ, defined as

$$\gamma = \frac{\sigma^0}{\sin \psi} \qquad [7.10]$$

The parameter γ is said to be almost independent of the grazing angle in this angular regime. (Note that a perfectly rough surface that reradiates in the direction of the source a power per unit solid angle independent of the direction of the incident energy will result in $\sigma^0 = 2 \sin \psi$.[7] Substituting in Eq. (7.10), γ in this case is 2, or 3 dB.) Nathanson[2] states that the maximum value of γ for grazing angles from 6 to 70°, all frequencies from 0.4 to 35 GHz, and for all polarizations is −3 dB. The median is −14 dB, and the minimum is −29 dB. In this oversimplification, these values are a maximum of various experiments rather than a peak value in time. Barton[8] adds that for rural terrain covered by crops, bushes, and trees, the value of γ lies between −10 and −15 dB, and that urban and mountain clutter might have a value of γ that approaches −5 dB. Billingsley's *X*-band data for all terrain types at depression angles from 1 to 8° can be approximated by $\gamma = -11$ dB.[4]

These values of γ are said to apply over a wide range of frequencies; but it is known that they are frequency dependent, as was indicated in Fig. 7.10. Nathanson suggests that since these values are based to large extent on *X*-band data, they might be considered as applicable for *X* band and that the frequency dependence can be represented by

$$\gamma = \gamma_{10} + 5 \log \left(\frac{f}{10} \right) \qquad [7.11]$$

where f is the frequency in GHz and γ_{10} is the value of γ at 10 GHz. For example, if $\gamma_{10} = -14$ dB at *X* band, γ will be −18.5 dB at *L* band. Equation (7.11) is shown by the dashed curve in Fig. 7.11.

The solid curves of Fig. 7.11 are derived from Table 7.16 of Ref 2. They plot the maximum value of γ for various terrains. These are an indication of the decibel average

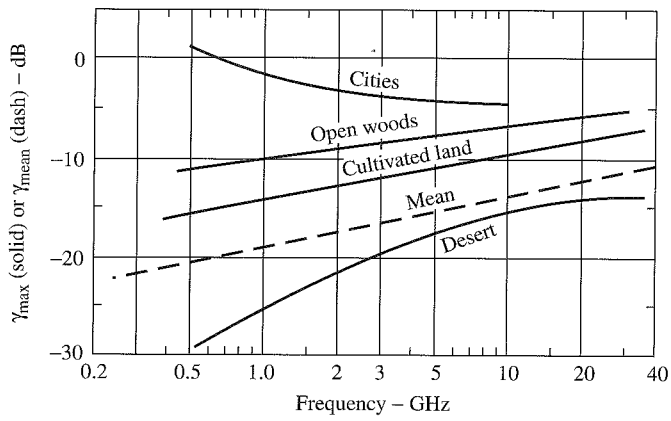

Figure 7.11 Dashed curve is the mean value of γ as given by Eq. (7.11) with $\gamma_{10} = -14$ dB at *X* band. The solid curves are the maximum values of γ as given by Table 2.16 of Ref. 2.

of the maximum values reported by various experimenters rather than an indication of the maximum expected return. (Because of the wide variation in the data, some liberties have been taken in smoothing the values from which Fig. 7.11 was derived.)

Land Clutter at High Grazing Angles (Near Vertical Incidence) The values of σ^0 can be large near vertical incidence. As mentioned previously, scattering in this regime is due to those facets (surfaces that are "flat" relative to a wavelength) that reflect incident energy back to the radar. The values of σ^0 near vertical incidence can also be affected by the antenna pattern and the antenna gain.

When determining the values of σ^0 at perpendicular incidence, the effect of the antenna pattern shape must be taken into account. Because of the finite antenna beamwidth, measured values of σ^0 at vertical incidence are sometimes lower than actual. This results from the averaging done over a finite beamwidth where the clutter echo is changing rapidly with angle. With a finite beamwidth antenna, the large value at the peak (90° grazing angle) is averaged with lower values at angles off normal so that the value obtained in this manner is less than it really is at 90°.

The antenna gain can influence, in some cases, the value of σ^0 near vertical incidence. Schooley[7] has shown that the value of σ^0 is $4/(\theta_{2B})^2$ at normal incidence (grazing angle = 90°) for an infinite perfectly smooth reflecting surface when the antenna is a pencil beam of two-way beamwidth θ_{2B}. The one-way beamwidth $\theta_B = \sqrt{2}\ \theta_{2B}$. Since the maximum gain G of an antenna is approximately equal to $\pi^2/(\theta_B)^2$, the value of sigma zero in this case is

$$\sigma^0 = \frac{8}{\theta_B^2} = \frac{8G}{\pi^2} \approx G \qquad [7.12]$$

Thus the antenna gain G can have a significant effect on the value of σ^0 at normal incidence and in the vicinity of normal incidence for a perfectly smooth surface. This probably applies, however, more to a perfectly smooth sea than to land. Over a perfectly flat earth with a reflection coefficient less than unity, the value of σ^0 will be reduced by the (power) reflection coefficient. If the surface is slightly rough (roughness small compared to a wavelength), the value of σ^0 will also be reduced similar to that for an antenna with errors in the aperture distribution.

Examples of the values of σ^0 near vertical incidence may be found in Chapter 12, Ground Echo, in the *Radar Handbook.*[9]

The value of σ^0 at normal incidence is generally larger than unity. That is, the radar cross section is greater than the area of the radar resolution cell.

Other Land Clutter Topics Other subjects of interest in the radar scattering from land are briefly summarized below.

Discrete Echoes Buildings and other constructed objects can result in large echoes, known as *discretes* or *point clutter.* They can range from 10^4 to 10^5 m^2 at *S* band.[10] They can be even larger at the lower frequencies. W. H. Long et al.[11] state that at the higher radar frequencies (assumed to be *S* band or above) discrete clutter echoes of 10^4 m^2 cross section might have a density of 1 per mi^2; 10^5 m^2 discretes, a density of 0.1 per mi^2; and

10^6 m^2 discretes, only 0.01 per mi^2. It takes a good MTI radar to eliminate large discrete echoes. Other techniques (such as blanking based on a clutter map) might be used to reduce the effects of discrete echoes when the MTI cannot eliminate them.

Snow The effect of snow covering the ground depends on its thickness, water content, and frequency. Dry snow (no liquid water) has a dielectric constant ranging from 1.4 to 2, so that significant transmission of energy can take place across the air-snow boundary over a wide range of angles.[12] Dry snow is of low loss so that radar energy is not highly attenuated when propagating through the snow. The ground beneath the snow, therefore, can have a major effect on σ^0, especially at low frequencies and shallow snow cover where the attenuation is quite low. It was found, for example, that 15 cm of dry powder-like snow had no effect on the measured backscatter over the frequency range from 1 to 8 GHz.[13] Any backscatter from snow under these conditions was completely dominated by the contribution from the underlying surface. With 12 cm of wet snow, however, σ^0 decreased approximately 5 to 10 dB at grazing angles between 30 and 80°.

The attenuation in propagating through snow depends on the amount of water in the snow. When the sun shines, it melts the snow and produces water, which increases attenuation. At night this water freezes. Thus there can be large variations in radar scattering, depending on whether it is night or day.[6] For example, it was reported that in the morning as the snow began to melt and produce water, the radar return decreased as much as 10 dB within half an hour (at the higher microwave frequencies, 40° grazing angle, and 48 cm snow depth). Figure 7.12 shows the effect of dry and wet snow as a function of frequency at a grazing angle of 40°.[14] At *L* band, the snow is essentially transparent and the echo is primarily from the underlying ground. At the upper end of the microwave frequency spectrum, at K_a band, the snow is likely to have a dominant effect on the backscatter.

Other examples of radar measurements of snow can be found in *Microwave Remote Sensing*, vol III.[15]

Snow and Altimeters The effect of snow (or ice) over the ground is dramatically illustrated by the problem it can introduce in some radar altimeters. Serious, life-threatening

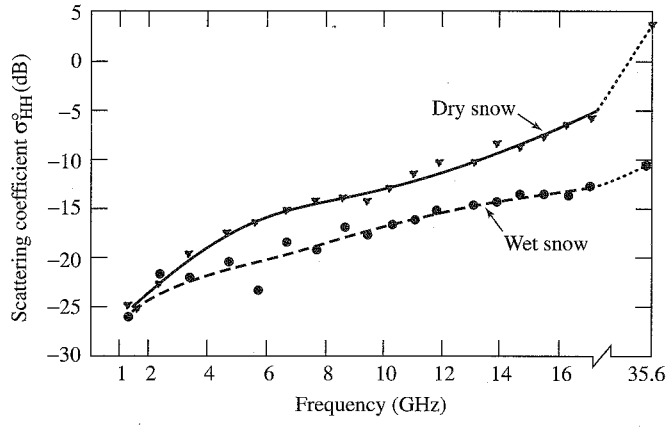

Figure 7.12 Effect of wet and dry snow as a function of frequency for a grazing angle of 40°.
(Reprinted from Ulaby and Stiles, Ref. 14, Copyright 1981, with permission from Elsevier Science.)

errors in the measurement of the aircraft altitude can result, especially at UHF or lower frequencies where the propagation loss in snow is low.[16] In some cases, the echo from the air-snow interface can be so small that it might be missed and the altitude measurement is falsely determined by the reflection from the ground underneath the snow. To make matters worse, the dielectric constant of snow compared to air results in a greater altitude measurement for a given time delay if the velocity of propagation in air rather than snow is assumed. (The velocity of propagation in snow is about 0.8 that in air; in ice it is 0.55 times that in air.) It can result in a pilot being misled as to the altitude of the aircraft above the snow and might crash into the snow, thinking that the plane's altitude was safely above the surface. This can be a serious problem with UHF altimeters when flying over a region such as the Greenland ice cap. Altimeters are now operated at the higher microwave frequencies (4.2–4.4 GHz) where the propagation loss is higher than that at UHF so that altimeter measurements are more likely to indicate the distance to the air-snow interface rather than to the ground beneath the snow.

Remote Sensing Much information on land backscatter reported in the literature has been obtained for purposes of developing radar for the remote sensing of the environment. The goal of the remote sensing radar designer is different from that of other radar designers. In remote sensing the interest is in acquiring information about the environment (such as soil moisture or crop census) while other radar engineers are interested in detecting targets in unwanted clutter. The data of interest to the remote sensing designer, therefore, might not always be useful to the radar designer, and vice versa. Examples of the backscatter from land obtained mainly for purposes of remote sensing design are given by Ulaby and Dobson[17] as well as in a computer database at the University of Massachusetts.[18]

Variability of Land Clutter As mentioned earlier in this chapter, the chief characteristic of clutter is its variability. There is seldom precise agreement among similar data taken by different investigators. Long[19] points out that "two flights over apparently the same type of terrain may at times differ by as much as 10 dB in σ^0." Another analysis of the problem of the variability of the value of σ^0 from eleven sets of measurements of agricultural crops under "similar" conditions and for approximately the same radar parameters (frequency, polarization, and grazing angle) found maximum differences of approximately 17 dB.[20] Some of these differences are due to the absence of good ground truth (that is, the measurements are not from similar terrain), accurate system calibration, or a lack of accurate data processing (including accounting for the effect of range variation of clutter as well as the effect of the antenna pattern shape). The variation and uncertainty in the value of land clutter is something the radar designer has learned to accept and compensate for by conservative system design.

Theory of Land Clutter There have been many attempts to describe scattering from land using empirical models; but these attempts have not been completely successful. In principle, if the shape and the dielectric properties of the scattering surface are known, Maxwell's equations can be solved numerically. In practice, however, the land features that cause scattering are generally too complex to describe simply.

Radar and Land Clutter Information about radar backscatter from land is required for several diverse applications, each with its own special needs that differ from the others. These applications include:

- *Detection of aircraft over land.* Clutter echoes might be 50 to 60 dB, or more, greater than aircraft echoes. MTI or pulse doppler radar (Chap. 3) is commonly used for this application to remove the large unwanted clutter.
- *Detection of moving surface-targets over land.* Vehicles or personnel can be separated from clutter by means of properly designed doppler processing radar.
- *Altimeters.* A large echo from the ground or the sea is desired for the measurement of the height of an aircraft or spacecraft since "clutter" is the target. The altimeter has also been used in "map matching" for missile guidance, as well as for remote sensing.
- *Detection and height measurement of terrain features.* This provides warning to an aircraft that it is approaching high ground so that the aircraft can fly around it (terrain avoidance) or follow the contour of the land (terrain following).
- *Mapping, or imaging, radars.* These utilize high resolution to recognize ground objects by their shape and by contrast with their surroundings. Such radars might be used by the military for navigation or target recognition. The synthetic aperture radar (SAR), sidelooking airborne radar (SLAR), and military air-to-surface radar are examples.
- *Remote sensing.* Imaging radars (such as SAR), altimeters, and scatterometers (a radar that measures sigma zero as a function of elevation angle) are used to obtain specific information about the characteristics of the earth's surface.

7.4 SEA CLUTTER

The radar echo from the sea when viewed at low grazing angles is generally smaller than the echo from land. It usually does not extend as far in range as land clutter and is more uniform over the oceans of the worlds than typical land clutter. It has been difficult, however, to establish reliable quantitative relationships between sea echo measurements and the environmental factors that determine the sea conditions. Another difficulty in dealing with sea echo is that the surface of the sea continually changes with time. Nevertheless, there does exist a large body of information regarding the radar echo from the sea that can be used for radar design and provide a general understanding of its effect on radar performance.

The nature of the radar echo (clutter) from the sea depends upon the shape of the sea surface. Echoes are obtained from those parts of the sea whose scale sizes (roughness) are comparable in dimension to the radar wavelength. The shape, or roughness, of the sea depends on the wind. Sea clutter also depends on the pointing direction of the radar antenna beam relative to the direction of the wind. Sea clutter can be affected by

contaminants that change the water surface-tension. The temperature of the water relative to that of the air is also thought to have an effect on sea clutter.

The *sea* generally consists of waves that result from the action of the wind blowing on the water surface. Such waves, called *wind waves,* cause a random-appearing ocean-height profile. *Swell waves* occur when wind waves move out of the region where they were originally excited by the wind or when the wind ceases to blow. Swell waves are less random and sometimes appear to be somewhat sinusoidal. They can travel great distances (sometimes thousands of miles) from the place where they originated. The echoes from an *X*-band radar viewing swell at low grazing angles will be small if there is no wind blowing, even if the swell waves are large. If a wind occurs, the surface will roughen and radar echoes will appear.

Sea state is a term used by mariners as a measure of wave height, as shown in Table 7.2. The sea state description shown in this table is that of the World Meteorological Organization. Sea state conditions can also be described by the Douglas scale, the Hydrographic Office scale, and the Beaufort scale. The Beaufort is actually a wind-speed scale.[21] Each gives slightly different values, so when a sea state is mentioned one should check which scale is being used.

Although sea state is commonly used to describe the roughness of the sea, it is not a complete indicator of the strength of sea clutter. Wind speed is often considered a better measure of sea clutter, but it is also limited since the effect of the wind on the sea depends on how long a time it has been blowing (called the *duration*) and over how great a distance (called the *fetch*). Once the wind starts to blow, the sea takes a finite time to grow and reach equilibrium conditions. When equilibrium is reached it is known as a *fully developed sea.* For example, a wind speed of 10 kt with a duration of 2.4 h and a fetch of at least 10 nmi produces a fully developed sea with a significant wave height (average height of the one-third highest waves) of 1.4 ft.[22] It corresponds to sea state 2. A 20 kt

Table 7.2 World Meteorological Organization sea state

	Wave Height		
Sea State	**Feet**	**Meters**	**Descriptive Term**
0	0	0	Calm, glassy
1	0–$\frac{1}{3}$	0–0.1	Calm, rippled
2	$\frac{1}{3}$–1$\frac{2}{3}$	0.1–0.5	Smooth, wavelets
3	2–4	0.6–1.2	Slight
4	4–8	1.2–2.4	Moderate
5	8–13	2.4–4.0	Rough
6	13–20	4.0–6.0	Very rough
7	20–30	6.0–9.0	High
8	30–45	9.0–14	Very high
9	over 45	over 14	Phenomenal

wind blowing for 10 h over a fetch of 75 nmi results in a significant wave height of about 8 ft and corresponds to sea state 4.

Average Value of σ^0 as a Function of Grazing Angle A composite of sea clutter data from many sources is shown in Fig. 7.13. This figure was derived from data for winds varying from approximately 10 to 20 kt, and can be considered representative of sea state 3. (Sea state 3 is roughly the medium value of sea state; i.e., about half the time over the oceans of the world, the sea state is 3 or less.) It is believed that Fig. 7.13 is representative of the average behavior of sea clutter, but there is more uncertainty in the data than is indicated by the thin lines with which the curves were drawn.

The curves of Fig. 7.13 provide the following conclusions for sea clutter with winds from 10 to 20 kt:

- At high grazing angles, above about 45°, sea clutter is independent of polarization and frequency.
- Sea clutter with vertical polarization is larger than with horizontal polarization. (At higher wind speeds the differences between the two polarizations might be less.)
- Sea clutter with vertical polarization is approximately independent of frequency. (This seems to hold at low grazing angles even down to frequencies in the HF band.)
- At low grazing angles, sea clutter with horizontal polarization decreases with decreasing frequency. This is apparently due to the interference effect at low angles between the direct radar signal and the multipath signal reflected from the sea surface.

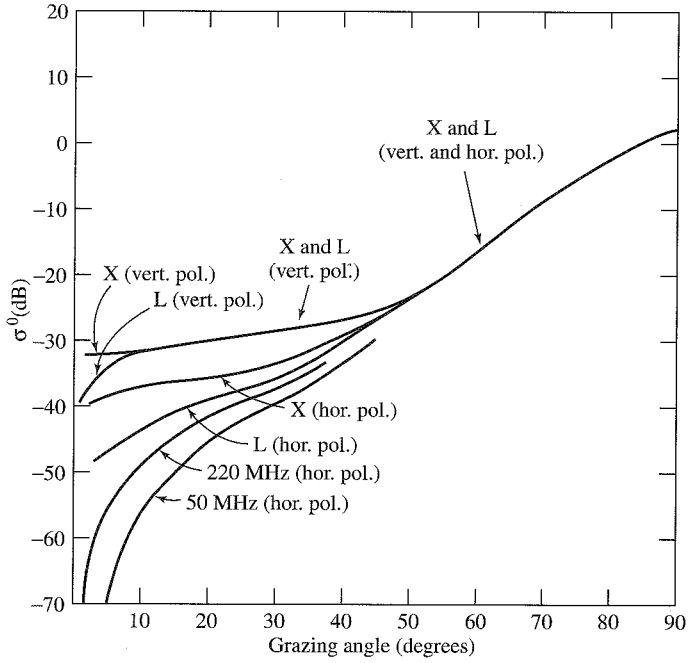

Figure 7.13 Composite of averaged sea clutter σ^0 data from various sources for wind speeds ranging from 10 to 20 kt.

There is no simple law that describes the frequency dependence of sea clutter with horizontal polarization.

Effect of Wind The wind is the most important environmental factor that determines the magnitude of the sea clutter. At low grazing angles and at microwave frequencies, backscatter from the sea is quite low when the wind speed is less than about 5 kt. It increases rapidly with increasing wind from about 5 to 20 kt, and increases more slowly at higher wind speeds. At very high winds, the increase is small with increasing wind.

Figure 7.14 was derived from experimental data of John Daley et al. using the Naval Research Laboratory Four-Frequency Airborne Radar.[23–25] As mentioned, sea clutter at the higher microwave frequencies and low grazing angles increases with increasing wind speed, but begins to level off at winds of about 15 to 25 kt. When viewed at vertical incidence (grazing angle of 90°) and with zero or low wind speed, the sea surface is flat and a large echo is directed back to the radar. As the wind speed increases and the sea surface roughens, some of the incident radar energy is scattered in directions other than back to the radar, so that σ^0 will decrease. According to Daley et al., the value of σ^0 at vertical incidence in Fig. 7.14 can be represented by $25\ w^{-0.6}$, where w is the wind speed in knots.

At low grazing angles, less than about one degree, it is difficult to provide a quantitative measure of the effect of the wind on sea clutter. This is due to the many factors that influence σ^0 at low angles, such as shadowing of parts of the sea by waves, multipath interference, diffraction, surface traveling (electromagnetic) waves, and ducted propagation.

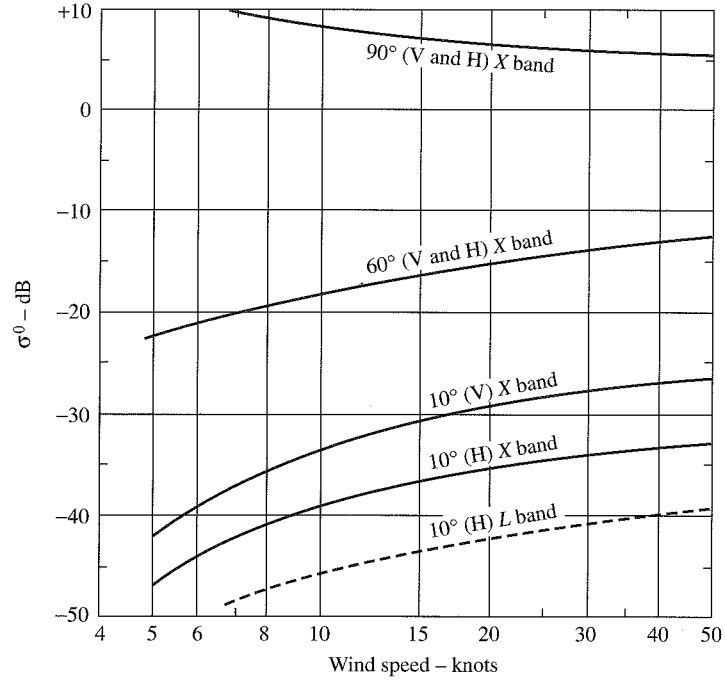

Figure 7.14 Effect of wind speed on sea clutter at several grazing angles. Radar looking upwind. Solid curves apply to *X* band, dashed curve applies to *L* band. (After J. C. Daley, et al.[23–25])

Another factor affecting the ability to obtain reproducible measurements of sea clutter is that a finite time and a finite fetch are required for the sea to become fully developed. Unfortunately, few measurements of sea clutter mention the fetch and duration of the wind.

Sea clutter is largest when the radar looks into the wind (upwind), smallest when looking with the wind (downwind), and intermediate when looking perpendicular to the wind (crosswind). There might be as much as 5 to 10 dB variation in σ^0 as the antenna rotates 360° in azimuth.[26] Backscatter is more sensitive to wind direction at the higher frequencies than at lower frequencies; horizontal polarization is more sensitive to wind direction than vertical polarization; the ratio of σ^0 measured upwind to that measured downwind decreases with increasing grazing angle and sea state; and at UHF the backscatter is practically insensitive to wind direction at grazing angles greater than 10°.

The orthogonal component of polarization from sea clutter (cross polarization response) at grazing angles from 5 to 60° appears to be about 5 to 15 dB less than the echo from the same polarization (co-pol) as transmitted.[25]

Sea Clutter with High-Resolution Radar (Sea Spikes) The use of a clutter density, σ^0 (clutter cross section per unit area), to describe sea clutter implies that the clutter echo is independent of the illuminated area. When sea clutter is viewed by a high-resolution radar, especially at the higher microwave frequencies (such as X band), sea clutter is not uniform and cannot be characterized by σ^0 alone. High-resolution sea clutter is spiky. The individual echoes seen with high-resolution radar are called *sea spikes.* They are sporadic and have durations of the order of seconds. They are nonstationary in time, spatially nonhomogeneous, and have a probability density function that is non-Rayleigh. Sea spikes are important since they are the major cause of sea clutter at the higher microwave frequencies at low grazing angles, with any radar resolution.

Fig. 7.15 is an example of the time history of sea spikes in sea state 3 for pulse widths varying from 400 to 40 ns and with vertical polarization.[27,28] With 40-ns pulse width (6-m range resolution), Fig. 7.15 shows that the time between sea spikes can be several tens of seconds and the duration of each spike is of the order of one or a few seconds. As the pulse width is increased, more sea spikes appear within the larger resolution cell of the radar and the time between spikes decreases. The peak radar cross section of sea spikes in this example is almost 10 m^2. (At times they have been observed to be of even higher cross section.) The relatively large cross section and time duration of sea spikes can result in their being mistaken for small radar targets. This is a major problem with sea spikes; they can cause false alarms when a conventional detector based on gaussian receiver noise is used.

Under calm conditions, sea state 1 or less, the echo signals still have the same spiky appearance as in Fig. 7.15, but are as much as 40 dB lower in cross section. A time history similar to that of Fig. 7.15, but for horizontal polarization, would show that sea spikes with this polarization occur slightly less frequently and are sharper (of briefer duration) than with vertical polarization.

Based on airborne radar measurements made at L, S, and X bands with pulse widths ranging from 0.5 to 5 μs, clutter is more spiky when the radar looks upwind or downwind rather than crosswind and with low rather than high grazing angles.[29]

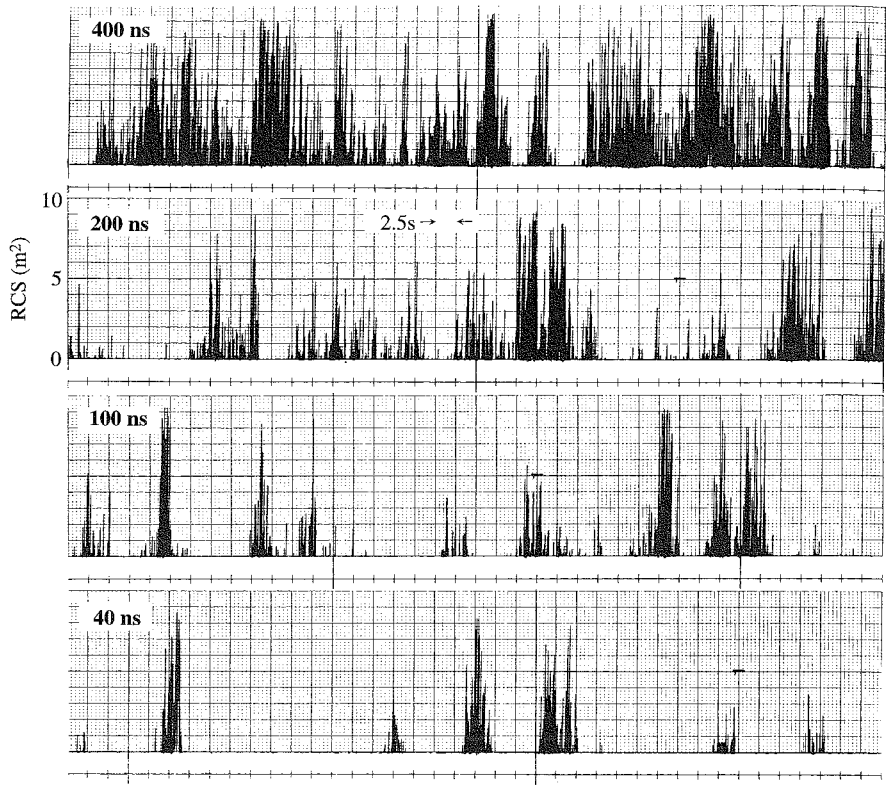

Figure 7.15 Amplitude as a function of time at a fixed range-resolution cell for low grazing angle *X*-band (9.2 GHz) sea clutter obtained off Boca Raton, Florida, with pulse widths ranging from 400 ns to 40 ns in a windblown sea with many white caps (sea state 3). Cross-range resolution is approximately 9 m, grazing angle of 1.4°, and vertical polarization.
(From J. P. Hansen and V. F. Cavaleri.[27])

Sea spikes are evident when the radar resolution is less than the water wavelength. The physical size of sea spikes usually is less than the resolution of the radar which observes them, and it is said they appear to move at approximately the surface wave velocity.[30] Sea spikes obviously are present with low as well as high resolution. At low resolution, the sum of many individual sea spikes within the resolution cell produces an almost continuous noiselike echo. At the lower frequencies where the radar wavelength is large compared to the sea-surface features that give rise to sea spikes, it would be expected that the backscatter is no longer characterized by sea spikes.

Another characteristic of sea spikes is a relatively rapid and high-percentage pulse-to-pulse amplitude modulation. According to Hansen and Cavaleri,[27] measured modulation frequencies at *X* band vary from 20 to 500 Hz. The modulating frequency seems to be affected by the type of physical surface (breaking water, sharp wave crests, ripples, etc.), the relative wind speed and direction, and polarization of the radar. The

characteristic amplitude modulations can be used for recognizing and rejecting sea spike echoes from true target echoes.[31]

In addition to changes in clutter characteristics with narrow pulse widths, as illustrated in Fig. 7.15, similar effects have been noted with narrow antenna beamwidths.[32] In some cases, target detection in clutter can actually be enhanced when a smaller antenna with a lower resolution is used rather than one with a high resolution that is bothered by sea spikes.[32] On the other hand, with very high resolution, targets can be seen in the clear regions between the sea spikes, so that subclutter visibility in the traditional sense might not be required.

Origin of Sea Spikes Sea spikes are associated with breaking waves or waves about to break. Visible whitecaps are also associated with breaking waves, but whitecaps themselves do not appear to be the cause of sea spikes since whitecaps are mainly foam with entrapped air (which does not result in significant backscatter). It has been reported[33] that about 50 percent of the time the whitecap is seen visually either simultaneously or a fraction of a second later than the appearance of a sea spike on the radar display. About 35 to 40 percent of the time a spike is observed when the waves have a very peaked crest, but with no whitecap developed. A sea spike echo can appear without the presence of a whitecap, but no whitecap is seen in the absence of a radar observation of a spike. Thus it can be concluded that the whitecap is not the cause of the sea spike echo.

Wetzel[34] has offered an explanation for the origin of sea spikes based on the entraining plume model of a spilling breaker.[35] In this model "a turbulent plume emerges from the unstable wave crest and accelerates down the forward face of the breaking wave, entraining air as it goes." Wetzel further assumes "that the breaking 'event' involves a cascade of discrete plumes emitted along the wave crest at closely spaced times." Based on this model and some assumptions about the characteristics of the plume, Wetzel was able to account for the peak radar cross section, frequency dependence, the spikier nature of horizontal polarization, similarity of the appearance of sea spikes with both horizontal and vertical polarizations at very low grazing angles, appearance of the characteristic modulation, and other properties. He has pointed out that this model is based on a simplistic hypothesis that requires further elaboration. It does not account, however, for the scattering when the radar views the sea downwind and it does not adequately explain the internal amplitude modulations of the sea spikes.

Detection of Signals in High-Resolution Sea Clutter The nature of sea spikes as seen by high-resolution radar results in a probability density function (pdf) that is not Rayleigh. Therefore, conventional methods for detection of signals in gaussian noise do not apply. (A Rayleigh pdf for clutter power is equivalent to a gaussian pdf for receiver noise voltage.) Non-Rayleigh pdfs have "high tails"; that is, there is a higher probability of obtaining a large value of clutter than when it is Rayleigh. A receiver detector designed as in Chap. 2 on the basis of gaussian noise, or Rayleigh clutter, will result in a high false-alarm rate when confronted with sea spikes. The statistics of non-Rayleigh sea clutter are not easily quantified and can vary with resolution and sea state. Thus conventional receiver detector-design based on the assumption of gaussian noise cannot be applied. To avoid excessive false alarms with non-Rayleigh sea clutter, the detection-decision

threshold might have to be increased (perhaps 20 to 30 dB). The high thresholds necessary to avoid false alarms reduce the probability of detecting desired targets. When sea spikes are a concern, detection criteria other than those based on gaussian or Rayleigh statistics must be used if a severe penalty in detection capability is to be avoided.

One method for dealing with a sea spike is to recognize its characteristic amplitude modulations and delete the sea spike from the receiver.[31] Another method is to employ a receiver with a log-log output-input characteristic whose function is to provide greater suppression of the higher values of clutter than a conventional logarithmic receiver. In a log-log receiver, the logarithmic characteristic progressively declines faster than the usual logarithmic response by a factor of 2 to 1 over the range from noise level to +80 dB above noise.[36]

Conventional pulse-to-pulse integration does not improve the detection of targets in spiky clutter because of the long correlation time of sea spikes. However, a high antenna scan rate (several hundred rpm) allows independent observations of the clutter to be made, so that scan-to-scan integration can be performed.[37] Similarly, if the target is viewed over a long period of time before a detection decision is made, the target can be recognized by its being continuously present on the display while sea spikes come and go. One method for achieving this is *time compression,* as mentioned later in Sec. 7.8.

The effect of sea spikes is less important for radars that are to detect ships since ship cross sections are large compared to the cross sections of sea spikes. Sea spikes might interfere, however, with the detection of small targets such as buoys, swimmers, submarine periscopes, debris, and small boats. With ultrahigh resolution (ultrawideband radar) where the range resolution might be of the order of centimeters, sea spikes are relatively sparse in both time and space so that it should be possible to see physically small targets when they are located in between the spiky clutter.

Sea Clutter at Very Low Grazing Angles[38] Clutter at very low grazing angles differs from that at higher angles because of shadowing, ducted propagation (Sec. 8.5), and the changing angle at which the radar ray strikes the fluctuating sea surface.

The surface of the sea is seldom perfectly flat. It usually has a time-varying angle with respect to the radar. A grazing angle might be defined with respect to the horizontal, but it is difficult to determine the angle made with respect to the dynamic sea surface. Refraction by the atmosphere can also change the angle the radar ray makes with the surface.

Shadowing of wave troughs by wave crests can occur. Scatterers as seen by the radar are thought to be mainly those from the crests, especially for horizontal polarization. Attempts to compute the effect of shadowing by simple geometrical considerations (to determine how much of the sea surface is masked) have not proven successful. One reason for failure of geometrical shadowing is that scattering features (such as sloshes, plumes, and other effects of breaking waves) are not uniformly distributed and are more likely to be near the crests of the waves. Diffraction effects can occur which complicate shadowing calculations. Thus the effect of shadowing is more complicated than just simple masking.[38,39]

Another factor to consider when searching for a theoretical understanding of sea spikes (and microwave sea clutter in general) is the effect of a surface traveling radar wave that

is launched when the incident wave has a component of electric field in the plane of incidence.[40] The effect was mentioned in Sec. 2.7 and shown in Fig. 2.10 for scattering from a long thin road. The surface traveling wave and its reflection from a discontinuity can be a reason why microwave sea clutter seen with vertical polarization usually is larger than sea clutter seen with horizontal polarization.

At very low grazing angles (less than about one degree), sea clutter should decrease rapidly with decreasing grazing angle, especially for horizontal polarization. Figure 7.3, which is a generic plot of clutter echo strength as a function of grazing angle, attempts to show this behavior. The decrease of clutter at low angles results from the cancellation of the direct and surface scattered waves as illustrated in the ideal representation given in Sec. 8.2. Measurements[41] have demonstrated this rapid decrease in sea clutter below some *critical angle* (the angle at which clutter changes from a R^{-3} dependence at short range to an R^{-7} at longer range and low grazing angle, where R = range). Not all low-angle sea clutter measurements, however, show this effect. For example, the curve for X-band sea clutter in Fig. 7.13 does not show the presence of a critical angle below which the clutter decreases rapidly.

One reason for the lack of a critical angle in some cases is that at very low grazing angles ducted propagation can occur.[42] Erroneous measurements of σ^0 can be made unless propagation effects are separated from sea-surface scattering. This requires that ducting propagation be accounted for using the proper propagation models.[43] The commonly encountered evaporation duct, which occurs a large portion of the time over most of the oceans of the world, probably is the dominant factor that gives rise to larger values of sea clutter than expected with normal (nonducting) refractive conditions.

It is difficult to obtain reliable empirical information on sea clutter at very low grazing angles that is correlated with environmental conditions. It is also difficult to obtain a theoretical understanding of the nature of the scatterers and the propagation medium at low angles. Fortunately, sea clutter is quite low at very low grazing angles and might not be a serious factor in most radar applications that have to detect targets in a sea clutter background. For example, at X band and sea state 3, σ^0 is less than -40 dB at 1.0°, less than -45 dB at 0.3°, and less than -50 dB at 0.1° grazing angle.[44] At lower frequencies, sea clutter is even less than at X band when the polarization is horizontal.

Sea Clutter at Vertical (Normal) Incidence Although sea clutter usually is much lower than land clutter at low grazing angles, it is higher than land clutter at perpendicular incidence. In the discussion of clutter at vertical (normal) incidence over a flat, perfectly reflecting land surface, it was mentioned that the value of σ^0 is approximately equal to the antenna gain G. The same is true over the sea. Thus when examining measured values of sea (or land) clutter at or near normal incidence, it needs to be kept in mind that the antenna has a significant effect on the value of the backscatter clutter power per unit area when the surface is flat or even when it is slightly rough.

Theory of Sea Clutter Many theoretical models have been proposed over the years to explain sea clutter. Most of the discussion here applies to moderate or low grazing angles. Scattering near vertical incidence generally requires a different theoretical model than at the lower grazing angles.

Past attempts to explain sea echo have been based on two different approaches. In one, the clutter is assumed to originate from scattering features at or near the sea surface. Examples include reflection from a corrugated surface,[45] backscatter from droplets of spray thrown into the air above the sea surface,[46] and backscatter from small facets, or patches, that lie on the sea surface.[41] Each of these can be applied to some limited aspect of sea echo, but none has provided an adequate explanation that accounts for the experimental evidence.

The other approach is to derive the scattering field as a boundary-value problem in which the sea surface is described by some kind of statistical process. One of the first attempts assumed that the surface disturbances could be described by a gaussian probability density function. It has been said[47] that gross observation of the sea characterized by large water wavelengths shows that the surface can be considered to be approximately gaussian, but observation of the sea's fine structure (which is what is of interest for radar backscatter) shows it is not so. Calculations of the scattering of the sea based on a gaussian surface[48] produce results that appear at first glance to be reasonable, but on close examination do not match experimental data. The conclusion that the sea cannot be represented as a gaussian statistical surface was also found by application of the theory of chaos in nonlinear dynamical systems to experimental sea clutter data.[49]

Bragg Scatter A model that has been successfully used to describe sea echo at long radar wavelengths (HF and VHF) is Bragg resonance, or Bragg scatter. This type of backscatter is so named because of its similarity to X-ray diffraction in crystals as originally put forward by Sir Lawrence Bragg and his father, Sir William Bragg, for which they jointly received the 1915 Nobel Prize in Physics. Bragg scatter is based on the coherent reinforcement of scattering from a periodic scatterer. Although real seas driven by the wind do not appear periodic, the sea can be considered as made up of a large number of individual sinewaves of different wavelengths and directions, similar to the manner in which an electrical engineer describes a noiselike voltage waveform by its frequency spectrum (also a collection of individual sinewaves of different frequencies). The Fourier transform is the means by which one can convert the voltage waveform to the frequency spectrum, and vice versa. The sea spectrum is two-dimensional (wave height as a function of frequency and direction), which differs from the one-dimensional frequency spectrum usually considered by the electrical engineer.

A rough sea surface can be described by its vertical displacement from the mean. A Fourier transform of this surface displacement gives a spectrum. Scattering from such a surface can be characterized as scattering from that particular (sinewave) frequency component of the surface spectrum that is *resonant* with the radar frequency. By resonant is meant backscattering such that the echo energy from each cycle of the sinewave reinforces coherently, as depicted in Fig. 7.16. In this figure, the radar wavelength λ_r is twice that of the spectral component λ_w (water wavelength) so that coherent addition takes place. Echoes, from any other spectral component that is not at the resonant frequency, add noncoherently and result in much smaller amplitude than the echo that experiences coherent addition from each cycle. Hence, the major scattering effect is from the resonant component and not from the other components of the sea-surface spectrum.

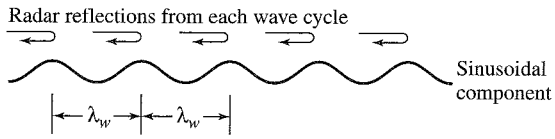

Figure 7.16 Representation of "resonant," or Bragg, scatter from a sinusoidal component of the sea-surface spectrum. Grazing angle = 0°. When the radar wavelength λ_r equals twice the wavelength λ_w of the resonant spectral component of the sea spectrum, then in-phase (coherent) addition of scattering takes place.

In general, the grazing angle is not zero, as was shown in Fig. 7.16. The Bragg resonant condition relating the radar wavelength λ_r and the water wavelength λ_w for a grazing angle ψ is given as

$$\lambda_r = 2\lambda_w \cos \psi \qquad [7.13]$$

The first to successfully apply the Bragg scattering model to sea clutter was Douglas Crombie,[50] who used it to explain the distinctive nature of the sea clutter doppler spectrum from HF radar. Bragg scatter forms the theoretical basis for remote sensing of sea and wind conditions over the sea with HF radar.[51,52] The Bragg model, however, has not been successful in explaining experimental observations of sea echo at the higher microwave frequencies.

Composite Surface Model At the higher microwave frequencies, the resonant water waves of the classical Bragg model that might contribute to backscatter have wavelengths of the order of centimeters. These short water waves are said to ride on the higher-amplitude long waves. The short-wavelength water waves are primarily responsible for the backscattering, and the long-wavelength water waves act to tilt the shorter waves. The effect of tilt can be taken into account by averaging over the tilt angles. The sea surface is thus modeled as a composite surface with two scales of roughness.[53] It has been called the *two-roughness* model or the *composite surface* model.

Long-wavelength water waves are called *gravity waves* because their velocity of propagation is determined primarily by gravity. *Capillary waves,* also called *ripples,* are small waves whose velocity is determined mainly by the surface tension of the water. Waves less than about 1.73 cm are capillary waves; waves of longer wavelength are considered gravity waves. At *X* band, the composite surface model is said to consist of short capillary waves riding on longer gravity waves. (There are, however, other surface effects in addition to capillary waves that can give rise to scattering at the higher frequencies; and these surface effects can produce greater backscatter than capillaries.)

The combination of the Bragg theory of sea echo and the composite-surface model has had considerable acceptance by some theorists since it is one of the few theories that provides an analytical basis for computation. Bragg theory, however, has serious limitations at microwave frequencies, which make its validity suspect. These include:

- The composite-surface model for microwave sea echo does not explain many of the important experimental observations of sea clutter, especially at low grazing angles.

- The theoretical formulation of Bragg scattering as a global boundary-value problem is based on the assumption that the sea-surface displacements are small compared to the radar wavelength, an assumption usually not satisfied at microwave frequencies.[54]
- Examination of sea echo obtained with high-resolution radar indicates that the dominant scattering features (sea spikes) are of relatively large amplitude (order of a few square meters radar cross section) and have a time duration of seconds. When observed with sufficient resolution, they are seen by the radar intermittently. This is far different from the view that small waves ride on top of big waves as in the composite model. Most proponents of Bragg scatter tend to consider the capillaries or ripples as the small waves. In photographs of rough sea that show capillaries or ripples, however, there are almost always present other, more significant, sea-surface features. These are generally larger than capillaries and have sharp features that can give rise to larger echoes than the capillaries. Any theory of microwave sea clutter has to be based on the observed nature of the sea and what the radar sees, which at low grazing angle is predominantly (maybe even exclusively) sea spikes.

Scattering by Surface Features One of the limitations to obtaining a satisfactory theory of sea echo is the lack of a quantitative description of the sea surface. If the exact nature of the sea surface is described, the calculation of electromagnetic scattering is achieved by solution of Maxwell's equations using more or less standard methods. Oceanographers and hydrodynamicists, however, have not been very interested in the small-scale features of the sea surface that give rise to radar scattering at microwave frequencies. The lack of a full understanding of these small-scale features has been a limitation in formulating a suitable model.

At the beginning of this discussion on sea echo theory, it was mentioned that early theorists tried to explain sea echo by postulating rather simple surface features (sinewaves, facets, and spray). Wetzel[55] has enumerated several other sea-surface features that could account for sea scatter. These are:

- *Plumes:* which slide down the front faces of breaking waves
- *Sloshes or hydraulic shocks:* structures associated with localized wind-puffs or the passage of a steep wave
- *Pools of surface roughness:* associated with breaking waves
- *Wedgelike structures*[56]
- *Pyramidal cusplike structures*

In addition, scattering from the tops of the disturbed crests might be included in the list. If the size, shape, distribution, and transient behavior of these surface features were known, one might begin to formulate a theory of sea echo.

Sea Spikes Whatever its cause and nature, the scattering feature known as the sea spike has to be a major part of any theory of sea clutter at low grazing angles at the higher microwave frequencies. Experiments show that the sea spike is all that a high-resolution radar sees. There are no other major scatterers present in the echo. Thus the sea spike should be the basis for any radar sea scatter theory at microwave frequencies (*L* band and

higher), and Bragg scatter is the basis for sea scatter theory at the lower radar frequencies (HF and VHF).

Sea Clutter Models and Radar Design As indicated, it has been difficult to formulate a satisfactory theory of microwave sea clutter that starts from fundamental principles and fully describes the experimental observations of electromagnetic scatter from the sea. A satisfactory theory should allow the radar engineer to determine optimum waveforms and related signal processing to maximize radar performance when sea clutter limits detection. Lacking a suitable theory, radar engineers have been able to design radars that operate satisfactorily in the presence of sea clutter by using simplified models and conservative design. Empirical observations are still a widely used basis for specifying a sea clutter model for engineering design or procurement specification. This is an engineering expedient that will be used until a theory suitable for reliable design is formulated.

There exist several collections of averaged values of σ^0 used to describe sea clutter. Two of the most popular are the tables given in Nathanson's book[57] and the formulas of Georgia Tech.[58] Other models have been described by Morchin.[59]

The values of σ^0 in the literature are usually the mean or the median. There is less information on the statistical properties of sea clutter. Design of the radar signal processor and detector by the methods of classical detection theory requires knowledge of the probability density function of the clutter. The spatial as well as temporal variations of clutter are also necessary, especially with high radar-resolution. These descriptions have been difficult to obtain. It has been even more difficult to relate them to the environmental parameters that affect sea clutter. There has been only limited success in devising a theory of signal processing and detector design that can be used by the radar designer when the clutter with which the radar echo must compete is time varying (nonstationary) and spatially nonhomogeneous.

If there were a satisfactory model for sea clutter, it would also provide information about the physical mechanisms occurring at the sea surface. In remote sensing, the radar is used as an instrument to measure some characteristic of the sea, such as the sea state, surface currents, and the winds that drive the sea. One can obtain empirical relations between the radar echo and some environmental parameters of the sea to be measured; but a satisfactory theory of sea clutter could advance one's ability to perform remote sensing of the environment, as well as improved detection of aircraft, missiles, ships, and other targets.

Backscatter from Sea Ice[60–62] At low grazing angles, as might occur with a shipboard radar, there is little backscattered energy from smooth, flat ice. On a PPI or similar display the areas of ice will be dark except perhaps at the edges. If areas of water are present along with the ice, the sea clutter seen on the display will be relatively bright in contrast with the ice echoes. Backscatter from rough ice, such as floes and pack ice, can produce an effect on the radar display similar to sea clutter. Clutter echoes from rough ice, however, can be distinguished from sea clutter since its pattern will remain stationary from scan to scan but the sea clutter echo pattern will change with time.[63] Measurements of ice fields near Thule, Greenland indicated that the radar backscatter (σ^0) varied linearly with frequency over a range of grazing angles from 1° to 10°, was proportional

to the grazing angle from 2° to 10°, but was inversely proportional to grazing angle from 1° to 2°.[64] The scatterometer, a radar that measures σ^0 as a function of elevation angle in the region near vertical incidence, has been used as an ice sensor to differentiate between first-year ice and multiyear ice (ice that doesn't completely melt in the summer). Shipboard radars with multiple polarizations are also able to distinguish between first-year ice, multiyear ice, and icebergs.[65] Multiyear ice is harder, and more difficult for a ship to penetrate, than first-year ice. Imaging radars, such as SAR and SLAR, have been used to image ice fields to determine the nature of the ice and inform shipping of the best routes to travel through the ice.[66]

Radar can also detect icebergs, especially if they have faces that are nearly perpendicular to the radar direction of propagation.[63] Icebergs with sloping surfaces can have a small echo even though they may be large in size. Icebergs can be readily identified in radar images by the characteristic shadows (absence of echo) they produce when viewed at low grazing angles.[67] Growlers, which are small icebergs that are large enough to be of danger to ships, are poor radar targets because of their small size and shape.

Oil Slicks[68] Oil on the surface of the sea has a smoothing effect on breaking waves. Oil slicks, therefore, are readily detectable since they appear dark on a radar PPI compared to the surrounding sea. Vertical polarization produces greater contrast in radar images of oil slicks than horizontal polarization.

7.5 STATISTICAL MODELS FOR SURFACE CLUTTER

Because of the highly variable nature of clutter echoes it is often described by a probability density function (pdf) or a probability distribution (Sec. 2.4). This section describes several statistical models that have been suggested for characterizing the fluctuations of the surface-clutter cross section per unit area, or σ^0. They can apply to both sea and land clutter. The term *distribution,* as in *Rayleigh distribution,* is used here to indicate the statistical nature of the phenomenon and applies to either the pdf or the probability distribution function. In this chapter, however, the pdf rather than the probability distribution is usually used to describe clutter statistics.

Rayleigh Distribution[69] This popular model is based on the assumption that there are a large number of randomly located independent scatterers within the clutter surface area illuminated by the radar. (The assumption of a large number is usually satisfied with as few as ten scatterers.) It is further assumed that none of the individual scatterers is significantly larger than the others.

If the radar receiver uses a linear detector, the probability density function of the voltage envelope of the Rayleigh distributed clutter at the receiver output is[17]

$$p(v) = \frac{2v}{m_2} \exp\left(-\frac{v^2}{m_2}\right) \qquad v \geq 0 \qquad \text{[7.14a]}$$

where m_2 is the mean-square value (second moment) of the envelope v. (This equation differs slightly from the form given in Ref. 17.) The mean m_1 (first moment) is $(m_2\pi/4)^{1/2}$, and

the median is $(m_2\ ln\ 2)^{1/2}$ so that the mean-to-median ratio is $[\pi/(4\ ln\ 2)]^{1/2} = 1.06$, or 0.27 dB. The mean of the Rayleigh distribution is proportional to the standard deviation, or

$$\text{standard deviation} = \sqrt{\frac{4}{\pi} - 1} \times \text{mean} = 0.523 \times \text{mean}$$

The Rayleigh pdf of v normalized to its median v_m, rather than the mean-square value, is

$$p(v_n) = 2(ln\ 2)v_n \exp\left[-(ln\ 2)\ v_n^2\right] \qquad v_n \geq 0 \qquad \textbf{[7.14b]}$$

where $v_n = v/v_m$.

The Rayleigh pdf also describes the envelope of the output of the receiver when the input is gaussian noise, as was discussed in Chap. 2 for the detection of signals in noise. The theory given in Chap. 2 for signals in noise applies to the detection of signals in clutter when the clutter statistics are Rayleigh and the clutter echoes are independent pulse to pulse (as is receiver noise). However, this is not often true with clutter. The noise voltage from a receiver is independent from pulse to pulse since it is decorrelated in a time $1/B$, where B = bandwidth. The decorrelation time of clutter can be much longer. This is important when attempting to integrate pulses for improving detection since clutter echoes are generally not decorrelated pulse to pulse. (Correlation of clutter echoes was discussed in relation to the surface-clutter radar equation in Sec. 7.2.) To apply the methods of Chap. 2 based on Rayleigh statistics, the clutter might be decorrelated by changing the frequency pulse to pulse or by waiting a sufficiently long time between pulses to allow the temporal decorrelation of the clutter to occur (if there is clutter motion). However, these methods for decorrelating clutter are not practical in all applications. For example, frequency agility cannot be used with doppler processing. Waiting for the clutter to decorrelate due to its own internal motion might take too long.

If the receiver uses a square-law detector, the output voltage is proportional to the input signal power P. The probability density function in this case is the exponential, or[17]

$$p(P) = \frac{1}{\overline{P}} \exp\left(-\frac{P}{\overline{P}}\right) \qquad P \geq 0 \qquad \textbf{[7.15]}$$

where $\overline{P}$ is the mean value of the power. The standard deviation of the exponential pdf is equal to the mean.

Although the output of a linear receiver is described by the Rayleigh pdf, as in Eq. (7.14), and the output of the square-law receiver is given by the exponential pdf of Eq. (7.15), they both are considered to belong to the Rayleigh model. The term *Rayleigh clutter* derives from the basic nature of the clutter model rather than whether a linear or a square-law receiver is used.

Log-Normal Distribution As mentioned, the Rayleigh clutter model usually applies when the radar resolution cell is large so that it contains many scatterers, with no one scatterer dominant. It has been used to characterize relatively uniform clutter. However, it is not a good representation of clutter when the resolution cell size and the grazing angle are small. Under these conditions, there is a higher probability of getting large values of clutter (higher "tails") than is given by the Rayleigh model.

One of the first models suggested to describe non-Rayleigh clutter was the log-normal pdf since it has a long tail (when compared to the Rayleigh).[70] In the log-normal pdf the clutter echo power expressed in dB is gaussian. The log-normal pdf for the echo power when the receiver has a square-law detector is[17]

$$p(P) = \frac{1}{\sqrt{2\pi}\, sP} \exp\left[-\frac{1}{2s^2}\left(ln\frac{P}{P_m}\right)^2\right] \qquad P \geq 0 \qquad [7.16]$$

where s = standard deviation of $ln\ P$, and P_m = median value of P. The ratio of the mean to the median is exp ($s^2/2$). With a linear receiver, the pdf for the normalized output voltage amplitude $v_n = v/v_m$, with v_m = median value of v, is

$$p(v_n) = \frac{2}{\sqrt{2\pi}\, sv_n} \exp\left[-\frac{2}{s^2}(ln\ v_n)^2\right] \qquad v_n \geq 0 \qquad [7.17]$$

where s remains the standard deviation of $ln\ P$.

The log-normal distribution is specified by two parameters (the standard deviation and the median), whereas the Rayleigh is specified by only one parameter (the mean square value). Log-normal clutter is often characterized by the ratio of its mean to median.[71] Based on measurements by different experimenters, as reported in Ref. 71, the mean-to-median ratio for sea clutter varies from about 0.6 dB for a grazing angle of 4.7° and low sea state, to 5.75 dB for a high sea state and low grazing angle of 0.5°. For a particular ground clutter measurement at low grazing angles, it had a value of about 2.6 dB.

It should be expected that because of its two parameters the log-normal pdf can be made to fit experimental data better than can the one-parameter Rayleigh. However, it is sometimes said that the log-normal tends to predict higher tails for the pdf than normally experienced with most non-Rayleigh clutter, just as the Rayleigh model tends to predict lower values.

Weibull Distribution[17,72] The Weibull distribution is a two-parameter family that can be made to fit clutter measurements that lie between the Rayleigh and the log-normal. The Rayleigh is actually a special case of the Weibull; and with appropriate selection of the distribution's parameters, the Weibull can be made to approach the log-normal.

If v is the amplitude of the voltage out of a linear detector, the Weibull pdf for the normalized amplitude $v_n = v/v_m$ is

$$p(v_n) = \alpha(ln\ 2)v_n^{\alpha-1} \exp\left[-(ln\ 2)v_n^{\alpha}\right] \qquad v_n \geq 0 \qquad [7.18]$$

where α is a parameter that relates to the skewness of the distribution (sometimes called the *Weibull skewness parameter*), and v_m is the median value of the distribution. When $\alpha = 2$, the Weibull takes the form of the Rayleigh; and when $\alpha = 1$, it is the exponential pdf. The mean-to-median ratio is $(ln\ 2)^{-1/\alpha}\ \Gamma(1 + 1/\alpha)$, where $\Gamma(\cdot)$ is the gamma function. With a square-law detector, the Weibull pdf for the power $P = v^2$ is

$$p(P_n) = \beta(ln\ 2)P_n^{\beta-1} \exp\left[-(ln\ 2)P_n^{\beta}\right] \qquad P_n \geq 0 \qquad [7.19]$$

where $\beta = \alpha/2$, $P_n = P/P_m$, and $P_m = v_m^2$ is the median value of P.

The Weibull distribution has been applied to land clutter,[73,74] sea clutter,[75,76] weather clutter,[77] and sea ice.[78] Table 7.3 lists examples of the Weibull skewness parameter α for several types of land and sea clutter.[79]

Table 7.3 Weibull clutter parameters.[79]

Terrain/Sea State	Frequency	Beamwidth (deg)	Pulse Width (μs)	Grazing Angle	Weibull Parameter
Rocky mountains	S	1.5	2	.....	0.52
Wooded hills	L	1.7	3	~0.5	0.63
Forest	X	1.4	0.17	0.7	0.51–0.53
Cultivated land	X	1.4	0.17	0.7–5.0	0.61–2.0
Sea state 1	X	0.5	0.02	4.7	1.45
Sea state 3	K_u	5	0.1	1.0–30.0	1.16–1.78

With regard to land clutter at small depression angles, Billingsley[4] states: "Weibull formulations of clutter amplitude statistics represent better engineering approximations to clutter spatial amplitude distributions than do log normal formulations. Log normal formulations of clutter amplitude statistics tend to provide too much spread in the statistics."

K-Distribution This two-parameter probability distribution for modeling the statistics of clutter, proposed by Jakeman and Pusey,[80] is described as a compound distribution that consists of two components. The K-distribution probability density function describing the voltage amplitude x is

$$p(x) = \frac{2b}{\Gamma(\nu)}\left(\frac{bx}{2}\right)^{\nu} K_{\nu-1}(bx) \qquad [7.20]$$

where b is a scale parameter[81] that relates only to the mean of the clutter or σ^0, $\Gamma(\cdot)$ is the gamma function, ν is the shape parameter which depends on the higher moments in relation to the mean, and K_ν is the modified Bessel function of the second kind. (The parameter x has been used in the above instead of the more usual v for voltage so as to not confuse it with the Greek letter ν which is the shape parameter.) The statistical moments of the K-distribution lie between those of the Rayleigh and the log-normal distributions, which is sometimes used as a justification for the K-distribution since experimental sea clutter measurements seem to have the same property. Although it can be applied to land,[82] there appears to have been more interest in its application to the sea.

For sea clutter, the K-distribution is said to be made up of two components that might be associated with experimental observations.[83] There is a fast varying component, with a correlation time on the order of 5 to 10 ms. (This applies for a particular set of data obtained at X band, with a 30 ns pulse duration and a two-way 3-dB beamwidth of 1.2°.) The fast component can be decorrelated pulse to pulse by means of frequency agility. It is sometimes called the *speckle component* and its statistics can be represented by a Rayleigh distribution. The other component has a longer decorrelation time, of the order of seconds, and is unaffected by frequency agility. The slowly varying component can be represented by a gamma distribution.[84] Thus the model assumes a Rayleigh-distributed

rapidly fluctuating component modulated by a slowly fluctuating gamma-distributed component which results in the compound K-distribution of Eq. (7.20).

In the literature it has been said that the rapid component "occurs because of the multiple nature of the clutter in any illuminated patch."[85] The slowly varying component is "thought to be associated with the sea swell structure." There is not universal agreement about this description. (It is also possible to describe sea clutter as consisting of two components with different correlation times because of the observed behavior of sea spikes, as was discussed in Sec. 7.4.)

Based on measurements with an X-band radar having a 30-ns pulse width, and a 1.2° (two-way) beamwidth (resulting in a cross-range resolution of 100 to 800 m), the shape parameter ν in the K-distribution generally falls within the range 0.1 and ∞.[81] The value of ν increases with increasing cell size; and when $\nu = \infty$, the K-distribution is the same as the Rayleigh. An empirical estimate of the shape parameter ν, based on the above radar characteristics, is

$$\log \nu = \frac{2}{3} \log \psi + \frac{5}{8} \log \Delta + \zeta - k \qquad [7.21]$$

where ψ = grazing angle in degrees (from 0.1 to 10°); Δ = cross-range resolution in meters; $\zeta = -1/3$ for up or down swell directions, $+1/3$ for across swell directions, and 0 for intermediate directions or when no swell waves exist; and k gives the effect of polarization with $k = 1$ for vertical and $k = 1.7$ for horizontal polarization. No significant statistical trend was noted for variations in the sea state, wind speed, or aspect angle relative to the wind direction. It has been suggested[86] that changes in the range resolution might have a similar effect on ν as the cross-range resolution Δ, and that the parameter ζ can be expressed as $-1/3 \cos 2\theta$, where the angle θ is zero when the radar antenna points in the direction of the swell. [There is also a slightly different version of Eq. (7.21).[86]] As the range-resolution cell becomes smaller, the clutter distribution deviates from Rayleigh and ν becomes smaller. The smaller the ν, the higher the threshold for a given false-alarm probability. However, the higher the resolution, the smaller will be the clutter echo. In one analysis of range resolution,[87] it was concluded that better performance will generally be achieved with the higher resolution radar, provided the K-distribution model is maintained.

It should be cautioned that Eq. (7.21) was obtained with measurements from only a single radar and might not be universally applicable to other situations. (It would seem that ν should vary to some extent with sea state, since experiments show that the probability density function of sea clutter changes with the sea state.[88]) Although most of the above information is based on X-band data, similar behavior of the parameter ν was also observed at S band and K_u band.[89]

The above discussion has applied mainly to the noncoherent detection of targets in K-distributed clutter. The model has been extended to coherent detection,[90,91] the addition of thermal noise,[92] and the performance of CFAR.[93]

Other Statistical Distributions Other distributions that have been proposed for describing the statistics of clutter include contaminated normal,[88] Ricean,[94] Rice squared,[95] gamma,[96] and log-Weibull.[97] Shlyakhin[98] provides an extensive listing of probability density

functions for describing non-Rayleigh fluctuating radar signals. He lists twelve two-parameter, six three-parameter, and seven multiparameter distributions.

Application of the Statistical Descriptions of Clutter Probability distributions such as those given in this section have been of interest for providing a concise description of the amplitude statistics of clutter. As mentioned previously, except for the Rayleigh, there is no physical basis for the use of these distributions. They are curve-fitting models used to describe experimental data. Analyses in the literature of the detection of targets in non-Rayleigh clutter can be found that employ log-normal clutter,[99,100] Weibull clutter,[88,101] and K-distribution clutter.[102,91]

The probability distributions that contain two parameters, such as the Weibull and the K, can be made to fit experimental data better than can a single-parameter distribution. Generally, the Weibull and K-distributions have similar curve-fitting capability; but it has been said that the Weibull is easier to use. However, curve fitting of a particular distribution is not always of sufficient help to the radar engineer trying to determine how to design a signal processor to detect signals in non-Rayleigh clutter since a single statistical expression does not do well in fitting the wide variety of real-world clutter.

A comparison of the Rayleigh pdf with examples of log-normal and Weibull is shown in Fig. 7.17. (The equivalence of the Rayleigh and the Weibull with $\alpha = 2$ is noted in the figure.) The ability of a two-parameter distribution like the Weibull to fit experimental data is illustrated by the quite different shapes for the $\alpha = 0.5$ and $\alpha = 2$ curves.

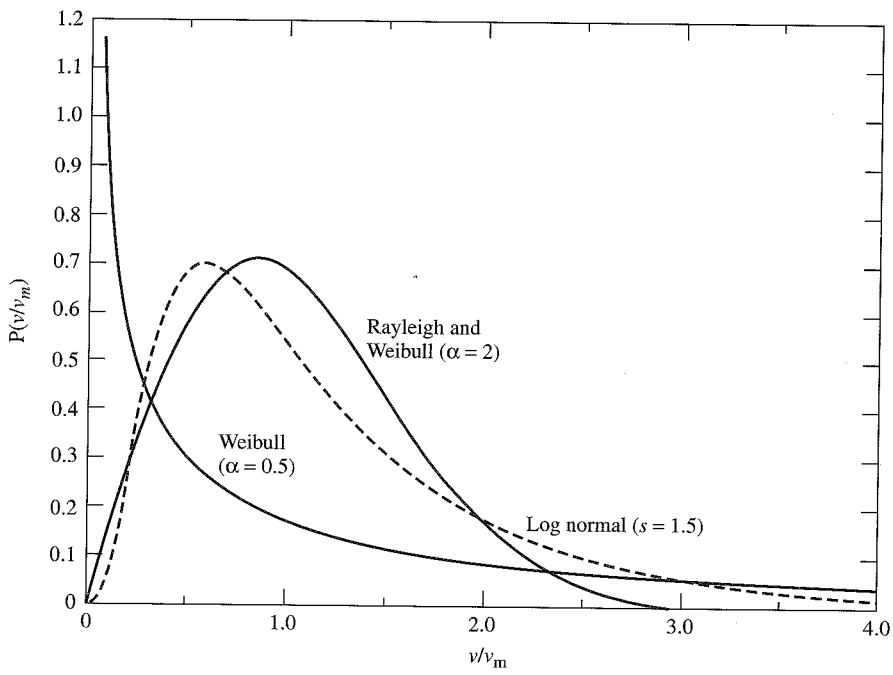

Figure 7.17 Probability density functions of the envelope v of the output of a linear detector, normalized by the median value v_m, for Rayleigh [Eq. (7.14b)], log-normal [Eq. (7.17)], with a mean-to-median ratio of 5 dB], and Weibull [Eq. (7.18) with a skewness parameter of 0.5].

The theory for the detection of signals in clutter that is non-gaussian, partially correlated in time, nonhomogeneous, and nonstationary (which is the nature of real-world clutter) is a difficult problem. Classical detection-theory methods have generally been inadequate. They either contain restricting assumptions that might not be applicable or are difficult to apply to the varying nature of real-world clutter. The radar designer, when confronted with such a problem, has to design conservatively and from experience.*

7.6 WEATHER CLUTTER

Radar is much less affected by weather than are optical and infrared sensors; but weather can seriously degrade radar performance at the higher microwave and millimeter wave frequencies. Backscatter from precipitation that masks the desired target echo is the chief problem. Attenuation of the electromagnetic signal in propagating through precipitation also occurs; but at most microwave frequencies it is seldom strong enough to be of serious concern for the detection of targets.

Radar Equation for Detection of Rain[1,103–105] The radar equation describing the echo from meteorological particles such as rain, hail, sleet, and snow is of interest to the meteorologist as well as the radar engineer. The engineer needs to understand the effect weather has on the detection of targets. The meteorologist, on the other hand, is interested in using radar to determine the rate of fall of precipitation and the direction and speed of the wind. The radar equation derived below is based on the detection of rain, but it can be extended to other forms of precipitation.

Within the radar resolution cell there are many individual rain drops, each with some radar cross section σ_i. The total radar cross section, σ_c, from volume-distributed rain is the summation of the echoes from all the individual scatterers, and can be represented as

$$\sigma_c = V_c \eta = V_c \sum_i \sigma_i \qquad [7.22]$$

where η = radar cross section per unit volume, and V_c = volume of the radar resolution cell. The summation is taken over the unit volume. The volume V_c is

$$V_c = \frac{\pi}{4}(R\theta_B)(R\phi_B)\left(\frac{c\tau}{2}\right)\frac{1}{2\ ln\ 2} \qquad [7.23]$$

where R = range, θ_B = horizontal half-power beamwidth of the radar antenna, ϕ_B = vertical half-power beamwidth, τ = pulse duration, c = velocity of propagation, and ln is the natural logarithm. The factor $\pi/4$ is included to account for the elliptical shape of the antenna-beam projected area. In the interest of accuracy, the radar meteorologist reduces the

*A similar statement has been made before in this text, referring to those times when full information is not available to the radar designer. *Conservative* means being cautious and the inclusion of "safety factors" where appropriate. *Experience* implies that the designer learns from his or her own experience and the experience of others. The role of experience in engineering design, especially that which comes from failure, has been described by Duke University Civil Engineering Professor Henry Petroski in *To Engineer is Human—The Role of Failure in Successful Design*. New York: Vintage, 1992.

volume of Eq. (7.23) by a factor of 2 *ln* 2 to account for the fact that the effective volume of uniform rain illuminated by the *two-way* radar antenna pattern (described by a gaussian beamshape) is less than that indicated if the half-power (one-way) beamwidths are used in Eq. (7.23).

The echo power P_r, received from rain of radar cross section σ_c, is given by the simple radar equation of Sec. 1.2:

$$P_r = \frac{P_t G^2 \lambda^2 \sigma_c}{(4\pi)^3 R^4} \qquad [7.24]$$

where P_t = transmitted power, G = antenna gain, λ = wavelength, and R = range. Using Eqs. (7.22) and (7.23), the radar equation becomes

$$P_r = \frac{P_t G^2 \lambda^2 \theta_B \phi_B c\tau}{1024(ln\ 2)\pi^2 R^2} \sum_i \sigma_i \qquad [7.25]$$

The antenna gain is approximated by $G = \pi^2/\theta_B \phi_B$, if the antenna pattern can be described by a gaussian function.[1] With this substitution, the radar equation becomes

$$\bar{P}_r = \frac{P_t G \lambda^2 c\tau}{1024(ln\ 2)R^2} \sum_i \sigma_i \qquad [7.26]$$

The bar over P_r denotes that the received power is averaged over many independent samples to smooth the fluctuations of the rain echo. (The radar meteorologist might average 30 or 40 samples to make the standard deviation of the received signal power less than one dB.)

The above radar equation assumes that the volume of the radar resolution cell is completely filled with uniform rain. If not, a correction must be made by introducing a dimensionless beam-filling factor, which is the fraction of the cell filled by rain. It is difficult to accurately estimate this correction. The resolution cell is not likely to be completely filled at long range or when the beam is viewing the edge of a precipitation cell.

If a single drop of rain can be considered as a sphere of diameter D_i, with circumference small compared to the radar wavelength (Rayleigh scattering region), the radar cross section is given by

$$\sigma_i = \frac{\pi^5 D_i^6}{\lambda^4} |K|^2 \qquad [7.27]$$

where $|K|^2 = (\epsilon - 1)/(\epsilon + 2)$, and ϵ = dielectric constant of water. The value of $|K|^2$ for water varies with temperature and wavelength. At 10°C and 10 cm wavelength, it is approximately 0.93. Equation (7.27) also applies for ice. The value of $|K|^2$ for ice is about 0.197 and is independent of frequency in the centimeter-wavelength region. Substituting Eq. (7.27) into (7.26) yields

$$\bar{P}_r = \frac{\pi^5 P_t G c\tau}{1024(ln\ 2)R^2 \lambda^2} |K|^2 \sum_i D_i^6 \qquad [7.28]$$

Since the diameter D_i appears as the sixth power, in any distribution of drop sizes the small number of large drops will dominate the contribution to the radar echo.

Equation (7.28) does not include the attenuation of radar energy by rain. Attenuation usually is not of concern at microwave frequencies, except when accurate measurements of rainfall rate are required. (It is for this reason that the meteorological radar known as Nexrad is at *S* band, where the effects of attenuation are small.) The two-way attenuation of the radar signal in traversing the range R and back through uniform rain is $\exp(-2\alpha R)$, where α is the one-way attenuation coefficient. If rain is not uniform, the total attenuation must be expressed as the integrated value of $\exp(-2\alpha R)$ over the two-way path. When the radar equation has to include the effect of attenuation, it cannot be readily solved for the range R. (In practice, it can be solved by trial and error.)

The parameter $\sum D_i^6$ in Eq. (7.28) is called the *radar reflectivity factor* by the radar meteorologist and is denoted by Z. Experimentally, Z can be related to the rainfall rate r by

$$Z = \sum_i D_i^6 = ar^b \qquad [7.29]$$

where a and b are empirically determined constants. Equation (7.29) allows the echo signal power P_r to be related to the rainfall rate r. A number of experimenters have attempted to determine the constants in Eq. (7.29), but considerable variability exists among the reported results.[103] One form of Eq. (7.29) that has had wide acceptance is

$$Z = 200r^{1.6} \qquad [7.30]$$

where Z is in units of mm^6/m^3 and the rainfall rate r is in mm/h. (Sometimes the expression $Z = 300\,R^{1.4}$ has been used for the Nexrad WSR-88D weather radar system for rainfall estimation.) The units of Z must be properly accounted for when substituting into the radar equation. Equation (7.30) applies to stratiform rain which, in temperate climates, is relatively uniform over distances of 100 km or more (except for embedded showers that might have dimensions of the order of 10 km).[106] Intensities rarely exceed 3 mm/h except in the imbedded showers that can have rates up to 20 mm/h or more. Their vertical extent is from 4 to 6 km, and durations are of several hours. For orographic rain $Z = 31r^{1.71}$ and for thunderstorm rain $Z = 48r^{1.37}$. (Orographic rain is the rain produced when a mountain deflects moisture-laden wind upward.)

When Eq. (7.30) is substituted into Eq. (7.28) the radar equation becomes

$$\overline{P}_r = \frac{2.4P_tG\tau r^{1.6}}{R^2\lambda^2} \times 10^{-8} \qquad [7.31]$$

where r is in mm/h, R and λ in m, τ in seconds, and P_t in watts. This is the form of the equation used to measure rainfall. The received power varies as $1/R^2$ rather than the $1/R^4$ found in the usual radar equation for conventional "point" targets.

The backscatter cross section of rain per unit volume, η, as a function of wavelength and rainfall rate is shown plotted in Fig. 7.18. The dashed lines apply to Rayleigh scattering when $D_i << \lambda$, and were obtained by summing the values of σ_i given by Eq. (7.27) over the unit volume and using Eqs. (7.29) and (7.30) to give

$$\eta = \sum_i \sigma_i = 7f^4r^{1.6} \times 10^{-12} \quad \text{m}^2/\text{m}^3 \qquad [7.32]$$

where f is the radar frequency in GHz and r the rainfall rate in mm/h. The solid curves are exact values computed by Haddock.[107] Rayleigh scattering is seen to be a good approximation over most of the frequency range of interest to radar.

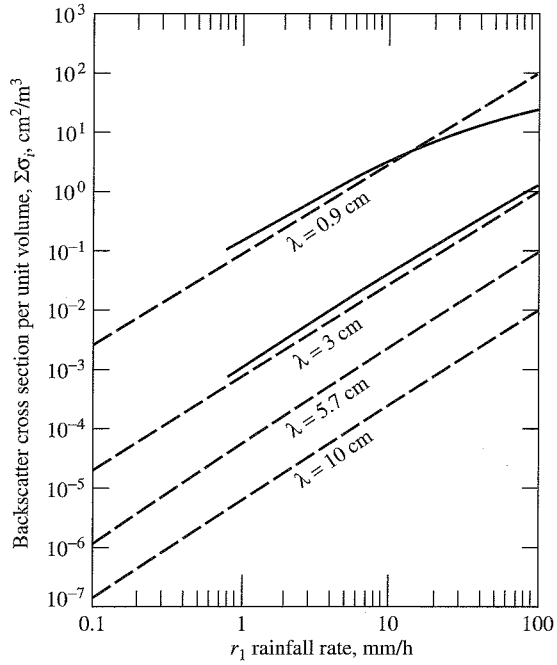

Figure 7.18 Exact (solid curves) and approximate (dashed curves) backscattering cross section per unit volume of rain at a temperature of 18°C. (From Gunn and East,[104] Quart. J. Roy. Meteor. Soc.)

The radar meteorologist prefers to describe the output of a weather radar by the parameter Z [Eq. (7.29)] rather than rainfall rate r. It would not be unusual for a weather radar to observe a rain cloud filled with rain that had not yet reached the ground or which evaporated before hitting the ground. Therefore a radar measurement of r in mm/h from such a cloud would have no meaning to an observer on the ground with a conventional rain gauge. By using Z rather than r, the meteorologist avoids this problem. The parameter Z is usually given in dB and denoted as dBZ. Using the relationship of Eq. (7.30), a rainfall rate of 1 mm/h equals 23 dBZ, 4 mm/h equals 33 dBZ, and 16 mm/h equals 42 dBZ. (This may be an incorrect usage of the precise definition of decibels as a power ratio, but it is the jargon of the radar meteorologist.) With the parameter Z instead of rainfall rate, Eq. (7.31) becomes (ignoring attenuation)

$$\overline{P}_r = \frac{1.2P_tG\tau Z}{R^2\lambda^2} \times 10^{-10} \qquad [7.33]$$

Sometimes the radar meteorologist uses, instead of Z, an equivalent radar reflectively factor Z_e when the assumption of Rayleigh scattering does not apply. It is defined as[108]

$$Z_e = \lambda^4\eta/(\pi^5|K|^2) \qquad [7.34]$$

The measurement of rainfall based on the Z-r relationship discussed in this section is not always sufficiently accurate for the meteorologist. Other microwave methods for obtaining potentially more accurate measurements are based on attenuation measured at one or two frequencies, or at two polarizations; differential reflectivity (comparison of

reflectivity measured with both horizontal and vertical polarizations); polarization differential propagation phase shift (difference in rates of phase change with increasing distance between vertically and horizontally polarized waves); and others.[109]

Radar Equation for Detection of Targets in Rain Rain can be a serious limitation to the detection of targets, especially at *L*-band and higher frequencies. The radar equation derived here indicates the important parameters that affect detection of targets in rain.

We derive the radar equation for detection of a target in rain by taking the ratio of the echo from the target and the echo from rain. It is assumed that the rain echo is much larger than receiver noise. The received signal power S from the target is (Sec. 1.2)

$$S = P_r = \frac{P_t G^2 \lambda^2 \sigma_t}{(4\pi)^3 R^4} \qquad [7.35]$$

where σ_t = target radar cross section, and the other parameters are defined as in Eq. (7.24). The rain clutter C is similar to that of Eq. (7.33), and is written

$$C = \frac{K_1 P_t G \tau Z}{R^2 \lambda^2} \qquad [7.36]$$

where K_1 is a constant $= 1.2 \times 10^{-10}$. (The constant K_1 includes the velocity of propagation which has units of m/s.) The ratio of Eqs. (7.35) and (7.36) gives the signal-to-clutter ratio for a *single* pulse. If the maximum range $R_{\max}$ corresponds to the minimum detectable signal-to-clutter ratio $(S/C)_{\min}$, then

$$R_{\max}^2 = \frac{K_2 G \lambda^4 \sigma_t}{\tau Z (S/C)_{\min}} \qquad [7.37]$$

where $K_2 = 4.2 \times 10^6$. Attenuation has not been included. (For Z, one can substitute $200r^{1.6}$, or any other suitable ar^b relationship.) It should be noted that the statistics of rain echo can be different from those of receiver noise, and the value of $(S/C)_{\min}$ might not be easy to determine. We see from Eq. (7.37) that for long-range detection of targets in rain, the radar wavelength should be large (low frequency), the pulse width small, and the beamwidths small (high antenna gain).

The radar equation derived above for detection of targets in rain applies for one pulse. When a number of pulses are available from a target, they may be added together (integrated) to get larger signal-to-clutter ratio if the echoes are not correlated. It was mentioned that for land and sea clutter the pulses might not be decorrelated pulse to pulse, and the use of an effective number of pulses n_{eff} must be done with caution. Rain clutter, however, is likely to be decorrelated quicker than other clutter echoes and have the statistics of the Rayleigh pdf if the radar resolution cell is not too small and the prf is not too high. Therefore, it might be appropriate to include an effective number of pulses in the numerator of Eq. (7.37) when the conditions for independent pulses apply. The decorrelation (or independence) time of rain in seconds has been said to be

$$T_I = 0.2\lambda/\sigma_v \qquad [7.38]$$

where λ = radar wavelength in meters and σ_v = standard deviation of the velocity spectrum of the rain echo in m/s.[110] For example, at S band ($\lambda = 10$ cm) and $\sigma_v = 1$ m/s, the

decorrelation time is 0.02 s, which means there are only 50 independent samples of rain echo available per second. (The value of σ_v depends on wind shear, turbulence, and the terminal fall velocities of the precipitation.[111] It varies from 0.5 m/s for snow to 1 m/s for rain. In convective storms it might reach 5 m/s.)

Scattering from Snowfall Dry snow particles are essentially ice crystals, either single or aggregated. The relationship between Z and snowfall rate r is of the same form as that given by Eq. (7.29) for rain, but with different values of a,b. This allows the radar equation derived for rain, Eq. (7.28) or (7.31), to be applied to snow with the proper value of $|K|^2$ inserted (typically 0.197) and the snowfall rate r at the ground in millimeters of water measured when the snow is liquid (melted).

There have been fewer measurements of the Z-r relationship for snow than rain. The following two expressions have been suggested[112,113]

$$Z = 2000\, r^2 \qquad [7.39]$$

$$Z = 1780\, r^{2.21} \qquad [7.40]$$

Other values have been proposed, but there does not seem to be universal agreement.[114,115]

A radar is less affected by snow and ice than by rain since $|K|^2$ is smaller for ice than rain, and the snowfall rates (equivalent water content) are generally smaller than rainfall rates.

Scattering from Water-Coated Ice Spheres Moisture at altitudes where the temperature is below freezing takes the form of ice crystals, snow, or hail. As frozen particles fall to the warmer lower altitudes, they melt and form water-coated ice before becoming rain. Radar scattering by water-coated ice or snow is similar in magnitude to that of water drops of the same size and shape. Therefore, when an ice particle begins to change to liquid, radar backscatter increases since water-coated particles reflect more strongly than ice. Even for comparatively thin coatings of water, the composite particle scatters nearly as well as an all-water particle. One effect of this phenomenon is to give rise to what is called the *bright band.*

Radar observations of light precipitation show a horizontal bright band at an altitude at which the temperature is just above 0°C. It can be seen with a RHI display (range-height indicator). The center of the bright band might be 100 to 400 m below the 0°C isotherm. The echo in the center of the bright band is typically about 12 to 15 dB greater than the echo from the snow above it and about 6 to 10 dB greater than the rain beneath it.[103]

The bright band is due to changes in snow falling through the freezing level.[104] As snow just begins to melt, it changes from flat or needle-shaped particles which scatter feebly to similarly shaped particles which scatter relatively strongly due to their water coating. As melting progresses, the particles lose their extreme shapes and their velocity of fall increases. This results in a decrease in the number of particles per unit volume, and a reduction in the backscatter.

Scattering from Clouds and Fog Most water droplets in fair-weather (cumulus) clouds do not exceed 100 μm in diameter (1 μm = 10^{-6} m); consequently Rayleigh scattering

applies. Since the diameter of cloud droplets is small compared to the radar wavelength, echoes from fair-weather clouds are not of concern.

It might be possible to obtain weak echoes from a thick, intense fog at millimeter wavelengths; but at most radar frequencies, echoes due to fog may generally be regarded as insignificant.

Attenuation in Precipitation When precipitation particles are small compared to the radar wavelength (Rayleigh region), the attenuation due to absorption is small. This is the case for frequencies below S band. Since rain attenuation is usually small and unimportant at the longer wavelengths, the relative simplicity of the Rayleigh scattering approximation is of limited use for predicting attenuation through rain. The computation of rain attenuation must therefore be based on a more exact formulation, the results of which are shown in Fig. 7.19 as a function of wavelength and rainfall rate.[104] The attenuation produced by ice particles in the atmosphere, whether occurring as hail, snow, or ice-crystal clouds, is less than that caused by rain of an equivalent rate of precipitation.[116]

Effect of Weather on Radar Because the echo from precipitation varies as f^4, where f = frequency, UHF radars (420–450 MHz) are seldom bothered by weather effects. At L band weather echoes can be a problem, and some method for seeing aircraft targets in weather is usually needed. A radar at S band will have its range considerably reduced in modest rainfall if nothing is done to reduce the effect of rain. Radars at higher frequencies are even further degraded by rain. (Airborne weather-avoidance radars at X band, for example, can be severely degraded by heavy rain and prevent the radar from seeing hazardous weather.)

A typical specification for an air-surveillance radar might be that it has to detect its target when rainfall in the vicinity of the target is at the rate of 4 mm/h. This is called a

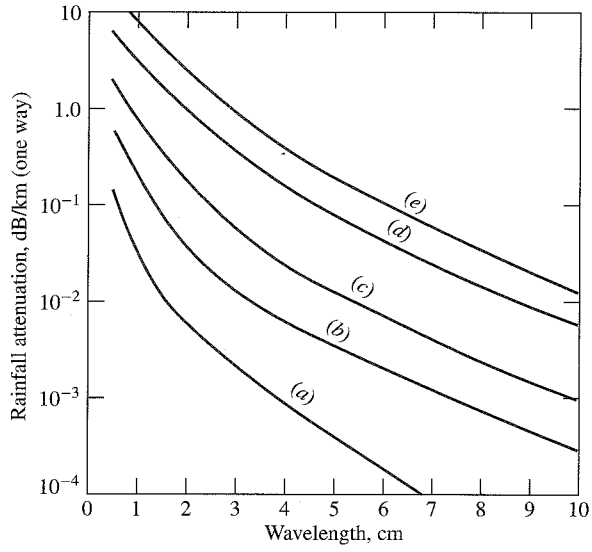

Figure 7.19 One-way attenuation in rain at a temperature of 18°C. (a) Drizzle—0.25 mm/h; (b) light rain—1 mm/h; (c) moderate rain—4 mm/h; (d) heavy rain—16 mm/h; (e) excessive rain—40 mm/h. In Washington, D.C., a rainfall rate of 0.25 mm/h is exceeded 450 h/yr, 1 mm/h is exceeded 200 h/yr, 4 mm/h is exceeded 60 h/yr, 16 mm/h is exceeded 8 h/yr, and 40 mm/h is exceeded 2.2 h/yr.

moderate rain. At Washington, D.C., this rainfall rate is equaled or exceeded approximately 60 h/yr.[117] As has been mentioned, attenuation is generally not a problem at frequencies below *X* band, unless the precipitation is very heavy.

7.7 OTHER SOURCES OF ATMOSPHERIC ECHOES

Radar echoes are sometimes obtained from regions of the atmosphere where no apparent reflecting sources seem to exist. Before the causes of these echoes were understood they were called *angels.* Today we know that discrete or "point" angel echoes are usually due to birds or insects. Even though the echo from a single bird or insect is small, it can be detected by radar if the range is short enough. For example, a radar that can detect a target with a radar cross section of 1 m^2 at a range of 200 nmi can detect a 10^{-2} m^2 target (a large bird) at a range greater than 60 nmi, and a 10^{-4} m^2 target (a large insect) at a range of 20 nmi. Angel echoes also can be caused by large flocks of birds, especially during migration season, or by large numbers of insects.

Distributed angel echoes can be due to inhomogeneities in the atmosphere such as clear-air convective cells and other turbulent atmospheric effects. Echoes from atmospheric turbulence are weak and can only be detected by powerful radars or at short range. Echoes from birds and insects, on the other hand, can be quite substantial in numbers and can be seen within a large area of the radar coverage. They can present a problem to an unprepared radar designed to detect aircraft. Operation at VHF or UHF can reduce the backscatter of insects and, to some extent, the echo from small birds when their cross sections are within the Rayleigh scattering region where the cross section is proportional to the fourth power of the frequency.

Knowledge of the scattering characteristics of birds and insects is important for understanding their effect on radar performance. In addition, radar has proven to be an important instrument for the study of the flight characteristics of insects (entomology) and birds (ornithology). It can obtain information not possible by other sensing means.

Birds Table 7.4 gives examples of the radar cross sections of birds taken at three frequencies with vertical polarization.[118] The largest values occur at *S* band. It is difficult, however, to be precise about the radar cross section of birds since echoes can fluctuate over quite large values, with the maximum and minimum differing at times by more than two orders of magnitude.[118]

The effect of birds on radar depends on the total cross sections that can be expected from large flocks. Table 7.5 gives representative estimates of the area over which bird echoes might be expected, the number of birds within the area, their density, individual cross section, and the volume reflectivity η (or radar cross section per unit volume). The value of η can be used in Eq. (7.2) to find the clutter cross section σ_c for the radar equation. This table is taken from an excellent review paper[119] published in the *Proceedings of the IEEE* by Charles Vaughn of NASA, Wallops Island, VA. (References to the sources of this information can be found in Vaughn's paper.) According to Table 7.5, most birds fly at altitudes less than a few hundred meters; but at times they have been observed much

Table 7.4 Radar cross sections of birds.[118]

Bird	Frequency Band	Mean Radar Cross Section (cm^2)	Median Radar Cross Section (cm^2)
Grackle	*X*	16	6.9
	S	25	12
	UHF	0.57	0.45
Sparrow	*X*	1.6	0.8
	S	14	11
	UHF	0.02	0.02
Pigeon	*X*	15	6.4
	S	80	32
	UHF	11	8.0

higher.[120] Over the ocean, the altitudes of migrating land birds have been reported as high as 4000 m.[121] Birds generally fly at speeds of from 15 to 40 kt,[122] and some have been observed at greater than 50 kt. These speeds are too high to be rejected by conventional microwave MTI radars without special design consideration.

The radar echo from a bird exhibits a periodic modulation that is caused by the beating of the bird's wings. A wing-beat fluctuation in radar cross section of 10 dB is common. A single tracked bird has sometimes been observed to fluctuate as much as 30 to 40 dB at the wing-beat rate.[119] The wing-beat frequency might vary from a few Hz to 10 to 20 Hz. The nonsinusoidal nature of the wing-beat modulation results in a spectrum with significantly higher harmonics. One estimate of the wing-beat frequency is given by $fL^{0.827} = 572$, where f is the wing-beat frequency in hertz and L is the length of the bird's wing in millimeters.[123] The spectral components of the wing-beat modulation has been said to be remarkably stable and suited for recognition.[124]

Williams and Williams[121] state that the great majority of radar observations of birds over the ocean are straight tracks at altitudes of more than 100 m, and are found at the season of peak land-bird migration on nearby continents. Migrating land and sea birds move over the oceans in massive waves that can extend up to a thousand kilometers wide and a hundred kilometers deep. The maximum density of radar echoes over the ocean is said to be significantly less than that detected with similar radars at continental sites. Williams and Williams also report that radar will often detect no bird echoes over the ocean for several days and then suddenly the display will be filled with small echoes, all moving at about the same direction and speed. Sea birds are usually seen close to the surface of the sea and move in curving paths rather than in the large number of parallel tracks typical of migrating land birds. Land birds cannot feed or rest over the sea and must make nonstop flights. Sea birds, on the other hand, feed from the sea and make use of dynamic soaring.

A statistical prediction of radar bird clutter was reported for the Distant Early Warning (DEW) line of aircraft surveillance radars that were located in northern Canada and

Table 7.5 Representative order of magnitude values for some high average areal number densities of birds (integrated over altitude), most of which are averaged over wide geographical areas. The cross section values apply for frequencies from *S* to *X* bands.

Type of Concentration	Area Affected (km^2)	No. of Birds	n ($Birds/m^3$)	σ (cm^2)	η (cm^{-1})
Blackbird roosts lower Miss. Valley (winter)	10^5	10^8	$10^{-6(1)}$	5–50	10^{-11}–10^{-10}
Single blackbird roost (Winter feeding area)	10^3–10^4	10^7	10^{-6}–$10^{-5(1)}$	5–50	10^{-11}–10^{-9}
Crows, gulls, geese, and ducks costal areas, wildlife refuges (winter)	10^3	10^4–10^6	10^{-9}–$10^{-6(2)}$	10–500	10^{-13}–10^{-9}
Shearwater migration, California coast	10^3	$> 10^6$	$10^{-5(3)}$	50–500	10^{-9}–10^{-8}
Greater Shearwater (*Puffinus gravis*) Georges Banks, non-breeding	10	10^5	$10^{-4(3)}$	50–500	10^{-9}–10^{-8}
Wading and seabird (breeding) U.S. Gulf Coast	10^5	10^6	$10^{-9(2)}$	50–500	10^{-13}–10^{-12}
Nocturnal fall migration U.S. east of Rocky Mts.	10^7	10^9	$10^{-7(4)}$	1–50	10^{-13}–10^{-12}
Nocturnal fall migration, one location, eastern U.S.	$> 10^3$	?	$10^{-6(4)}$	1–50	10^{-12}–10^{-10}
Quelea (*Quelea quelae*) breeding colony, semi-arid African savannahs	2	$> 10^7$	$10^{-2(1)}$	5–50	10^{-7}–10^{-6}
Quelea, semi-arid African Savannahs	10^9	10^9–10^{11}	10^{-9}–$10^{-7(1)}$	5–50	10^{-14}–10^{-11}

[1] [(1)]10 percent within 100 m of the ground.

[2] [(2)]50 percent within 200 m of the ground.

[3] [(3)]50 percent within 20 m of the surface.

[4] [(4)]50 percent within a 500 m interval.

[5] Sources of this information can be found in Vaughn,[119] from which this table was taken. (*Copyright 1985 IEEE*)

Alaska.[125] Birds in this region can be relatively large, and can have mean cross sections of about 0.02 m^2 at *L* band and 0.05 m^2 at UHF. A migrating flock might contain between 25 and 100 birds, but at times can be as large as 1000. The probability that a flock of Elders, a common northern bird, will have a radar cross section greater than 0.1 m^2 was said to be 90 percent, and the probability that the cross section will be greater than 1.0 m^2 is 50 percent. In northern Alaska, for example, from July to September, approximately 1.5 million large size birds such as ducks, swans, and geese can be expected to migrate across the length of the DEW line. It was estimated that the maximum number of birds

that might be seen on a particular radar screen at various locations along the DEW line during the peak of the migratory season could vary from 8,000 to 30,000.

There are times when birds or insects can cause serious degradation of radar performance if the radar operator and/or designer are not aware of the effects that birds can have as moving clutter echoes. Radars that have to operate reliably under all conditions need to account for clutter from birds and insects. Most civil air-traffic control air-surveillance radars employ sensitivity time control (to be described later in this chapter) to turn down the receiver gain at short ranges so as to reduce the clutter from nearby birds and insects. Military air-surveillance radars cannot reduce their gain by means of sensitivity time control in order to avoid low cross section birds and insects, since a military radar's target of interest can also have low cross section. During migratory seasons, bird echoes can extend over a wide area and can cause great concern to those who are not aware of what is happening. In addition to times of migration, Vaughn[119] states that mass bird concentrations can occur in the vicinity of breeding colonies, nocturnal roosts, premigratory staging areas, and concentrated feeding areas.

Vaughn summarizes the effect of birds on radar as follows:

> "From spring through fall, birds and/or insects are generally common to abundant in the atmosphere to an altitude of 1 or 2 km over most land areas of the world—especially at night. Some migrant bird species regularly fly above 4-km altitude and more than 1000 km from the nearest land. From the surface to 2-km altitude a density of 10^{-7} to 10^{-6} m^{-3} birds is not uncommon; in areas with social gatherings, 10^{-5} m^{-3} birds can be encountered during the day. A radar resolution cell of 10^6 to 10^7 m^3 (which will occur within 20 km of many radars) will result in a significant fraction of these cells occupied by at least one bird. Single birds typically have mean σ [radar cross section] from 10^0 to 10^2 cm^2, while migrant flocks, which often occur during the day, can have a mean σ greater than 10^4 cm^2."

Insects Despite their small size, insects can be detected by radar, especially at short range. In sufficient numbers, insects can *clutter* the display and prevent the detection of desired targets. It has been said that the density of airborne insects can be many orders of magnitude greater than the density of birds.[119]

Figure 7.20 is an approximate plot of the *X*-band radar cross section of insects as a function of their mass. This particular curve is taken from E. F. Knott,[126] who based it on a much more complete presentation of insect cross sections given by J. R. Riley.[127] The reader is referred to Riley's paper for the complete list of insects that make up this plot. Riley states that the data indicate that "the radar cross section of an insect may be very approximately represented by that of a spherical water droplet of the same mass, and that this representation holds true over a mass range of 10,000:1." This is only approximate since the cross section of insects is aspect dependent. Insects have been observed to have echoes at broadside aspect of from 10 to 1000 times greater than when viewed end-on.[128] Insects generally travel with the wind. Because of the aspect dependence, when a radar looks into or away from the wind, the radar echoes from a swarm of insects will be smaller than the echo when looking broadside to the wind direction. Thus the configuration of a large area of insects on a PPI display will not be uniform with angle, but more like a figure-eight. (The orientation of the figure-eight can indicate the approximate direction of

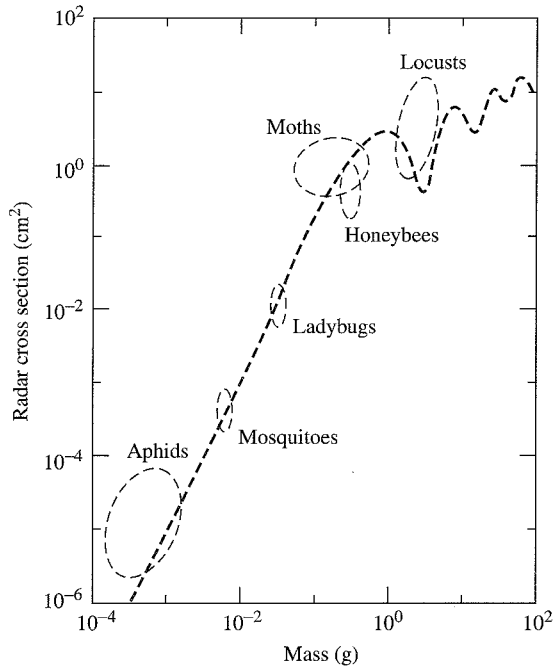

Figure 7.20 Sample of measured radar cross section of insects as a function of insect mass, as drawn by E. Knott[126] from data presented in a paper by J. Riley.[127] The dashed curve is the calculated cross section of spherical water drops, and is shown for comparison.
| (Copyright, 1985 IEEE.)

the wind, with a 180° ambiguity.) The wing beat of insects is also observed to produce a distinctive modulation on the radar echo. It has been said,[128] "Male and female grasshoppers and locusts usually differ significantly in size and hence in wing-beat frequency, making it possible to distinguish sexes under favorable circumstances."

Radar echoes can be produced by insect concentrations that would scarcely be noticed visually. Insect echoes are more likely to be found at the lower altitudes, near dawn and twilight. The majority of insects do not fly at temperatures below 40°F (4.5°C) or above 90°F (32°C), so that large concentrations of insect echoes would not be expected outside this temperature range. As with clutter due to birds, sensitivity time control can reduce the adverse effects of clutter caused by insects.

Vaughn[119] summarizes his discussion of insects as follows:

> "Insect densities can easily exceed 10^{-5} to 10^{-4} m^{-3}, while 10^{-3} to 10^{-2} m^{-3} insects seem to be regularly encountered when a wind field convergence brings them together. The highest densities are very local, less than 100 km^2 probably being a typical area of concentration. Insects also trace many atmospheric boundary layer features, thus complicating data interpretation by radar meteorologists . . . . At a wavelength of less than 3–5 cm, a volume reflectivity due to insects of 10^{-8} cm^{-1} might reasonably be expected in a region of wind convergence; 10^{-11} to 10^{-10} cm^{-1} should be regularly expected elsewhere."

Table 7.6 is a summary of some relevant number densities compiled by Vaughn from a number of sources. His paper gives the references for the values shown in the table.

Table 7.6 Summary of number densities of insects; as presented by Vaughn[119] based on data from R. Rainey and C. G. Johnson. The altitude in the table is that at which the sample was taken. The cross section is at *X* band.

Sample	Altitude (m)	Insects (m^{-3})	σ (cm^2)	η (cm^{-1})
Medium sized butterflies (perids), heavy migration	surface	10^{-2}	10^{-2}–10^{0}	10^{-10}–10^{-8}
Major aphid migration	surface	10^{0}	10^{-3}–10^{-2}	10^{-9}–10^{-8}
Noctuid moths	surface	10^{-2}	10^{-1}–10^{0}	10^{-9}–10^{-8}
All insects in 1 h	surface	10^{1}	10^{-3}–10^{-1}	10^{-8}–10^{-6}
Stratified desert locust swarm	near surface	10^{0}	10^{-1}–10^{0}	10^{-7}–10^{-5}
Suction trap during passage of intertropical front, Africa	15	10^{-2}	10^{-3}–10^{0}	10^{-11}–10^{-8}
Aircraft flying across intertropical front	300	10^{-3}	10^{-3}–10^{0}	10^{-11}–10^{-8}
Mean over 50-km traverse. Mostly *Aiolopus simulatrix*	450	10^{-3}	10^{-2}–10^{0}	10^{-11}–10^{-9}
Spodoptera exempta, average over 12-h period	2	10^{-2}	10^{-2}–10^{0}	10^{-10}–10^{-8}

[Copyright 1985 IEEE.]

Clear-Air Turbulence Radar echoes from clear air (no birds, insects, clouds, dust, or precipitation) are caused by inhomogeneities in the refractive index (index of refraction) of the atmosphere that result from turbulence.[129,130] (The index of refraction is the square root of the dielectric constant.) The refractive index of the atmosphere is a function of the water vapor (humidity), temperature, and pressure. At microwave frequencies, inhomogeneities in the water vapor are usually more important than inhomogeneities in the temperature or pressure. Reflections from clear-air turbulence are small in terms of radar cross section and are detectable only by large radars or at close range.

The atmosphere can be considered turbulent everywhere, but its intensity varies widely both in space and time. It is only when turbulence is concentrated into regions of greater or lesser intensity than its surroundings (so that there is a contrast that can be detected) is it of interest as an electromagnetic scatterer. There are at least two types of turbulent atmospheric phenomena that result in clear-air echoes. One is the *convective cell,* or *plume,* that occurs in the lower part of the atmosphere. Atmospheric convective cells, also called *thermals,* are the means by which birds and gliders soar. The other turbulent phenomenon is the *atmospheric horizontal layer,* which can occur at any altitude and is the turbulent effect that aircraft encounter at the higher altitudes. To radar, the atmospheric layer is generally weaker than the convective cell.

The basic theory for scattering from homogeneous, isotropic turbulence was first given by Tatarskii.[131] The radar reflectivity (cross section per unit volume) of a homogeneous turbulent medium is given as

$$\eta = 0.38 C_n^2 \lambda^{-1/3} \qquad [7.41]$$

where C_n^2 is the *structure constant* (a measure of the intensity of refractive-index fluctuations), and λ is the radar wavelength. At altitudes of several hundred meters, values of C_n^2 can be between 10^{-9} and 10^{-11} $m^{-2/3}$, which correspond to a volume reflectivity of about 0.8×10^{-9} to 0.8×10^{-11} m^{-1} at S band ($\lambda = 10$ cm). This is quite low, as can be seen by comparison with the volume reflectivity of rain in Fig. 7.18. The value of C_n^2 is variable and decreases with increasing height. At an altitude of 10 km, it can have values in the vicinity of 10^{-14} $m^{-2/3}$. An S-band radar with a 1° beamwidth and a 1-μs pulse width viewing a turbulent medium with $\eta = 10^{-9}$ (a very high value) sees a radar cross section at 10 km of about 3×10^{-3} m^2. Thus even with large values of C_n^2, echoes from clear-air turbulence are not likely to bother most radars.

Doppler weather radars, such as Nexrad[133] and the Terminal Doppler Weather Radar,[134] are used to detect wind shear, including that caused by the dangerous microburst, or downburst.* Wind shear caused by a downburst can be a hazard to aircraft during landing or take-off. It has sometimes been said that these radars detect clear-air wind shear, but the atmospheric wind-shear pattern is usually inferred from the radar echo of wind-driven rain rather than clear-air turbulence. When a downburst occurs without the presence of rain, wind-blown dust and insects provide the echoes that allow wind shear to be detected.

Other "Angel" Echoes Radar has been reported to detect the passage of an invisible sea breeze as it moves toward the shore.[103] Echoes have also been reported from the vicinity of forest fires, dump fires, and oil fires.[135,136] The reflectivity of smoke from such fires is too small to account for these echoes. Such echoes might be caused by numerous large particles and debris lifted into the air above the fires and/or by the generation of atmospheric turbulence due to the high heat from the fire.

Another example of clear-air echoes that are detectable by radar is gas seepage from underground oil and gas deposits.[137,138] Although these echoes are weak and the radar used for this purpose is small (a modified civil marine radar), the observations are performed at short range (500 to 1000 ft). This radar technique has been used commercially on many occasions for oil and gas exploration. It is speculated that the radar is detecting turbulent water vapor included with the gas seepage.

Ring echoes, or ring angels, are sometimes observed on PPI displays.[139] They start as a point and form a rapidly expanding ring. After one ring grows to a diameter of several miles, a second ring forms. Other rings can form in succession. They expand at velocities typically ranging from 20 to 30 kt and can attain diameters of 30 km or more. Over time, their appearance is similar to the outward moving ripples that occur when a pebble is dropped in a pond of water. These ring echoes have been associated with birds, such as starlings, flying away from their roosting areas at sunrise.

7.8 DETECTION OF TARGETS IN CLUTTER

Chapters 2 and 5 discussed the radar detection of targets when radar sensitivity is limited by receiver noise. When clutter is larger than receiver noise, different radar design methods

*Wind shear in radar meteorology is the local variation of wind velocity in range, altitude, or azimuth (or x, y, and z in a rectangular coordinate system). According to Theodore Fujita of the University of Chicago, a downburst is a strong downdraft that induces an outburst of damaging winds on or near the ground.

need to be employed for target detection. This section discusses the various techniques that might allow the detection of desired targets in the presence of undesired clutter echoes.

There is no one method that works equally well for the detection of all targets in various types of clutter. In brief, the major techniques available to the radar designer may be summarized as follows:

- The *doppler frequency shift* in MTI and pulse doppler radar is a powerful method for separating moving targets from stationary clutter.
- *High resolution in range and/or angle* reduces the amount of clutter with which the target must compete, thus increasing the signal-to-clutter ratio.
- Generally, for many types of clutter the *lower radar frequencies* produce smaller echo power. (An exception is an ionized media such as meteor trails and aurora).
- The use of *polarization discrimination* can increase the target-to-clutter ratio from some types of clutter, such as rain.
- *Clutter-echo decorrelation* by observing the target and clutter at different times or with different frequencies has some limited potential for allowing improved detectability.
- There are also techniques that help to *avoid saturation* of the receiver due to large clutter echoes. These can be important to good radar performance even though they do not increase the target-to-clutter ratio.

Doppler Frequency Shift (Target Radial Velocity) The doppler frequency shift of the echo signal is widely used for separating a moving target's echo signal from large, unwanted stationary clutter echoes. Doppler filtering allows echoes of moving targets to be separated from those of stationary clutter even though the clutter might be greater by many orders of magnitude. This is the basis for moving target indication radar (MTI), pulse doppler radar, and CW radar (Chap. 3). In spite of limitations, doppler filtering works well and can provide far greater suppression of the clutter echoes than any other technique.

Since radar echoes from land usually are much larger than those from the sea, the use of doppler filtering to detect aircraft is more demanding over land than over the sea. In the absence of ducted propagation or mountainous terrain, clutter usually does not extend more than a few tens of miles when the radar is at or near the surface. Airborne radars, however, can look down on extensive land or sea clutter and can experience surface clutter at relatively long ranges compared to what is observed from land or ship-based radars. When doppler filtering is employed to detect moving targets in rain, the rain itself is moving and the doppler processor must be designed differently from a doppler processor designed for stationary clutter. The MTD radar described in Sec. 3.6 is an example of how aircraft can be detected in the presence of moving rain clutter.

High Resolution The smaller the radar resolution cell, the less will be the competing clutter echo. The benefit of small resolution cells is indicated in the radar equations for detection of targets in surface clutter [Eq. (7.8)] and in rain [Eq. (7.37)]. Short pulses (or the equivalent pulse compression) and narrow-beamwidth antennas, therefore, can reduce

the amount of clutter with which the target echo signal must compete. High resolution usually is the preferred method for detection of ships.

With large resolution cells, the clutter statistics can be described by the Rayleigh probability density function (pdf). With small resolution cells, however, sea clutter is no longer Rayleigh and is likely to produce higher values (such as from sea spikes) than predicted by Rayleigh clutter. The result is that serious false alarms can occur when small targets are to be detected if the clutter is non-Rayleigh but the receiver is designed on the basis of Rayleigh statistics. Increasing the detection threshold can reduce the false alarms from non-Rayleigh clutter, but it results in the undesired lowering of the probability of detection. Other solutions are required.

A knowledge of clutter statistics is necessary for receiver design based on classical detection theory. It is also needed to design CFAR (Sec. 5.7) when an optimum detector is not practical. Unfortunately, the statistics of the sea clutter are variable, and it is not always possible to specify a single statistical description of the clutter when the statistics are not Rayleigh.

High resolution is usually a good method for enhancing the signal-to-clutter ratio, even when the statistics of the clutter are not Rayleigh. It is one of the few methods available for increasing the target-to-clutter ratio when the target is stationary (no doppler shift).

The clutter echo must be large compared to receiver noise in order for the clutter radar equations [Eqs. (7.8 and 7.37)] to apply. If this condition is not met, it is not necessarily bad since it means that radar detection will be noise limited rather than clutter limited—which is to be preferred. It is cautioned that the resolution cell size cannot be decreased without limit when considering detection of signals in clutter. With a small enough resolution cell size, the radar becomes noise limited and there is no need for a further decrease.

High-Resolution Clutter and Detector Design With sea clutter, non-Rayleigh clutter statistics might be expected to appear when the beamwidth is less than about one degree and the pulse width is less than about one μs (as indicated in the previous discussion of sea spikes in this chapter). Non-Rayleigh sea clutter is especially obvious when pulse widths are on the order of nanoseconds. Attempts have been made to model the statistics of high-resolution sea clutter, but without total success. The Rayleigh pdf generally underestimates the range of values obtained from real sea clutter. On the other hand, the log-normal pdf tends to overestimate the range of values. Several other analytical pdfs that lie between these two extremes have been suggested for modeling the statistics of sea clutter, some of which were mentioned in Sec. 7.5.

Any particular probability density function might be able to fit some particular set of data; but there does not seem to exist a single analytical form of probability density function that fits all the observed data and can be correlated with environmental parameters. For this reason it has not been practical to design a detector in a classical manner when sea clutter is dominant. (*Classical manner* means that the optimum detector is found based on the statistics and correlation properties of the background clutter and target signals.)

Billingsley[140] has said that on the basis of many measurements of various types of land clutter at low depression angles, "measured amplitude distributions almost never pass

rigorous statistical hypothesis tests for belonging to Weibull, log normal, or other theoretical distributions that have been tried." Thus the fitting of experimental data to arbitrary statistical models has not been successful as a method for describing clutter to aid in radar design.

When the clutter cannot be described by a specific pdf, *robust detection* and *distribution-free detection* are often considered. A robust detector is one that works satisfactorily when the clutter (or noise) statistics can be described as one of a family of pdfs or a number of different classes of pdf. It is not necessarily optimum for any of them. A distribution-free detector makes as few assumptions as possible regarding the statistics of the clutter or noise.[141] Its probability of false alarm is supposed to be constant under weak assumptions on the statistical character of the clutter. Distribution-free detectors have not been used much in practice because they are not easy to implement and the loss in detectability is larger than might be desired. The term *nonparametric detector* is sometimes used interchangeably with the term *distribution-free detector.*

The *median detector* and the *m-out-of-n detector* (Sec. 5.6) are examples of robust detectors that have been considered for detecting targets in high-resolution sea clutter. A median detector is one that bases its detection decision on the median value* of n received pulses. Trunk and George[142] showed that the *median detector* gave better performance in non-Rayleigh clutter than the conventional receiver (which can be called a *mean detector*). A median detector is robust in that the threshold values and detection probabilities do not depend on the detailed shape of the clutter pdf, but only on its median value. For instance, if one of the n received pulses happens to be very large, it can have a significant effect on the mean value; but it would have no greater effect on the median value than a pulse that is only slightly larger than the median. Trunk[143] has shown that the *trimmed-mean detector* is even better than the median detector for non-Rayleigh clutter. If there are n pulses available from which to make a detection decision, the trimmed-mean detector discards the smallest and the largest of the n pulses before finding the mean and making a detection decision. Although its performance may be attractive, the trimmed mean is more difficult to implement in practice since the n pulses must be rank-ordered to find the smallest and the largest.

According to Schleher,[144,145] the median detector is inferior to both the m-out-of-n detector and the logarithmic detector when clutter can be described by the Weibull pdf. The optimum value of m for an m-out-of-n detector will depend on the nature of the pdf. When the optimum m is used with non-Rayleigh clutter, Schleher states that the m-out-of-n detector is better than other detection criteria.

The logarithmic detector has an output voltage whose amplitude is proportional to the logarithm of the input envelope. A logarithmic characteristic provides a constant false-alarm rate (CFAR) when the clutter is described by the Rayleigh pdf (see the log-FTC discussion presented later in this section). The performance of the logarithmic detector in non-Rayleigh clutter is almost as good as the m-out-of-n detector and is probably easier to implement.[145] A variant sometimes useful for reducing the false-alarm rate in non-Rayleigh clutter is the *log-log detector.* In one implementation, this is a logarithmic receiver in which the slope of the logarithmic characteristic progressively declines by a

* The middle value of a statistical distribution, above and below which lie an equal number of values.

factor of 2 to 1 over the range from noise level to +80 dB.[146,147] In the log-log detector, the higher clutter values (tails of the distribution) are subjected to greater suppression.

Land Interclutter Visibility The patchiness of land clutter, when viewed with high-resolution radar at low grazing angles, usually is beneficial for target detection. Patches of large clutter are separated by areas with little or no clutter. Typical sizes of clutter patches can be several kilometers on a side. Billingsley[140] states that the macropatches of clutter might typically occupy about one half of the resolution cells of discernible clutter. However, for level terrain in which only isolated discrete clutter echoes appear, the percentage of cells with clutter might be as low as 25 percent. For high radar sites and/or steep terrain "in which relatively full illumination exists, it can approach 100%." Interclutter visibility is a result of masking caused by hills or higher levels of terrain which create shadow areas where clutter echoes are absent. Aircraft targets can be detected in regions with low or no clutter even though they might be undetectable when within patches of high clutter.[148] It has been said that at low grazing angles over land, interclutter visibility can be expected with beamwidths less than a degree and pulse widths less than one μs.[149]

Weather Reducing radar beamwidth and/or pulse width is generally considered good for decreasing the weather clutter with which the target must compete. There is, however, little information on the characteristics of rain with high-resolution radar.[150] Most forms of rain are not uniform when viewed with high resolution; but for purposes of radar design, it is usually assumed so. Reducing the radar resolution cell to improve signal-to-clutter ratio is an acceptable technique, but the designer should be aware that a small resolution cell size might cause the statistics of the clutter to become non-Rayleigh and increase the probability of false alarm.

Target Break-up with High-Resolution Waveforms In some cases, the range resolution cell might be smaller than the dimensions of the target, resulting in "break-up" of the target echo. This means that the cross section of each resolved area of the target will be less than the total cross section as seen by a lower resolution radar. A serious reduction of detectability need not occur because of target break-up. Reduction of clutter by high range-resolution is still a good tactic.

If echoes from the various parts of the target viewed with high-resolution radar are properly displayed to an operator, and if the operator knows the general shape of the target or even that it is a distributed target, there appears to be little, if any, loss in detectability. The operator seems to be able to provide a form of noncoherent integration. Even if the recognition ability of an operator is not utilized, detectability will likely be reduced only slightly with high resolution since many targets tend to consist of one or a few large scatterers and a large number of small scatterers.[151] The echo in the largest resolution cell and in surrounding cells might still be of significant value to produce adequate detection.

Hughes[152] has investigated detection strategies when the radar resolution is less than the target dimensions. He assumed, for sake of discussion, that a range cell was 10 ns (5 ft) and that a 100-ns window was examined. The distributed target was completely

within the 100-ns window. Clutter was homogeneous and described by a gaussian distribution. In one strategy, a threshold decision was made every resolution cell (10 ns), and any threshold crossing within the 100 ns window was declared a detection. This is similar to an m-out-of-n detector with $m = 1$. The other strategy, called the integrated detector, was to integrate 10 cells and make a detection decision every 100 ns. As reference case with which to judge these two procedures, Hughes took a 100-ns range cell with a detection decision made every 100 ns. The reference case was always significantly worse than either of the two strategies. Hughes concluded that the strategy that is better depends on the a priori knowledge of the target's nature that is available to the designer. If about two-thirds or more of the target echo energy comes from a single "flare" point, or individual scatterer, the m-out-of-n detector will be better. He stated that the correct strategy to use can be chosen if detailed knowledge of the target is known. Without such knowledge or when a variety of targets must be detected, the second strategy—integration before detection—is better.

Frequency Radar echoes from rain, sea (with horizontal polarization), and (to some extent) land decrease with decreasing frequency. Although this favors the lower frequencies, it is more difficult at the lower frequencies to achieve narrow beamwidths and high range-resolution. Thus some of the benefits of reduced clutter at the lower frequencies might be partially offset by the poorer resolution that results.

Rain The radar equation for detection of targets in rain, Eq. (7.37), shows that for a constant-gain antenna the range varies as the square of the wavelength. (For an antenna with a constant effective aperture, however, the range is directly proportional to wavelength.) There can be great benefit in using lower frequencies to reduce rain clutter. It is unlikely, for instance, that a radar at UHF or lower frequencies will be degraded by rain clutter. Unfortunately, as indicated above, in some applications it is not always possible to operate radars at frequencies low enough to make rain clutter negligible because of other undesirable constraints such as broad beamwidth, narrow bandwidth, a crowded frequency spectrum, external noise, and poor low altitude coverage.

Radars at L band or higher frequencies are likely to be affected by rain clutter. Some higher frequency radars might even be rendered useless in rain if no corrective measures are taken.

Sea The plot of σ^0 versus grazing angle that was shown in Fig. 7.13 for sea clutter indicates that at low grazing angles and horizontal polarization, the lower the frequency the lower will be the echo from the sea when everything else remains the same. There are some reservations, however, about how low in frequency one might wish to go. The lower the frequency, the more difficult it is to direct the radar energy at low angles. This is illustrated in Sec. 8.2, which shows that the elevation angle of the lowest interference lobe is $\lambda/4h_a$, where λ = wavelength and h_a = antenna height above the water. If the target of interest is a small boat, buoy, submarine periscope, swimmer, or low altitude (sea skimming) missile, the higher microwave frequencies might be preferred even though the sea clutter might be greater.

Another reason higher frequencies might be preferred in some overwater applications in spite of higher sea clutter is the better range and angle resolution that can be obtained. In addition to providing less clutter, the higher resolutions obtainable at the higher frequencies might be required for particular applications. An example is the civil marine radar, which is commercially available at both X and S bands. When radars at both frequencies are operated on a ship, it is the higher frequency radar (X band) that is generally depended upon, except in bad weather when rain clutter degrades the higher frequency much more than S band. The fact that sea clutter is less at the lower frequencies is but one of several factors to be considered in the selection of the best frequency for a particular radar application.

Land Although it was shown in Fig. 7.10 that land clutter at high grazing angles decreases with decreasing frequency, the frequency dependence is not usually a major consideration in radar design. At low grazing angles, Fig. 7.5 and the discussion of Sec. 7.3 show that for any particular type of terrain there might be significant variation of clutter with frequency, but the mean value of clutter taken over all types of terrain (excluding urban area) is essentially independent of frequency.

Polarization

Rain Circular polarization is often employed to reduce weather clutter in microwave air-surveillance radars. Discrimination of a target located in the midst of rain results because the echo from an aircraft (an asymmetrical scatterer) differs from that of a raindrop (a circularly symmetric scatterer) when using circular polarization. This difference in scattering can be used to enhance the echo from the target and suppress echoes from rain.

A circularly polarized wave incident on a spherical scatterer will be reflected as a circularly polarized wave of opposite sense of rotation (when viewed in the direction of propagation) and will be rejected by the same antenna that originally radiated it. On the other hand, when a circularly polarized wave is incident on an asymmetrical target such as an aircraft, it has been found experimentally that the reflected energy is more or less equally divided between the two senses of polarization rotation.[153] The two senses of circular polarization are (1) right-hand circular, when the electric field rotates clockwise when viewed in the direction of propagation and (2) left-hand circular, when the electric field rotates counterclockwise. Since about half of the reflected energy is of the same sense of circular polarization as that transmitted, it will be accepted by the antenna that originally radiated it. The circularly polarized echo from spherical raindrops is of the opposite sense of polarization (when viewed in the direction of its propagation) and will be rejected by the radar antenna; but an aircraft will have a significant amount of its reflected energy with a polarization that is accepted by the antenna. This then provides target-to-clutter enhancement.

Raindrops are seldom perfect spheres, especially when they are large. They deviate from a sphere when their radius is greater than about 1 mm, and have a shape more like that of an oblate spheroid with a flattened base (a hamburger bun).[154,155] This particular raindrop shape, which is quite different from that usually depicted by an illustrator or

cartoonist, is a result of aerodynamic forces as the drop falls.[156] The greater its deviation from a spherical shape, the less the echo signal will be rejected. Thus circular polarization is limited in the amount of rain cancellation it can provide and becomes less as the rain becomes heavier.

In addition to the nonspherical shape of raindrops, the ability to cancel rain echo using circular polarization is limited by practical considerations. It is difficult to obtain an antenna with pure polarization that does not accept energy from the orthogonal polarization. The cancellation of an orthogonally polarized signal by an exceptionally well designed, well maintained antenna might be limited to about 40 dB, a very good value.[157] Most antennas are not this good, and they can be even poorer because of the depolarizing effects of the nearby environment. Depolarization is also introduced when propagating through rain located between the radar and the target. The different reflection coefficients of horizontal and vertical polarization on reflection from the earth's surface also will cause a change in the signal's polarization when multipath reflection occurs from the surface. This factor has been said to limit the cancellation of rain clutter in certain cases to 13 dB over water[158] and 34 dB over desert.[159]

The various forms of depolarization that cause circular polarization to become elliptical suggest that better rain cancellation might be achieved if the optimum form of elliptical polarization were used rather than circular. With the optimum elliptical polarization, cancellation in some regions of heavy rain might be increased by as much as 12 dB.[160] However, the polarization that is optimum for one particular region of rain might not be optimum for some other region of rain, and might prove to be worse than the cancellation obtained with circular polarization. The optimum polarization will depend on the distance traveled and the nature of the rain. Thus the polarization on receive should be adaptive and made variable with range (time). Nathanson suggested that an improvement in cancellation of 6 to 9 dB can be obtained with adaptive polarization.[161] Adaptive polarization, however, has not been easy to implement successfully.

The radar cross section of aircraft is generally less with circular polarization than with linear polarization. As mentioned above, experimental measurements indicate that when an aircraft is illuminated with one sense of circular polarization, the echo power on a statistical basis is divided more or less equally between right-hand and left-hand circular polarization. Other experiments, however, have shown the circular polarized echo to be smaller than the linearly polarized echo by about 5 dB for aircraft and even greater reductions for missiles and satellites.[162]

An alternative to circular polarization is to transmit with a linear polarization (horizontal or vertical) and receive with the orthogonal linear polarization. Spherical scatterers will not produce an echo at the orthogonal linear polarization; but asymmetrical scatterers will have energy in the orthogonal component. It has been suggested that crossed linear polarization might give better rain rejection than conventional circular polarization.[163] Some measurements show, however, that the backscatter from aircraft with the orthogonal linear polarization can be as much as 7 dB below that reflected at the transmitted linear polarization.[164]

Although the use of circular polarization is often employed in surveillance radars during rainfall, at the higher microwave frequencies where the echo from rain can be a problem, cancellations of heavy rain might be 15 dB or less. In heavy rain that accompanies

thunderstorms cancellations of only 5 dB have been observed.[161] If detection of targets in rain is important, then circular polarization might not provide all that is needed. MTI designed for moving clutter will obtain much greater clutter rejection. Lowering the frequency by a factor of 2 or using a pulse-compression waveform with a 13-bit Barker code could likely provide in heavy rain as much cancellation as circular polarization.

Sea Over the sea, horizontal polarization at low and moderate sea states results in less sea clutter than vertical, as was indicated in Fig. 7.13. The majority of the radars that operate over the sea employ horizontal polarization. If a target, such as an oil slick or a swimmer's head, lies on the water, vertical polarization is preferred even though sea clutter may be larger than with horizontal polarization. Sea clutter is large with vertical polarization at low angles for the same reason the echo energy from targets on the water surface is large: these targets and the sea surface are illuminated with more energy than if horizontal polarization were used because of the behavior of the vertical polarization reflection coefficient (Sec. 8.2).

Land It was mentioned in Sec. 7.3 that there is no significant difference between horizontal and vertical polarizations from land clutter when viewed at low grazing angles. Although there are indications that horizontal polarization produces a lower clutter echo than vertical, the difference is not significant enough to affect the choice of polarization in most radar applications over land.

Time Decorrelation Unlike receiver noise, clutter echoes are generally correlated from pulse to pulse, and sometimes even from scan to scan. The techniques of *rapid antenna scan* for detection of small targets in the sea, and *time compression* for detection of moving targets in patchy land or sea clutter are examples of detection techniques that try to take advantage of the nature of correlated clutter echoes.

Antenna Scan Rate (Sea Clutter) As mentioned previously in this chapter, when clutter is stationary (not moving) there is no gain to be had by integrating pulses. The sea is always changing, but over a short time interval it might not change sufficiently for the radar echo to be decorrelated pulse to pulse. For a medium-resolution *X*-band radar observing the sea at low grazing angles, the time required for the sea to decorrelate is about 10 ms.[165] Any pulses received during this time will be correlated and no improvement in signal-to-clutter ratio will result by integrating pulses. The sea surface, however, will often change by the time of the next antenna scan so that sea clutter is generally decorrelated from scan to scan. To take advantage of the decorrelation of sea clutter from scan to scan, the antenna rotation rate can be increased, as was first demonstrated by J. Croney for civil marine radar.[166]

Consider, for example, a civil marine *X*-band radar with a 1.2° beamwidth, pulse repetition frequency of 6000 Hz, and a 20-rpm antenna rotation rate. There will be 60 pulses in the 10 ms it takes for the beam to scan past a target. No integration improvement is obtained from adding these 60 pulses together since they occur within a time that is less than the decorrelation time of *X*-band sea clutter. If the antenna rotation rate is speeded up to 600 rpm, two pulses will be received per scan. These will be correlated, but the two

echoes received on the next scan, one tenth of a second later, will be decorrelated from the two echoes from the previous scan. In 30 scans at 600 rpm, there will be 30 sets of two pulses each, and each set will be decorrelated from the others. Thus there can be an integration improvement corresponding to that obtained with 30 independent samples. Experimental measurements with a civil marine radar having a 1° beamwidth and 5000 Hz pulse repetition frequency show that increasing the antenna rotation rate from 20 to 420 rpm improves the target-to-clutter ratio from about 4 to 8 dB, depending on the sea state.[167] The smaller improvement corresponds to the higher sea state.

Radars that use a high antenna-rotation-rate to improve detection of small targets in sea clutter include the AN/APS-116,[168] and its successor the AN/APS-137. The antenna scan rate in these radars is 300 rpm (five scans per second). Scan-to-scan integration is performed with an m-out-of-n detector. With spiky clutter, analysis shows that the best ratio of m/n was 0.6, which is larger than the optimum value used in an m-out-of-n detector when only receiver noise is present.

The decorrelation time of sea clutter is approximated by the reciprocal of the width of the clutter doppler spectrum. Normally, the decorrelation time might be expected to be inversely proportional to frequency, if the decorrelation is due solely to doppler effects. However, experimental measurements show that when the decorrelation time is 10 ms at X band, it will be about 60 ms at L band instead of the 70 to 75 ms predicted on the basis of an inverse relationship of decorrelation time and frequency. Therefore, it is found that when clutter spectra are given in units of velocity rather than frequency, the velocity spectra are broader at the lower frequencies.[169]

Time Compression Even if a target seen with a high-resolution non-MTI radar can be resolved in the midst of patchy land clutter or spiky sea clutter, it might be difficult to recognize the target from the clutter on the basis of a single observation. If the target is in motion, however, an operator can eventually distinguish it from the stationary clutter. One method that has been proposed to accomplish this is time compression, in which the last N scans of a radar are stored and then repeatedly displayed speeded up to accentuate the target motion. (The number of scans N might be from 5 to 10.) An operator's attention is called to the moving targets by the flickering of the repeated speeded-up scans. Even with a fixed target, time compression can separate the short duration sea spikes from the more persistent target echoes. As a target at long range comes within the coverage of the radar, there will be a delay of N scans before time compression can be fully effective. In the time needed to accumulate the N scans, however, a trained and alert operator might be expected to detect the moving target even without time compression.

Frequency Agility If the RF frequency of a pulse of duration τ is changed by more than $1/\tau$, the echo from uniformly distributed Rayleigh type clutter will be decorrelated. This can be shown by calculating the change in frequency Δf that causes the difference in the phase between the clutter echo from the leading edge of the range-resolution cell and the clutter echo from the trailing edge of the range-resolution cell to be greater than 2π radians (as in Problem 7.15). Pulse-to-pulse frequency changes (called *frequency agility*) greater than $1/\tau$ Hz will therefore decorrelate the clutter and permit an increase in target-to-clutter ratio when the decorrelated pulses are integrated. This assumes the target's physical size is small compared to the size, $c\tau/2$, of the radar resolution cell. When the

clutter is non-Rayleigh, as when there are one or a few dominate scatterers, there might be little benefit in the use of frequency agility. Spiky sea clutter, for example, is highly non-Rayleigh and frequency agility is not expected to offer much improvement. If land clutter is dominated by only one or a few large clutter scatterers in a resolution cell, the benefit of frequency agility also is lessened. Weather clutter is probably more uniform than either sea or land clutter, and frequency agility might be more effective than with other forms of clutter.[170]

The effect on the target and the clutter by changing frequency from pulse to pulse is illustrated in the A-scope presentations of Fig. 7.21.[171] The left-hand trace is that of a single frequency at *X* band. The clutter is shown on the left side of each figure. Its amplitude decreases with increasing range. A single target is shown on the right side. Its appearance indicates that it is composed of multiple scatterers. The right-hand trace is with pulse-to-pulse frequency agility. Two changes are noted: The clutter is smoothed in appearance and the target echo is larger. The increase in target echo is due to some of the individual frequencies returning large echoes from the target, at least as compared to the particular single frequency used in the upper trace. If a different frequency were chosen in the upper trace, it might have been larger or it might have been smaller. But by using multiple frequencies, the composite of the echoes is not as likely to produce a small echo as might a single frequency. If the target on the right side of the A-scope presentation were located in the midst of the clutter in the left-hand trace, it might not be detected. However, the target signal in the right-hand trace would likely be detected. It seems from this example that the real benefit of frequency agility is in the greater target cross section rather than the suppression of clutter.

It should be cautioned that conventional doppler filtering, as in MTI or pulse doppler radar, is not possible with pulse-to-pulse frequency agility.

Although frequency agility is sometimes claimed to be an attractive method for obtaining increased target-to-clutter ratio, it has not had the full success that its proponents

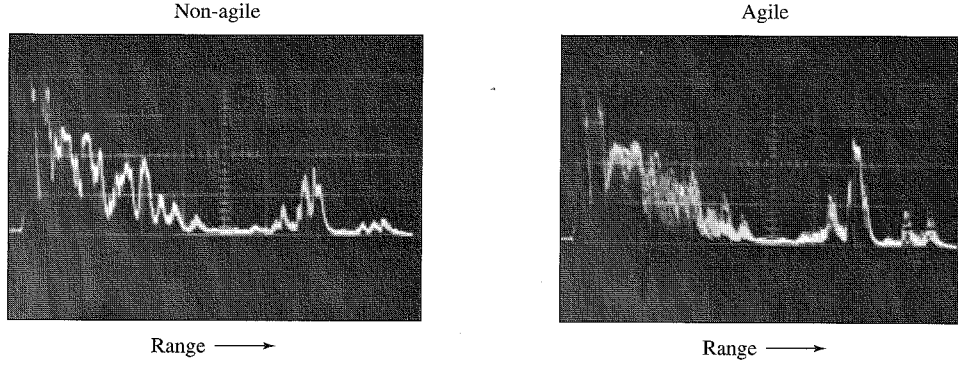

Figure 7.21 Effect of frequency agility on clutter and target. This A-scope presentation of clutter (left-hand side of each illustration) and a target (right-hand side of each illustration) was made with an *X*-band radar and a 0.2-μs pulse width. Left-hand trace is for a single frequency. Right-hand trace is for pulse-to-pulse frequency agility over a 100-MHz bandwidth.
(Courtesy of CPI Beverly Microwave Division, Beverly, MA.)

have desired since most clutter is non-Rayleigh. When a large frequency band is available, the bandwidth is usually better used to provide high range-resolution to decrease the clutter rather than to attempt to decorrelate the clutter by pulse-to-pulse frequency change.

Clutter Fence Reflections from nearby mountains and other large clutter might not be fully suppressed by conventional clutter reduction techniques. These echoes can be so large that they can enter the radar via the antenna sidelobes. At a fixed radar site it is possible to reduce the effects of such clutter by surrounding the radar with an electromagnetically opaque fence to prevent direct viewing of the clutter. The two-way attenuation provided by a typical clutter fence with a straight edge might be about 40 dB. Greater attenuation can be achieved by incorporating two continuous slots close to, and parallel with, the upper edge of the fence to cancel a portion of the energy diffracted by the fence. The increase in two-way attenuation by this method is 20 dB or more.[172]

A clutter fence can produce effects that are not always desirable. It can limit the accuracy of the elevation-angle measurement because of blockage and because of radar energy diffracted by the fence. Energy diffracted by the fence will interact with the direct energy and cause lobing of the radiation pattern in the angular region just above the fence. Radar energy backscattered by the fence towards the radar can sometimes damage the receiver front-end. In one design, the fence was tilted 15° away from the vertical to prevent damage to the receiver from occurring.[173]

Clutter fences are useful only when the targets are at higher elevation angles than the clutter. They have not been an attractive method to enhance target-to-clutter ratios for most applications.

Methods to Avoid Receiver Saturation by Clutter Echoes The finite dynamic range of radar receivers means that they can be saturated by large clutter signals, with the result that target echoes can be prevented from being detected even though they might be larger than clutter. Several methods have been used to minimize the effect of large clutter but they have no subclutter visibility in that they do not enhance the target-to-clutter ratio. They are useful, however, in preventing saturation or overload of the receiver, automatic processor, automatic tracker, or display.

Sensitivity Time Control (STC) The fourth-power relationship between the received echo-signal power and range means that clutter echoes at close ranges will be large and can saturate a radar receiver. A solution is to reduce the receiver gain at short ranges where the clutter echo signals are large, continually increase the gain as the pulse travels out in range, and finally operate at maximum gain (maximum sensitivity) at ranges beyond which clutter is expected. This is called *sensitivity time control* (STC). It has also been called *swept gain.* STC is used in air-traffic control radars to reduce nearby clutter from birds and insects as well as from land. The rate at which the gain is changed with time depends on the nature of the environment. It will be different, for example, when the radar is looking over water or desert than when the radar is looking over rugged or mountainous terrain. An air-surveillance radar might have more than one STC gain-versus-time characteristic that can be selected depending on the type of clutter the radar encounters. The

variation of gain with range might be as R^2 for rain, R^3 or R^4 for surface clutter, to R^7 over water at long range (as in a civil marine radar for targets below the lowest interference lobe[174]).

Even without the presence of clutter, STC can be used to compensate for the large change in the magnitude of the received target echo signal as a function of range. The change of target cross section with range has been said to overshadow other causes of echo variation.[175]

The use of STC causes the sensitivity of a 2D air-surveillance radar with a cosecant-squared antenna elevation radiation pattern (Secs. 2.11 and 9.11) to be reduced for targets at high angles and short range since the gain is lowered in these directions just as it is at low angles and long range. This can cause echoes from aircraft at short range and high altitude to be too weak to be detected. By modifying the cosecant-squared antenna pattern to direct more energy at the higher angles, it is possible to see these close-in aircraft even with STC applied. Multiple-elevation-beam (stacked beam) 3D radars can have a separate STC variation with range to match the clutter conditions found as a function of elevation angle.

STC usually cannot be used with pulse doppler and other radars that have prfs high enough to result in ambiguous range echoes. It can also cause degradation to pulse compression radars that employ very long uncompressed pulses, such as required with solid-state transmitters.

Raising the Antenna Beam Surface clutter can be decreased by raising the antenna beam in elevation and not illuminating the clutter. This technique can be applied only if the targets of interest (e.g., aircraft) are at a higher altitude than the clutter. Tilting an antenna beam upward reduces coverage at long range and low altitudes. A better technique is to use two beams in elevation, with one pointing higher than the other. Most civil air-traffic control radars use this method to reduce unwanted echoes from cars and trucks. In the ARSR-3 long range (nominally 200 nmi) air-traffic control radar, the gain of the upper beam is 16 dB less along the horizon than the gain of the lower beam along the horizon. The radar signal is transmitted on the lower beam and received only on the higher beam at short range so that surface clutter at short range is illuminated with less energy. After the pulse travels beyond the range of expected surface targets (typically 50 nmi in the ARSR-3), the receiver is shifted to the low beam to allow detection of aircraft at long range.

Log-FTC This is a receiver with a logarithmic input-output characteristic followed by a high-pass filter (sometimes called a *fast time-constant,* or FTC). When the input clutter or noise is described by the Rayleigh probability density function, the output clutter or noise is constant, independent of the input amplitude. Thus it acts to provide a constant false alarm rate, or CFAR.

The Rayleigh pdf can be written

$$p(v) = \frac{2v}{m_2} \exp\left(-\frac{v^2}{m_2}\right) \qquad v > 0 \qquad \textbf{[7.41b]}$$

where m_2 is the mean square value of v. The rms amplitude of the fluctuations about the mean (denoted here by δv_{in}) is proportional to the mean $\overline{v_{in}}$ or $\delta v_{in} = k\overline{v_{in}}$. (This is Problem 2.4.) A logarithmic receiver has the characteristic

$$v_{out} = a \log (bv_{in}) \qquad [7.42]$$

The slope of the logarithmic receiver characteristic at $\overline{v_{in}}$ is

$$\frac{\Delta v_{out}}{\Delta v_{in}} = \frac{a}{\overline{v_{in}}} \qquad [7.43]$$

If the input clutter fluctuations δv_{in} are small compared to the total range of the logarithmic characteristic, the output fluctuations δv_{out} are approximately

$$\delta v_{out} = \text{slope} \times \delta v_{in} = \frac{a}{\overline{v_{in}}} \delta v_{in} = ak \qquad [7.44]$$

Thus the output fluctuations are constant, independent of the input mean.

Although the output fluctuations about the mean are constant, the output mean is not. A high-pass filter removes the mean value of the output, leaving the fluctuation at a constant value on the display. The high-pass filter is equivalent to a differentiation.

The noise or clutter fluctuations that appear at the output of a logarithmic receiver are not symmetrical in amplitude since large amplitudes are suppressed more than normal. To make the output more like that of a linear receiver, the log-FTC may be followed by an amplifier with the inverse of the logarithmic characteristic (antilog).

A true logarithmic characteristic cannot be maintained down to zero input voltage since $v_{out} \to -\infty$ as $v_{in} \to 0$. At some point the receiver characteristic must deviate from logarithmic and go through the origin. Therefore, the practical receiver will have a linear characteristic at low signal levels and logarithmic at higher levels. This is called a *lin-log receiver.* The logarithmic receiver must be maintained at about 20 dB below the receiver rms noise level.[176]

Log-FTC prevents clutter from saturating the limited dynamic-range radar display and obscuring the presence of desired targets even though the targets may be of greater amplitude than the clutter. It is an example of a CFAR, but its effectiveness depends on the clutter having a Rayleigh pdf, which is not always the case.

The log-FTC was originally considered for the detection of targets in sea clutter;[176] however, it is probably more useful for operation in precipitation clutter. Precipitation is more likely to be described by a Rayleigh pdf than is sea or land clutter. When log-FTC when used for reducing the effect of rain, it has sometimes been called *weather fix.*

CFAR Circuitry for maintaining the false alarm rate constant (CFAR) has been described in Sec. 5.7 and by Taylor[177] in the *Radar Handbook.* As mentioned, CFAR does not provide an improvement in signal-to-clutter ratio, and it maintains the false-alarm constant at the expense of probability of detection. It also has the disadvantage of poorer range resolution and results in a loss in signal-to-noise ratio. It should be used only when necessary.

REFERENCES

1. Probert-Jones, J. R. "The Radar Equation in Meteorology." *Quart. J. Roy. Meteor. Soc.* 88 (1962), pp. 485–495.
2. Nathanson, F. E. *Radar Design Principles.* 2nd ed. New York: McGraw-Hill, 1991, p. 316.
3. Billingsley, J. B., and J. F. Larrabee: "Multifrequency Measurements of Radar Ground Clutter at 42 Sites," MIT Lincoln Laboratory, Lexington, MA, Technical Report 916, November 15, 1991, Vol. 1, Principal Results (ESD-TR-91-061); Vol. 2 Appendices A through D (ESD-TR-91-175); Vol. 3 Appendix E (ESD-TR-91-176). A condensation appears in Billingsley, J. B. "Radar Ground Clutter Measurements and Models, Part 1, Spatial Amplitude Statistics," paper No. 1 in *Target and Clutter Scattering and Their Effects on Military Radar Performance,* NATO Advisory Group for Aerospace Research and Development, AGARD Conf. Proceedings 501, September 1991. AD-A244 893.
4. Billingsley, J. B. "Ground Clutter Measurements for Surface-Sited Radar." MIT Lincoln Laboratory, Lexington, MA, Tech. Rep. 786, Revision 1, February 1, 1993.
5. Billingsley, J. B. "A Handbook of Multifrequency Land Clutter Coefficients for Surface Radar." MIT Lincoln Laboratory, Lexington, MA, Tech. Rep. 958. This will appear in the book *Low-Angle Radar Land Clutter* by J. B. Billingsley.
6. Moore, R. K., K. A. Soofi, and S. M. Purduski. "A Radar Clutter Model: Average Scattering Coefficients of Land, Snow and Ice." *IEEE Trans.* AES-16 (November 1980), pp. 783–799.
7. Schooley, A. H. "Some Limiting Cases of Radar Sea Clutter Noise." *Proc. IRE* 44 (August 1956), pp. 1043–1047.
8. Barton, D. K. *Modern Radar System Analysis.* Norwood, MA: Artech House, 1988.
9. Moore, R. K. "Ground Echo." In *Radar Handbook,* 2nd ed., M. Skolnik (Ed.). New York: McGraw-Hill, 1990, chap. 12.
10. Ref. 2, Table 7.17.
11. Long, W. H., D. H. Mooney, and W. A. Skillman. "Pulse Doppler Radar." In *Radar Handbook,* 2nd ed., M. Skolnik (Ed.). New York: McGraw-Hill, 1990, chap. 17, pp. 17.11–17.16.
12. Ulaby, F. T., R. K. Moore, and A. K. Fung. *Microwave Remote Sensing,* vol. II, Reading, MA: Addison-Wesley, 1982, Sec. 11-4.2.
13. Ulaby, F. T., W. H. Stiles, L. F. Dellwig, and B. C. Hansen. "Experiments on the Radar Backscatter of Snow." *IEEE Trans.* GE-15 (October 1977), pp. 185–189.
14. Ulaby, F. T., and W. H. Stiles. "Microwave Response of Snow." *Adv. Space Res.* (1981), pp. 131–149. (Also found in Refs. 15 and 17.)
15. Ulaby, F. T., R. K. Moore, and A. K. Fung. *Microwave Remote Sensing,* vol. III. Dedham, MA: Artech House, 1986, Sec. 21-7.

16. Waite, A. H., and S. J. Schmidt. "Gross Errors in Height Indication from Pulsed Radar Altimeters Operating over Thick Ice or Snow." *Proc. IRE* 50 (June 1962), pp. 1515–1520.

17. Ulaby, F. T., and M. C. Dobson. *Handbook of Radar Scattering Statistics for Terrain.* Norwood, MA: Artech House, 1989.

18. Borel, C. C., R. E. McIntosh, R. M. Narayanan, and C. T. Swift. "File of Normalized Radar Cross Sections (FINRACS)—A Computer Program for Research of the Scattering of Radar Signals by Natural Surfaces." *IEEE Trans.* GE-24 (November 1986), pp. 1020–1022.

19. Long, M. W., *Radar Reflectivity of Land and Sea,* 2nd ed. Norwood, MA: Artech House, 1983.

20. Bush, T. F., F. T. Ulaby, and W. H. Peake. "Variability in the Measurement of Radar Backscatter." *IEEE Trans.* AP-24 (November 1976), pp. 896–899.

21. Bowditch, *American Practical Navigator,* U. S. Hydrographic Office, H. O. Publication No. 9, 1966, Appendix R.

22. Pierson, W. J., G. Neumann, and R. W. James. *Observing and Forecasting Ocean Waves,* U. S. Naval Oceanographic Office, H. O. Publication No. 603, 1955.

23. Daley, J. "An Empirical Sea Clutter Model." Naval Research Laboratory, Washington, D.C., Memorandum Report 2668, October 1973.

24. Daley, J. C., J. T. Ransone, Jr., and W. T. Davis. "Radar Sea Return—JOSS II." Naval Research Laboratory, Washington, D.C., Rep. 7534, February 21, 1973.

25. Daley, J. C., J. T. Ransone, Jr., and J. A. Burkett. "Radar Sea Return—JOSS I." Naval Research Laboratory, Washington, D.C., Report 7268, May 11, 1971.

26. Daley, J. C., et al. "Upwind-Downwind-Crosswind Sea Clutter Measurements." Naval Research Laboratory, Washington, D.C., Report 6881, April 14, 1969.

27. Hansen, J. P., and V. F. Cavaleri. "High-Resolution Radar Sea Scatter, Experimental Observations and Discriminants." Naval Research Laboratory, Washington, D.C., Rep. 8557, March 5, 1982.

28. Lewis, B. L., and I. D. Olin. "Experimental Study and Theoretical Model of High-Resolution Radar Backscatter from the Sea." *Radio Science.* 15 (July–August 1980), pp. 815–828.

29. Macdonald, F. C. "Characteristics of Radar Sea Clutter, Pt. 1—Persistent Target-Like Echoes in Sea Clutter." Naval Research Laboratory, Washington, D.C., Report 4902, March 19, 1957.

30. Ewell, G. W., M. T. Tuley, and W. F. Horne. "Temporal and Spatial Behavior of High Resolution Sea Clutter 'Spikes.'" *Proc 1984 IEEE National Radar Conf.* pp. 100–104, IEEE Catalog no. 84CH1963-8.

31. U. S. Patent 3,971,997: "Sea Spike Suppression Technique," issued to B. L. Lewis and I. D. Olin, July 27, 1976.

32. Williams, P. D. L. "Limitations of Radar Techniques for the Detection of Small Surface Targets in Clutter." *The Radio and Electronic Engineer* 45 (August 1975), pp. 379–389.

33. Long, M. W. Ref. 19, Sec. 5.6.

34. Wetzel, L. B. "On Microwave Scattering by Breaking Waves." In *Wave Dynamics and Radio Probing of the Ocean Surface.* O. M. Phillips and K. Hasselmann (Ed.). New York: Plenum, 1986, pp. 273–284.

35. Longuet-Higgins, M. S., and J. S. Turner. "An 'Entraining Plume' Model of a Spilling Breaker." *J. Fluid Mech.* 63 (1974), pp. 1–20.

36. Croney, J., A. Woroncow, and B. R. Gladman. "Further Observations on the Detection of Small Targets in Clutter." *The Radio and Electronic Engineer* 45 (March 1975), pp. 105–115.

37. Croney, J. "Improved Radar Visibility of Small Targets in Sea Clutter." *The Radio and Electronic Engineer* 32 (September 1966), p. 135–148.

38. Wetzel, L. B. "Electromagnetic Scattering from the Sea at Low Grazing Angles." In *Surface Waves and Fluxes.* Vol. II Netherlands: Kluwer Academic, 1990, chap. 12, pp. 109–171.

39. Wetzel, L. B. "A Model for Sea Backscatter Intermittency at Extreme Grazing Angles," *Radio Science* 12 (September–October 1977), pp. 747–756.

40. Knott, E. F., J. F. Shaffer, and M. T. Tuley. *Radar Cross Section,* 2nd ed. Norwood, MA: Artech House, 1993, Secs. 5.9 and 6.3.

41. Katzin, M. "On the Mechanisms of Radar Sea Clutter." *Proc. IRE* 45 (January 1957), pp. 44–54.

42. Helmken, H. H., and M. J. Vanderhill. "Very Low Grazing Angle Radar Backscatter from the Ocean Surface." *Record of the IEEE 1990 International Radar Conf.* pp. 181–188, IEEE Catalog No. 90CH-2882-9

43. Dockery, G. D. "Method for Modelling Sea Surface Clutter in Complicated Propagation Environments." *IEE Proc.* 137, Pt. F (April 1990), pp. 73–79.

44. Nathanson, F. E. Ref. 2, Sec. 7.2

45. Kerr, D. E. (Ed.): *Propagation of Short Radio Waves.* MIT Radiation Laboratory Series. New York: McGraw-Hill, 1951, vol. 13.

46. Goldstein, H. "Frequency Dependence of the Properties of Sea Echo." *Phys. Rev.* 70 (Dec. 1 and 15, 1946), pp. 938–946.

47. Kinsman, B. *Wind Waves.* Upper Saddle River, NJ: Prentice Hall, 1965, Sec. 7.4.

48. Beckmann, P., and A. Spizzichino. *The Scattering of Electromagnetic Waves from Rough Surfaces.* New York: Macmillan, 1963, Secs. 5.3 and 18.2.

49. Leung, H., and S. Haykin. "Is There a Radar Clutter Attractor?" *Appl. Phys. Lett.* 56 (February 1990), pp. 593–595.

50. Crombie, D. D. "Doppler Spectrum of Sea Echo at 13.56 Mc/s." *Nature* 175 (1955), pp. 681–682.

51. Maresca, J. W., and T. M. Georges. "Measuring RMS Wave Height and the Scalar Ocean Wave Spectrum with HF Skywave Radar." *J. Geophys. Res.* 85 (1980), pp. 2759–2771.

52. "Special Issue on High-Frequency Radar for Ocean and Ice Mapping and Ship Location." *IEEE J. Oceanic Engr.* OE-11, No. 2 (April 1986).

53. Wright, J. W. "A New Model for Sea Clutter." *IEEE Trans.* AP-16 (March 1968), 217–223.

54. Wetzel, L. B. "Sea Clutter." In *Radar Handbook,* 2nd ed., M. Skolnik (Ed.). New York: McGrall-Hill, 1990, Chap. 13, Sec. 13.4.

55. Wetzel, L. B. Ref. 38, Chap. 12.

56. Lyzenga, D. R., A. L. Moffett, and R. A. Shuchman. "The Contribution of Wedge Scattering to the Radar Cross Section of the Ocean Surface." *IEEE Trans.* GE-31 (October 1983), pp. 502–505.

57. Nathanson, F. E: Ref. 2, Chap. 7.

58. Horst, M. M., F. B. Dyer, and M. T. Tuley. "Radar Sea Clutter Model." *Inter. Conf. on Ant. and Prop.* IEE Pub. No. 169, Pts. 1 and 2, London, 1978. (Also available in Ref. 2, pp. 307–308.)

59. Morchin, W. *Radar Engineer's Sourcebook.* Norwood, MA: Artech House, 1993, Sec. 3.3.2.

60. Ulaby, F. T., R. K. Moore, and A. K. Fung. Ref. 15, Sec. 20–4.

61. Lewis, E. O., B. W. Currie, and S. Haykin. *Detection and Classifcation of Ice.* New York: John Wiley, 1987.

62. Haykin, et al. *Remote Sensing of Sea Ice and Icebergs.* New York: John Wiley, 1994.

63. Wylie, F. J. *The Use of Radar at Sea,* 5th ed. Annapolis, MD: Naval Institute Press, 1978.

64. Ringwalt, D. L., and F. C. Macdonald. "Terrain Clutter Measurements in the Far North." *Report of NRL Progress,* Naval Research Laboratory, Washington, D.C., pp. 9–14, December 1956.

65. Orlando, J. R., R. Mann, and S. Haykin. "Classification of Sea-Ice Images Using a Dual-Polarized Radar." *IEEE J. Oceanic Engr.* 15 (July 1990), pp. 228–237.

66. Curlander, J. C., and R. N. McDonough. *Synthetic Aperture Radar.* New York: John Wiley, 1991, Appendix C.

67. Orlando, J. R., and S. Haykin: "Real-Time Detection of Iceberg Shadows." *IEEE J. Oceanic Engr.* 15 (April 1990), pp. 112–118.

68. Pilon, R. O., and C. G. Purves. "Radar Imagery of Oil Slicks." *IEEE Trans.* AES-9 (September 1973), pp. 630–636.

69. Ulaby, F. T., and M. C. Dobson. Ref.17, Chap. 3.

70. Trunk, G. V., and S. F. George. "Detection of Targets in Non-Gaussian Sea Clutter." *IEEE Trans.* AES-6 (September 1970), pp. 620–628.

71. Schleher, D. C. "Radar Detection in Log-Normal Clutter." *Record of the IEEE 1975 International Radar Conf.,* pp. 262–267. Reprinted in *Automatic Detection and Radar Data Processing,* D. C. Schleher (Ed.). Dedham, MA: Artech House, 1980.

72. Sekine, M., and Y. Mao. *Weibull Radar Clutter.* London: Peter Peregrinus, 1990.

73. Boothe, R. R. "The Weibull Distribution Applied to the Ground Clutter Backscatter Coefficient." U.S. Army Missile Command Report No. RE-TR-69-15, June, 1969; reprinted in *Automatic Detection and Radar Data Processing,* D. C. Schleher (Ed.). Dedham, MA: Artech House, 1980, pp. 435–450.

74. Sekine, et al. "Weibull Distributed Ground Clutter." *IEEE Trans.* AES-17 (July 1981), pp. 596–598.

75. Fay, F. A., J. Clarke, and R. S. Peters. "Weibull Distribution Applied to Sea Clutter," *Radar 77, IEE Conf. Publ.* 155, 1977, pp. 101–104; reprinted in *Advances in Radar Techniques.* London: Peter Peregrinus, 1985, pp. 236–239.

76. Sekine, M., et al. "Weibull Distributed Sea Clutter." *IEE Proc.* 130, Pt. F (1983), p. 476.

77. Sekine, M., et al. "On Weibull Distributed Weather Clutter." *IEEE Trans.* AES-15 (November 1979), pp. 824–830.

78. Ogawa, H., et al. "Weibull-Distributed Radar Clutter Reflected from Sea Ice." *Trans. IEICE* E70 (1987), pp. 116–120.

79. Schleher, D.C. "Radar Detection in Weibull Clutter." *IEEE Trans.* AES-12 (November 1976), pp. 736–743.

80. Jakeman, E., and P. N. Pusey. "A Model for Non-Rayleigh Sea Echo." *IEEE Trans.* AES-24 (November 1976), pp. 806–814.

81. Ward, K. D., and S. Watts. "Radar Sea Clutter." *Microwave J.* 28 (June 1985), pp. 109–121.

82. Jao, J. K. "Amplitude Distribution of Composite Terrain Radar Clutter and the K-Distribution." *IEEE Trans.* AES-32 (October 1984), pp. 1049–1062.

83. Ward, K. D. "A Radar Sea Clutter Model and Its Application to Performance Assessment." *International Conf. Radar-82* October 18–20, 1982. IEE Conference Publication No. 216, pp. 204–207.

84. Ward, K. D., C. J. Baker, and S. Watts. "Martime Surveillance Radar, Part 1: Radar Scattering from the Ocean Surface." *IEE Proc.* 137, Pt. F (April 1990), pp. 51–62.

85. Baker, C. J. "K-Distributed Coherent Sea Clutter." *IEE Proc.* 138, Pt. F (April 1991), pp. 89–92.

86. Watts, S. and D. C., Wicks. "Empirical Models for Detection Prediction in K-Distribution Radar Sea Clutter." *Record of the IEEE 1990 Int. Radar Conf.,* pp. 189–194, IEEE Catalog No. 90CH-2882-9.

87. Watts, S. and K. D. Ward. "Spatial Correlation in K-Distributed Sea Clutter." *IEE Proc.* 134, Pt. F (October 1987), pp. 526–532.

88. Trunk, G. V., and S. F. George. "Detection of Targets in Non-Gaussian Sea Clutter." *IEEE Trans.* AES-6 (September 1970), pp. 620–628.

89. Hair, T., T. Lee, and C. J. Baker. "Statistical Properties of Multifrequency High-Range-Resolution Sea Reflections." *IEE Proc.* 138, Pt. F (April 1991), pp. 75–79.

90. Baker, C. J. "K-Distributed Coherent Sea Clutter." *IEE Proc.* 138, Pt. F (April 1991), pp. 89–92.

91. Pentini, F. A., A. Farina, and F. Zirilli. "Radar Detection of Targets Located in a Coherent K Distributed Clutter Background." *IEE Proc.* 139, Pt. F (June 1992), pp. 239–245.

92. Watts, S. "Radar Detection Prediction in K-Distributed Sea Clutter and Thermal Noise." *IEEE Trans.* AES-23 (January 1987), pp. 40–45.

93. Armstrong, B. C., and H. D. Grifiths. "CFAR Detection of Fluctuating Targets in Spatially Correlated K-Distributed Clutter." *IEE Proc.* 138, Pt. F (April 1991), pp. 139–152.

94. Trunk, G. V. "Radar Properties of Non-Rayleigh Sea Clutter." *IEEE Trans.* AES-8 (March 1972), pp. 196–204.

95. Tough, R. J. A., C. J. Baker, and J. M. Pink. "Radar Performance in a Maritime Environment: Single Hit Detection in the Presence of Multipath Fading and Non-Rayleigh Sea Clutter." *IEE Proc.* 137, Pt. F (February 1990), pp. 33–40.

96. Oliver, C. J. "Representation of Radar Sea Clutter." *IEE Proc.* 135, Pt. F (December 1988), pp. 497–500.

97. Sekine, et al. "Log-Weibull Distributed Sea Clutter." *IEE Proc.* 127, Pt. F (June 1980), pp. 225–228.

98. Shlyakhin, V. M. "Probability Models of Non-Rayleigh Fluctuations of Radar Signals (A Review)." *Soviet J. Communications Technology and Electronics.* 33 (January 1988), pp. 1–16.

99. Schleher, D. C. "Radar Detection in Log Normal Clutter." *Record of the IEEE 1975 International Radar Conf.* pp. 262–267, IEEE Publication 75 CHO 938-1 AES.

100. Farina, A., A. Russo, and F. A. Studer. "Coherent Radar Detection in Log-Normal Clutter." *IEE Proc.* 133, Pt. F (February 1986), pp. 39–54.

101. Farina, A., et al. "Theory of Radar Detection in Coherent Weibull Clutter." *IEE Proc.* 134, Pt. F (April 1987), pp. 174–190.

102. Sangston, K. J. "Coherent Detection of Radar Targets in K-Distributed, Correlated Clutter." Naval Research Laboratory, Washington, D.C., Report 9130, August, 1988.

103. Battan, L. J. *Radar Observation of the Atmosphere.* Chicago, IL: Univ. of Chicago, 1973.

104. Gunn, K. L. S., and T. W. R. East. "The Microwave Properties of Precipitation Particles." *Quart. J. Roy. Meteor. Soc.* 80 (October 1954), pp. 522–545.

105. Sauvageot, H. *Radar Meteorology.* Norwood, MA: Artech House, 1992.

106. Personal communication from Raymond Wexler.

107. Haddock, F. T. "Scattering and Attenuation of Microwave Radiation Through Rain." Naval Research Laboratory, Washington, D.C., (unpublished manuscript), 1948. (Mentioned in Gunn and East, Ref. 104)

108. Smith, P. L. Jr., K. R. Hardy, and K. M. Glover. "Applications of Radar to Meteorological Operations and Research." *Proc. IEEE.* 62 (June 1974), pp. 724–745.

109. Jameson, A. R. "A Comparison of Microwave Techniques for Measuring Rainfall." *J. Applied Meteorology* 30 (January 1991), pp. 32–54.

110. Nathanson, F. E. Ref. 2, Sec. 3.6.

111. Sauvageot, H. Ref. 105, Sec. 1.5.3.

112. Gunn, K. L. S., and J. S. Marshall. "The Distribution with Size of Aggregate Snowflakes." *J. Meteor.* 15 (1958), pp. 452–466.

113. Sekhon, R. S., and R. C. Srivastava. "Snow Size Spectra and Radar Reflectivity." *J. Atmos. Sci.* 27 (1970), pp. 299–307.

114. Puhakka, T. "On the Dependence of the Z-R Relationship on the Temperature in Snowfall." *Preprints 16th Radar Meteorology Conf.* Am. Meteor. Soc., April 22–24, 1975, Houston, TX, pp. 504–507.

115. Austin, P. M. "Measurements of the Distribution of Precipitation in New England Storms." *Proc. 10th Weather Radar Conf.,* Am. Meteor. Soc., pp. 247–254, 1963.

116. Saxton, J. A. "The Influence of Atmospheric Conditions on Radar Performance." *J. Inst. Navigation* (London) 11, pp. 290–303, 1958.

117. Nathanson, F. E., Ref. 2, Fig. 6.4.

118. Konrad, T. G., J. J. Hicks, and E. B. Dobson. "Radar Characteristics of Brids in Flight." *Science* 159 (Jan. 19, 1968), pp. 274–280.

119. Vaughn, C. R. "Birds and Insects as Radar Targets: A Review." *Proc. IEEE* 73 (February 1985), pp. 205–227.

120. Eastwood, E. *Radar Ornithology.* London: Methuen, 1967.

121. Williams, T. C. and J. M. Williams. "Open Ocean Bird Migration." *IEE Proc.* 137, Pt. F (April 1990), pp. 133–137.

122. Houghton, E. W., F. Blackwell, and T. A. Wilmot. "Bird Strike and the Radar Properties of Birds." *Int. Conf. on Radar—Present and Future,* Oct. 23–25, 1973, pp. 257–262, IEE Conference Publication no. 105.

123. Flock, W. L., and J. L. Green. "The Detection and Identification of Birds in Flight, Using Coherent and Noncoherent Radars." *Proc. IEEE* 62 (June 1974), pp. 745–753.

124. Blackwell, F., and E. W. Houghton. "Radar Tracking and Identification of Wild Duck During the Autumn Migration." *Proc. World Conf. on Bird Hazards to Aircraft, Canada* (1969), pp. 361–376.

125. Antonucci, J. "A Statitical Model of Radar Bird Clutter at the DEW Line." Rome Laboratory (EEAS), Air Force Systems Command, Hanscomb AFB, MA, Report no. RL-TR-91-85, May, 1991.

126. Knott, E. F. "*Radar Cross Section.*" In *Radar Handbook*, 2nd ed. M. Skolnik (Ed.) New York: McGraw-Hill, 1990, Chap. 11.

127. Riley, J. R. "Radar Cross Section of Insects." *Proc. IEEE* 73 (February 1985), pp. 228–232.

128. Schaefer, G. W. "Radar Observations of Insect Flight," *Insect Flight,* R. C. Rainey (Ed.) London: Blackwell Scientific Publications, 1976, Chap. 8.

129. Gossard, E. E., and R. G. Strauch. *Radar Observations of Clear Air and Clouds.* New York: Elsevier, 1983.

130. James, P. K. "A Review of Radar Observations of the Troposphere in Clear Air Conditions." *Radio Sci.* 15 (March–April 1980), pp. 151–175. (The entire March-April 1980 issue of *Radio Sci.* is devoted to "Radar Investigations of the Clear Air.")

131. Tatarskii, V. T. *Wave Propagation in a Turbulent Medium.* New York: McGraw-Hill, 1961.

132. Skolnik, M. "Atmospheric Turbulence and the Extension of the Radar Horizon." Naval Research Laboratory, Washington, D.C., Memorandum Rep. 2903, October 1974.

133. Heiss, W. H., D. L. McGrew, and D. Sirmans. "Nexrad: Next Generation Weather Radar (WSR-88D)." *Microwave J.* 33 (January 1990), pp. 79–98.

134. Michelson, M., Shrader, W. W., and J. G. Wieler. "Terminal Doppler Weather Radar." *Microwave J.* 33, (February 1990), pp. 139–148.

135. Plank, V. G. "A Meteorological Study of Radar Angels." U.S.A.F. Cambridge Research Center Geophys. Resarch Papers, no. 52, July, 1956, AFCRC-TR-56-211, AD 98752.

136. Rogers, R. R., and W. O. J. Brown. "Radar Observations of a Major Industrial Fire." *Bull. Am. Meteorological Soc.* 78 (May 1997), pp. 803–814.

137. Skolnik, M., D. Hemenway, and J. P. Hansen. "Radar Detection of Gas Seepage Associated with Oil and Gas Deposits." *IEEE Trans.* GRS-30 (May 1992), pp. 630–633.

138. Skolnik, M., and T. C. Bailey. "A Review of Radar for the Detection of Gas Seepage Associated with Underground Oil and Gas Deposits." *Proc. of the Conf. on Applications of Emerging Technologies: Unconventional Methods in Exploration for Petroleum and Natural Gas V,* Institute for the Study of Earth and Man, Southern Methodist Univ., Dallas, Texas, 1997, pp. 207–228.

139. Eastwood, E. Ref. 120, Chap. 9; also V. G. Plank, Ref. 135.

140. Billingsley, J. B. "Ground Clutter Measurements for Surface-Sited Radar," MIT Lincoln Laboratory, Lexington, MA, Tech. Rep. 786, Revision 1, February 1, 1993.

141. Caspers, J. W. "Automatic Detection Theory." In *Radar Handbook,* 1st ed. M. Skolnik (Ed.). New York: McGraw-Hill, 1970, chap. 15, Sec.15.6.

142. Trunk, G. V., and S. F. George. "Detection of Targets in Non-Gaussian Sea Clutter." *IEEE Trans.* AES-6 (September 1970), pp. 620–628.

143. Trunk, G. V. "Further Results on the Detection of Targets in Non-Gaussian Sea Clutter." *IEEE Trans.* AES-7 (May 1971), pp. 553–556.

144. Schleher, D. C. "Radar Detection in Weibull Clutter." *IEEE Trans.* AES-12 (November 1976), pp. 736–743. Correction in AES-13 (July 1977), p. 435.

145. Schleher, D. C. "Radar Detection in Log-Normal Clutter." *IEEE International Radar Conf.* Arlington, VA, April 21–23, 1975, pp. 262–267.

146. Croney, J., A. Woroncow, and B. R. Gladman. "Further Observations on the Detection of Small Targets in Sea Clutter." *The Radio and Electronic Engineer* 45 (March 1975), pp. 105–115.

147. Williams, P. D. L. "Observations on the Further Optimization of Radar Signal Processing for the Display and Detection of Targets in Sea Clutter." *Int. J. Remote Sensing* 5 (1984), pp. 489–496.

148. Tonkin, S. P., and R. A. McCulloch. "Gross Spatial Structure of Land Clutter." *IEE Proc.* 138, Pt. F. (April 1991), pp. 99–108.

149. Shrader, W. W., and V. Gregers-Hansen. "MTI Radar." *Radar Handbook,* M. Skolnik (Ed.). New York: McGraw-Hill, 1990, Chap. 15, p. 15.13.

150. Gordon, W. B. "Analysis of Rain Clutter Data from a Frequency Agile Radar." *Radio Science* 17 (July-August 1982), pp. 801–816.

151. Queen, F. D., and J. J. Alter. "Results of a Feasibility Study for Determining the Yaw Angle of a Landing Aircraft." Naval Research Laboratory, Washington, D.C., Rep. 8480, May 27, 1981.

152. Hughes, P. K., II. "A High-Resolution Radar Detection Strategy." *IEEE Trans.* AES-19 (September 1983), pp. 663–667.

153. Gent, H., I. M. Hunter, and N. P. Robinson. "Polarization of Radar Echoes, Including Aircraft, Precipitation, and Terrain." *IEE Proc.* 110 (December 1963), pp. 2139–2148.

154. Sauvageot, H. *Radar Meteorology.* Norwood, MA: Artech House, 1992, Sec. 2.2.7.

155. Oguchi, T. "Electromagnetic Wave Propagation and Scattering in Rain and Other Hydrometeors." *Proc. IEEE* 71, (September 1983), pp. 1029–1078.

156. McDonald, J. E. "The Shape of Raindrops." *Scientific American* (February 1954).

157. Schneider, A. B., and P. D. L. Williams. "Circular Polarization in Radars." *The Radio and Electronic Engineer* 47, no. 1/2 (January/February 1976), pp. 11–29.

158. Kalafus, R. M. "Rain Cancellation Deterioration Due to Surface Reflections in Ground-Mapping Radars Using Circular Polarization." *IEEE Trans.* AP-23 (March 1975), pp. 269–271.

159. Beasley, E. W. "Effect of Surface Reflections on Rain Cancellation in Radars Using Circular Polarization." *Proc. IEEE* 54 (December 1966), pp. 2000–2001.

160. Hendry, A., and G. C. McCormick. "Deterioration of Circular-Polarization Clutter Cancellation in Anisotropic Precipitation Media." *Electronics Letters* 10 (May 16, 1974), pp. 165–166.

161. Nathanson, F. E. "Adaptive Circular Polarization." *IEEE 1975 International Radar Conf.,* April 21–23, 1975, pp. 221–225.

162. Nathanson, F. E. Ref. 2, Sec. 5.2.

163. Schneider, A. B., and P. D. L. Williams. Ref. 157.

164. Olin, I. D., and F. D. Queen. "Dynamic Measurement of Radar Cross Sections." *Proc. IEEE* 53 (August 1965), pp. 954–961.

165. Kerr, D. E. (Ed.). *Propagation of Short Radio Waves.* MIT Radiation Laboratory Series. New York: McGraw-Hill, 1951, vol. 13.

166. Croney, J. "Improved Radar Visibility of Small Targets in Sea Clutter. *The Radio and Electronic Engineer* 32 (September 1966), pp. 135–148.

167. Croney, J., and A. Woroncow. "Dependence of Sea Clutter Decorrelation Improvments Upon Wave Height." *IEE Int. Conf. On Advances in Marine Navigational Aids,* July 25–27, 1972, IEE (London) Conf. Publication no. 87, pp. 53–59.

168. Smith, J. M., and R. H. Logan. "AN/APS-116 Periscope Detecting Radar." *IEEE Trans.* AES-16 (January 1980), pp. 66–73.

169. Valenzuela, G. R., and M. B. Laing. "Study of Doppler Spectra of Radar Sea Echo." *J. Geophys. Res.* 75 (January 20, 1970), pp. 551–563.

170. Nathanson, F. E. Ref. 2, Sec. 6.6.

171. Fuller, J. B., and J. R. Martin. "Radar Subsystems," Varian Co. brochure, Beverly Division, Beverly MA, no date, Fig. 2. (Now known as CPI Beverly Microwave Division.)

172. Becker, J. E., and R. E. Millet. "A Double-Slot Radar Fence for Increased Clutter Suppression." *IEEE Trans.* AP-16 (January 1968), pp. 103–108.

173. Ruze, J., F. I. Sheftman, and D. A. Cahlander. "Radar Ground-Clutter Shields." *Proc. IEEE* 54 (September 1966), pp. 1171–1183.

174. Harrison, A. "Marine Radar Today—A Review." *The Radio and Electronic Engineer* 47 (April 1977), pp. 177–183.

175. Taylor, J. W., Jr. "Receivers." In *Radar Handbook,* M. Skolnik (Ed.). New York: McGraw-Hill, 1990, Chap. 3, Sec. 3.6.

176. Croney, J. "Clutter on Radar Displays." *Wireless Engr.* 33 (April 1956), pp. 83–96.

177. Taylor, J. W., Jr. Ref. 175, Sec. 3.13.

PROBLEMS

7.1 Find the range at which the radar echo from low grazing angle surface clutter equals receiver noise for the following radar: peak power = 100 kW, azimuth beamwidth = 1°, elevation beamwidth = 20° [see Eq. (9.5c)], wavelength = 3 cm, pulse width = 0.1 μs, and receiver noise figure = 4 dB. The radar is located at a height of 1 km over a flat sea surface. You may assume the following variation of σ^0 with grazing angle Ψ:

$$\text{sigma zero} = -46 \text{ dB at } 1.0^\circ \text{ grazing angle}$$
$$= -42 \text{ dB at } 3.0^\circ$$
$$= -37 \text{ dB at } 10.0^\circ$$

7.2 The ARSR-3 is a long-range, ground-based, fan-beam, *L*-band radar that was used by the FAA for enroute air-traffic control. It had an azimuth beamwidth of 1.25° and a pulse width of 2 μs. (a) If the clutter cross section per unit area, σ^0, for surface land clutter is -20 dB, what is the MTI clutter attenuation required to detect a 2 m^2 target at a range of 30 nmi with an output signal-to-clutter ratio of 15 dB? (Clutter is considered to be much greater than receiver noise.) (b) What will be the radar cross section of rain clutter (in m^2) seen by the ARSR-3 radar at a range of 30 nmi when the rainfall rate is 4 mm/h? You may assume a flat earth and that the rain uniformly fills the radar resolution cell from the ground up to a height h of 3 km. Take the radar frequency to be 1.3 GHz. (The elevation angle coverage should not be needed here.)

7.3 Derive a radar equation for the detection of a target in surface clutter when the grazing angle is 90° (normal incidence). Assume the antenna employs a pencil beam. (This is not a usual radar detection situation because the clutter echo is large when the antenna beam is perpendicular to the surface.)

7.4 An S-band pencil-beam radar (3.2 GHz) with a 1.5° beamwidth and 3-μs pulse width can detect a 2 m^2 target at a range of 200 nmi in a clear atmosphere (no rain). If a single-pulse signal-to-clutter ratio of 10 dB is required, what would be the range of the radar when observing a 2-m^2 target in rain of 4 mm/h? (Assume that clutter is uniformly distributed and is much greater than receiver noise, attenuation in rain at this frequency can be neglected, the antenna beam is pointing at a low elevation angle but doesn't strike the ground, and rain completely fills the radar resolution cell.)

7.5 Sketch as a function of rainfall rate (from 1 to 40 mm/h) the variation of the pulse echo power from rain for a radar with the following characteristics (which are those of Nexrad):

peak power = 1 MW
frequency = 3.0 GHz
pulse width = 1.57 μs
antenna gain = 45.5 dB (pencil beam)
effective number of hits integrated = 80
range = 150 km

(Assume that the beam is completely filled with rain, the beam is low to the ground but does not intercept it, and the attenuation due to rain can be neglected.)

7.6 What will be the attenuation due to rain uniformly distributed throughout the radar coverage and what will be the radar cross section of rain at a range of 20 km for a radar pointing at a low elevation angle with a 2° by 4° beamwidth and a 2-μs pulse width at frequencies of 3, 10, and 35 GHz? The rain falls at a rate of 4 mm/h.

7.7 Briefly comment on how the radar parameters listed below affect radar performance when detection is limited by (1) surface clutter and by (2) receiver noise. The radar parameters

are: (a) pulse width, (b) antenna gain, (c) transmitter power, (d) number of pulses returned from the target, (e) system losses, and (f) the sensitivity of the maximum detection range to changes in the radar cross section. (It may help to make a table.)

7.8 Show that the radar cross section per unit area, σ^0, for a radar with a narrow pencil-beam antenna viewing a large perfectly reflecting flat surface at perpendicular incidence is approximately equal to G, where G = antenna gain. The flat surface is much larger than the extent of the footprint of the radar beam hitting the surface. In other words, derive Eq. (7.12). [The key to this problem is solving for the received power in two different ways, and then equating them to find σ^0. Start with the simple form of the radar equation for the received echo signal power P_r from a radar directed perpendicular to a flat surface. The cross section of the target is $\sigma^0 A_c$, where A_c is the area of that portion of the flat surface which is illuminated by the radar beam. Find an expression for A_c. The half-power beamwidth is θ_B, but you have to account for the change in illuminated area due to the two-way beamwidth. The second way to find the received power is recognize that the flat plate creates an image of the radar antenna a distance R behind the plate. The receive signal power is found by considering the geometry as a one-way communication link between the radar antenna and its image located a distance R behind the surface. Derive a one-way communication equation for the signal received at the image antenna when the radar antenna transmits to its image a distance $2R$ away. The two values of P_r, found from the two different models of propagation path, are the same and may be equated. You might need to use Eq. (9.5b) for the antenna gain.]

7.9 This problem concerns finding the radar cross section (in square meters) of various forms of distributed volumetric clutter at low altitudes as might be seen at a range of 10 km by an X-band (10 GHz) radar with a 1° beamwidth and a 1-μs pulse width. The cross section per unit volume of the volumetric clutter is denoted by η. The clutter is assumed to occupy the entire radar resolution cell. (Be careful of units.) (a) Rain falling at 4 mm/h. (b) Migrating Shearwater birds with $\eta = 3 \times 10^{-9}$ cm^{-1}. Compare your answer with the radar cross section of a single Shearwater bird as given in Table 7.5. (c) Insects with $\eta = 10^{-10}$ cm^{-1}. (d) Clear-air turbulence with $C_n^2 = 10^{-10}$ m$^{-2/3}$.

7.10 List five options available to the radar designer for enhancing the detection of aircraft in rain. Briefly describe the operation of each and their chief limitation.

7.11 If an S-band radar is capable of detecting a 1 m^2 target at a range of 200 nmi, at what range will it be able to detect a single sparrow? (See Table 7.4.)

7.12 Assume an X-band radar (λ = 3.2 cm) has a range of 45 km in the absence of rain. If it is further assumed that the attenuation in rain is the only factor affecting range, what will be the radar range when rain is falling throughout the region at a rate of 4 mm/h? (You will probably have to solve for the range by trail and error. The ultimate in precision is not vital in the answer to this question.)

7.13 What radar parameters are under the control of the radar designer for increasing the range at which a target may be detected in rain? Which parameter do you think is most important for increasing the detectability of a target? Explain why.

7.14 The value of the cross section per unit volume of rain, η, varies as f^4, where f = radar frequency. Assume the rain completely fills the radar resolution cell. (a) What is the

variation of the echo from rain when the antenna gain G is independent of frequency? (b) What is the variation of the echo from rain when the antenna aperture area A_e is independent of frequency?

7.15 Show that the clutter echo seen by a pulse of width τ is decorrelated if the radar frequency is changed by an amount greater than $1/\tau$. [A decorrelated echo due to a change in frequency Δf means that the phase difference between the radar echo from the leading edge of the resolution cell and the trailing edge of the resolution cell changes by more than 2π radians when the frequency is changed an amount Δf. This occurs since phase is modulo 2π. Start by obtaining an expression for the two-way phase difference ϕ in terms of the radar resolution cell ΔR and wavelength λ. Note that the resolution cell is $\Delta R = c\tau/2$. The change in phase $\Delta\phi$ has to be greater than 2π radians when the frequency is changed by Δf in order to decorrelate the echo. The answer is now staring at you.]

7.16 Explain why frequency agility is not compatible with MTI (doppler) radar processing for detection of moving targets in clutter. (You may take as a model the single delay-line canceler.)

7.17 Why is the Bragg-scatter model not suitable for describing sea clutter at the higher microwave frequencies?

7.18 Briefly indicate what you think might be the preferred radar method or methods for detecting the targets listed below when in the presence of clutter. Assume the radar is located on the surface of the earth.

a. Aircraft over normal land clutter.
b. Aircraft over normal sea clutter.
c. Aircraft in the presence of large numbers of birds and insects.
d. Aircraft in the presence of moving ground targets.
e. Aircraft in rain clutter but beyond the range of surface clutter.
f. Ships and large buoys with corner reflectors.
g. Small boats, periscopes, buoys, and swimmers.
h. Stationary targets in distributed clutter.